UNIVERSIDAD DE LA FRONTERA

Facultad de Ingeniería y Ciencias

Doctorado en Ciencias de Recursos Naturales

"ROLE OF VOLATILE SULFUR COMPOUNDS (VSCS) EMITTED BY *Pseudomonas* SPP. IN THE BIOSYNTHESIS OF CdS QUANTUM DOT (QDs)"

DOCTORAL THESIS IN FULFILLMENT OF THE REQUERIMENTS FOR THE DEGREE DOCTOR OF SCIENCES IN NATURAL RESOURCES

CARLA DANIELA GALLARDO BENAVENTE

TEMUCO-CHILE

2020

“Role of volatile sulfur compounds (VSCs) emitted by *Pseudomonas* spp. in the biosynthesis of CdS quantum dot (QDs)”

Esta tesis fue realizada bajo la supervisión del Dr. ANDRÉS QUIROZ CORTEZ, perteneciente al Departamento de Ciencias Químicas y Recursos Naturales de la Universidad de La Frontera y del Dr. JOSÉ MANUEL PÉREZ DONOSO perteneciente a la Facultad de Ciencias de la Vida de la Universidad Andrés Bello. Se presenta el actual trabajo de tesis doctoral para la revisión por los miembros de la comisión examinadora.

CARLA DANIELA GALLARDO BENAVENTE

…….
Dr. Andrés Quiroz Cortez
Director Programa de Doctorado en Ciencias de Recursos Naturales

……
Dr. Andrés Quiroz Cortez (Tutor)
Universidad de La Frontera

…….
Dr. José Manuel Pérez Donoso (Co-Tutor)
Universidad Andrés Bello

.....
Dra. Mónica Rubilar Díaz
Directora Académica de Postgrado
Universidad de La Frontera

…….
Dr. Miguel Martínez Poblete
Universidad de Concepción

…….
Dra. Olga Rubilar
Universidad de La Frontera

…….
Dr. Cledir Santos
Universidad de La Frontera

To my family

Acknowledgements

First, I would like to thank my family for believing in me and for their unconditional love. Especially my parents, siblings, grandparents, and boyfriend for your permanent support, understanding, and encouragement during this process. Many thanks for always being interested in what I was doing, despite sometimes not fully understanding it. I am also grateful to my friends who have supported and encouraged me with their experience, laughs, or love along these years.

Very special gratitude goes out to my Thesis advisors, Dr. Andrés Quiroz and Dr. José Manuel Pérez Donoso, for their confidence, motivation, understanding, guide, and constant support during all this process. With particular recognition to Dr. Andrés Quiroz to his patience and help both with work and personal settings during these years.

I also want to thanks the members of the evaluation committee, Dr. Miguel Martínez Poblete, Dra. Olga Rubilar and Dr. Cledir Santos for their useful remarks and suggestions in each Thesis Advance.

Besides, I am grateful to Chemical Ecology Lab of the Universidad de La Frontera, a wonderful group of teachers and colleagues always willing to help and support the work of their members, as well as to the BioNanotechnology and Microbiology Lab of the Universidad Andres Bello for their constant friendship, collaboration and assistance in my work.

A special mention to the members of the Research Group of the School of Biological Sciences, University of East Anglia, Norwich, United Kingdom, especially to Dr. Jonathan Todd and Dr. Ornella Carrion as well as Dr. Amedea Seabra and Miss Joana Pieretti from the Research Group of Centro de Ciencias Naturais e Humanas,

Universidade Federal do ABC, Santo André, Brazil, for hosting me during my internships and for their valuable collaboration along with my research.

Finally, further acknowledgments go to the Doctoral Program in Science of Natural Resources of the Universidad de La Frontera for their academic support along these years, the National Commission of Scientific and Technological Research (CONICYT) for their financial support throughout the Doctoral Scholarship 21151066 and the Chilean Antarctic Institute (INACH) project DT_05_16**.**

Summary and thesis outline

The generation of a specific kind of nanoparticles named quantum dots (QDs) has emerged as a relevant tool for being used in a broad range of applications of high economic, technological, and biological values. The manufacture of these nanoparticles is carried out mainly by chemical methods of high cost, resulting in nanoparticles with high toxicity, which limits their applications. Thus, the biosynthesis of QDs, mainly produced by microorganisms, such as bacteria, emerges as an eco-friendly and inexpensive methodology. Some bacteria can release hydrogen sulfide (H_2S) for trapping exogenous cadmium, generating cadmium sulfide QDs (QDs CdS) by intra-or extracellular biosynthesis via cysteine desulfhydrase. However, not all bacteria respond to this mechanism, suggesting that there could be other volatile sulfur compounds that might be involved in the biosynthesis of CdS QDs, which have not been studied to date.

In Chapter I, we present a general introduction of this Doctoral Thesis, indicating the hypothesis and goals of this study.

In Chapter II, we study the role of volatile sulfur compounds (VSCs) released by *Pseudomonas* sp. GC01 in the biosynthesis extracellular of CdS QDs. Here, we assessed the biosynthesis of nanoparticles under several sulfur sources (sulfate, sulfite, thiosulfate, sulfide, cysteine, and methionine). Extracellular biosynthesis was observed only in cultures amended with cysteine (Cys) and methionine (Met), while intracellular biosynthesis occurred in all sulfur sources tested. Various methodologies for the characterization of extracellular QDs were applied, and the result showed cubic nanocrystals of CdS with diameters between 2 and 16 nm. The link of the CdS nanoparticles biosynthesis with volatiles compounds production in *Pseudomonas* sp. GC01 was evaluated by measuring VSCs under biosynthesis conditions (with Cadmium)

and using two mutants of the Antarctic strain *Pseudomonas deceptionensis* $M1^T$: megL- and mddA- unable to produce MeSH from Met and generate DMS from MeSH, respectively. The results revealed that *Pseudomonas* sp. GC01 produced hydrogen sulfide (H_2S), methanethiol (MeSH) and dimethyl sulfide (DMS) in the presence of sulfate, Met or Cys. While dimethyl disulfide (DMDS) only was detected in the presence of Met. MeSH was the main VSC generated and also was the only for which the concentration decreased in presence of cadmium for all the sulfur sources tested. The DMS role on Cds QDs biosynthesis was discarded due to the QDs production in the mddA- strain. No QDs biosynthesis was observed in the megL- strain, confirming the importance of MeSH in QD biosynthesis.

In Chapter III, we analyzed the genome of *Pseudomonas* sp. GC01 to searching genes associated with cadmium-resistance and sulfur metabolic pathways allowing explain the extracellular biosynthesis. The analysis was performed through genome sequencing of *Pseudomonas* sp. GC01 and comparative genetics using the genome sequence of 27 *Pseudomonas*. The general results showed a sequence with an identity of 99 % with *Pseudomonas* sp. Lz4W and *P. fragi* P121, both strains isolated from Antarctic and Arctic samples, respectively. Five genes involved in cadmium-resistance were found in *Pseudomonas* sp. GC01. Two genes, *cadR*, and *czcR*, code for regulatory elements involved in metal-resistance, while the other three genes belong to P-type ATPases (*cadA*, *zntA*, and *pbrA*) implicated in Cd efflux, which could favor the extracellular biosynthesis of CdS QDs.

Additionally, *Pseudomonas* sp. GC01 displays genes involved in sulfate assimilation, cysteine/methionine synthesis, and VSCs catabolic pathways, highlighting the absence of the genes *E4.4.1.11* and *megL* (coding methionine gamma-lyase) for MeSH generation because of *Pseudomonas* sp. GC01 produced high levels of these VSCs and was linked

with extracellular biosynthesis of nanoparticles using Met. Moreover, the *metC* gene (coding cystathionine beta-lyase) that produces MeSH from Met in bacteria was present in *Pseudomonas* sp. GC01 being able to fulfill this function.

Finally, overall results are discussed in Chapter IV, concluding the following: (1) *Pseudomonas* sp. GC01 biosynthesize extracellular CdS QDs through generating volatile sulfur compounds H_2S and MeSH from Cys and Met, respectively, (2) three P-type ATPases (*cadA*, *zntA*, and *pbrA*) involved in Cd efflux could contribute to the extracellular biosynthesis of CdS QDs in *Pseudomonas* sp. GC01, and (3) the enzyme cystathionine beta-lyase (*metC*) is presented as the main candidate to produce both H_2S and MeSH to the extracellular biosynthesis of CdS QDs from Cys and Met in *Pseudomonas* sp. GC01.

TABLE OF CONTENTS

CHAPTER I

General Introduction

1.1 General Introduction

Nanotechnology is a multi-disciplinary science field researching the nanoscale matter (size range 1 - 100 nm) manipulation to design and synthesize nanoparticles with an extensive range of applications (Sanchez and Sobolev, 2010; Solomon, 2018; Gour and Jain, 2019; Khan and Lee, 2020). One of the main groups of nanoparticles widely exploited for their dynamic applications in numerous science and technology areas is semiconductor nanocrystals or Quantum Dots (QDs) (Bajorowicz et al., 2018; Fontes and Santos, 2020).

QDs are considered bimetallic structures with a diameter range of 1 – 20 nm generally formed by elements in group 12-16 (IIB-VIA) (CdSe, CdS, ZnS), 13-15 (IIIA-VA) (GaN, GaP, InP), and 14-16 (IVA-VIA) (PbSe, PbS) (Mal et al., 2016; Jadhav et al., 2017; McHugh et al., 2018; Rengers et al., 2019; Gholami et al., 2020). These nanocrystals possess unique electrical and optical properties dependent on size and composition, such as highly photo-stability, broad absorption, narrow and size-tunable light emission, long fluorescence lifetime, and high quantum yield (Zhou and Ghosh, 2007; McHugh et al., 2018; Rengers et al., 2019; Cotta, 2020). The remarkable properties of QDs can apply in biomedicine and imaging, photovoltaics, optoelectronics, molecules quantification, and catalysis, among others (Faraon et al., 2007; Nozik et al., 2010; Durán-Toro et al., 2014; Nguyen et al., 2015; Wagner et al., 2019; Muthalif et al., 2019; Cotta, 2020).

Various approaches have been developed for QDs synthesis, including chemical, biological, and hybrid methods (Bajorowicz et al., 2018; Yang et al., 2017; Karimi et al., 2019; Mahle et al., 2020). Nevertheless, the biological synthesis or biosynthesis of QDs using microorganisms has emerged as a safe, cost effective, highly biocompatible, sustainable, and green alternative to classical production methods (Qin et al., 2018; Sekar

and Parvathi, 2019; Iravani and Varma, 2020; Khan and Lee, 2020). Bacterial biosynthesis of cadmium-based QDs has attracted growing interest due to their simplicity and the characteristic optical properties of the nanoparticles produced, becoming one of the most studied biosynthesis in recent years (Plaza et al., 2016; Ulloa et al., 2016; Yang et al., 2016; Oliva-Arancibia et al., 2017). The capacity to produce intra- and extracellular cadmium sulfide (CdS) nanoparticles has been reported in numerous bacterial genus such as *Klebsiella* (Holmes et al. 1997), *Rhodopseudomonas* (Bai et al. 2009), *Escherichia* (Mi et al. 2011; Venegas et al., 2017; Shivashankarappa and Konasur, 2020), *Stenotrophomonas* (Yang et al., 2015), *Acidithiobacillus* (Ulloa et al., 2016), *Halobacillus* (Bruna et al., 2019), *Idiomarina* (Ma et al., 2020), and *Pseudomonas* (Oliva-Arancibia et al., 2017; Gallardo et al., 2014; Plaza et al., 2016; Mahle et al., 2020; Gallardo-Benavente et al., 2019; Ashengroph et al., 2020), among others. However, despite the increasing knowledge generated during the last 10 years, the cellular mechanism involved in the biosynthesis of CdS QDs is still unknown. In general, the CdS QD biosynthesis involves cadmium ion (Cd^{2+}) addition into the system to react with sulfide anion (S^{2-}) generate by the bacterial metabolism to form nanoparticles (Bai et al., 2009a; Gallardo et al., 2014; Yang et al., 2016; Mahle et al., 2020).

Cadmium (Cd) is a heavy metal highly toxic for most organisms and with unknown cellular role. Cadmium toxicity in bacterial cells has been speculated to be associated with oxidative stress and damage to different cellular biomolecules such as lipids, proteins, and nucleic acids (Naz et al., 2005; Khan et al., 2015; Abbas et al., 2018; Abdelbary et al., 2019; Qin et al., 2019). Some bacteria have the ability to hydrogen sulfide (H_2S) generates to trap Cd and formed less toxic and insoluble metal-sulfide precipitates as a detoxifying strategy using cysteine desulfhydrase enzymatic activity (Holmes et al., 1997; Ma et al., 2020). This capacity has been widely explored and used

in the CdS nanoparticle biosynthesis during the last years (Bai et al., 2009b; Yang et al., 2015; Ulloa et al., 2016; Bruna et al., 2019; Ma et al., 2020). Biosynthesis methods described to date have been mainly associated with sulfur-containing molecules such as peptides, glutathione, cysteine, and H_2S (Monrás et al., 2012; Yang et al., 2016; Ma et al., 2020). To date, H_2S is the only volatile sulfur compound (VSCs) produced by bacterial related to QDs biosynthesis. However, the role of other VSCs such as dimethylsulfide (DMS), dimethyldisulfide (DMDS), and methanethiol (MeSH) (Schulz and Dickschat, 2007) produced from bacterial metabolism in CdS QDs biosynthesis has not been studied yet.

1.2 Hypothesis and research objectives

1.2.1 Hypothesis

Based on the previous background, we addressed the following hypothesis:

- The biosynthesis of CdS QDs by *Pseudomonas* spp. is favored by the production of other volatile organic sulfur compounds (VOSCs) than H_2S.

1.2.2 Research objectives

1.2.2.1 General objective

- To evaluate the role of volatile sulfur compounds (VSCs) released from *Pseudomonas* spp. in the biosynthesis of CdS QDs.

1.2.2.2 Specific objectives

1 To select the bacteria capable of producing CdS QDs under different sulfur sources.

2 To evaluate the VSCs production of the selected bacteria in presence and absence of cadmium through of the characterization of their volatiles profiles.

3 To identify the VSCs associated with the production of CdS QDs.

4 To propose a possible biosynthetic pathway of CdS QDs in bacteria by the action of VSCs.

CHAPTER II

Biosynthesis of CdS Quantum Dots Mediated by Volatile Sulfur Compounds Released by Antarctic Pseudomonas fragi

PUBLISHED

Gallardo-Benavente C., Carrión O., Todd J.D., Pieretti J.C., Seabra A.B, Durán N., Rubilar O., Pérez-Donoso J.M. and Quiroz A. 2019. Biosynthesis of CdS Quantum Dots Mediated by Volatile Sulfur Compounds Released by Antarctic *Pseudomonas fragi*. Front. Microbiol. 10:1866. doi: 10.3389/fmicb.2019.01866

Biosynthesis of CdS Quantum Dots Mediated by Volatile Sulfur Compounds Released by Antarctic *Pseudomonas fragi*

Carla Gallardo-Benavente[1,2], Ornella Carrión[3], Jonathan D. Todd[4], Joana C. Pieretti[5], Amedea B. Seabra[5], Nelson Durán[5,6], Olga Rubilar[2,7], José M. Pérez-Donoso[8]* and Andrés Quiroz[2,9]*

[1] Programa de Doctorado en Ciencias de Recursos Naturales, Universidad de La Frontera, Temuco, Chile.

[2] Centro de Excelencia en Investigación Biotecnológica Aplicada al Medio Ambiente (CIBAMA), Facultad de Ingeniería y Ciencias, Universidad de La Frontera, Temuco, Chile.

[3]School of Environmental Sciences, University of East Anglia, Norwich, United Kingdom.

[4]School of Biological Sciences, University of East Anglia, Norwich, United Kingdom.

[5]Centro de Ciencias Naturais e Humanas, Universidade Federal do ABC, Santo André, Brazil.

[6]Institute of Biology, Universidade Estadual de Campinas, Campinas, Brazil.

[7]Departamento de Ingeniería Química, Universidad de La Frontera, Temuco, Chile.

[8]BioNanotechnology and Microbiology Lab, Center for Bioinformatics and Integrative Biology, Facultad de Ciencias de la Vida, Universidad Andres Bello, Santiago, Chile.

[9]Departamento de Ciencias Químicas y Recursos Naturales, Facultad de Ingeniería y Ciencias, Universidad de La Frontera, Temuco, Chile.

*Corresponding author: jose.perez@unab.cl; andres.quiroz@ufrontera.cl

Abstract

Previously we reported the biosynthesis of intracellular cadmium sulfide quantum dots (CdS QDs) at low temperatures by the Antarctic strain *Pseudomonas fragi* GC01. Here we studied the role of volatile sulfur compounds (VSCs) in the biosynthesis of CdS QDs by *P. fragi* GC01. The biosynthesis of nanoparticles was evaluated in the presence of sulfate, sulfite, thiosulfate, sulfide, cysteine and methionine as sole sulfur sources. Intracellular biosynthesis occurred with all sulfur sources tested. However, extracellular biosynthesis was observed only in cultures amended with cysteine (Cys) and methionine (Met). Extracellular nanoparticles were characterized by dynamic light scattering, absorption and emission spectra, energy dispersive X-ray, atomic force microscopy, transmission electron microscopy, X-ray diffraction and X-ray photoelectron spectroscopy. Purified QDs correspond to cubic nanocrystals of CdS with sizes between 2 and 16 nm. The analysis of VSCs revealed that *P. fragi* GC01 produced hydrogen sulfide (H_2S), methanethiol (MeSH) and dimethyl sulfide (DMS) in the presence of sulfate, Met or Cys. Dimethyl disulfide (DMDS) was only detected in the presence of Met. Interestingly, MeSH was the main VSC produced in this condition. In addition, MeSH was the only VSC for which the concentration decreased in the presence of cadmium (Cd) of all the sulfur sources tested, suggesting that this gas interacts with Cd to form nanoparticles. The role of MeSH and DMS on Cds QDs biosynthesis was evaluated in two mutants of the Antarctic strain *Pseudomonas deceptionensis* $M1^T$: $megL^-$ (unable to produce MeSH from Met) and $mddA^-$ (unable to generate DMS from MeSH). No biosynthesis of QDs was observed in the $megL^-$ strain, confirming the importance of MeSH in QD biosynthesis. In addition, the production of QDs in the $mddA^-$ strain was not affected, indicating that DMS is not a substrate for the biosynthesis of nanoparticles. Here, we confirm a link between MeSH production and CdS QDs biosynthesis when Met

is used as sole sulfur source. This work represents the first report that directly associates the production of MeSH with the bacterial synthesis of QDs, thus revealing the importance of different VSCs in the biological generation of metal sulfide nanostructures.

Keywords: Antarctic bacteria, quantum dot, nanoparticle biosynthesis, volatile sulfur compounds, cadmium sulfide.

2.1 Introduction

Nanotechnology is the study, understanding, control and restructuring of matter in the scale of nanometers (size range 1 - 100 nm) to create materials with new properties and functions that remarkably differ from their bulk counterpart (Sanchez and Sobolev, 2010). Nanoscience research and its applications, developed in recent decades, has significantly affected a number of areas, such as information technology, agriculture, energy, environmental science, medicine and food safety, among others (Solomon, 2018). Consequently, there is a growing need to develop nanoparticles by using new, cheaper, reliable and eco-friendly synthesis methods that do not involve toxic chemicals. To achieve this, research on the use of natural sources such as biological systems becomes essential. Biological production or biosynthesis of metal nanoparticles has been widely studied through the use of microorganisms, such as fungi, yeast and bacteria (Wu et al., 2015; Chakraborty et al., 2018; Qin et al., 2018). Due to the convenience of this method, a cost-effective, environmentally friendly and highly biocompatible alternative based on the use of bacterial cells has emerged (Monrás et al., 2012).

Bacteria of the *Pseudomonas* genus have been employed as cell factories to produce different types of metal nanoparticles. In fact, several *Pseudomonas* strains have been reported to produce extracellular gold (Au) and silver (Ag) nanoparticles (Kumar and

Mamidyala, 2011; Baker et al., 2015; Ali et al., 2016; Jo et al., 2016). In addition, some *Pseudomonas* species can also synthesize a specific type of nanoparticles termed quantum dots (QDs) constituted of cadmium selenide (CdSe) (Ayano et al., 2015) or cadmium sulfide (CdS) (Oliva-Arancibia et al., 2017; Gallardo et al., 2014; Plaza et al., 2016).

Quantum dots (QDs) or semiconductor nanocrystals are bimetallic structures that generally contain II–VI or III–V elements such as CdS, CdSe, ZnS, ZnTe, CdTe, InP or GaAs (McHugh et al., 2018; Jadhav et al., 2017; Mal et al., 2016). The size and composition of the nanoparticles are responsible for their unique physical, chemical and optical properties, which arise through quantum confinement effect (Rengers et al., 2019; Alivisatos, 1996). The remarkable properties of QDs, such as broad absorption, narrow and size-dependent emission spectra, resistance to photobleaching, strong luminescence and long luminescent lifetimes (Zhou and Ghosh, 2007; Alivisatos, 1996) allow their use in a number of technology-based applications of high economic, technological and biological value as for example optoelectronics (Faraon et al., 2007), solar cells (Nozik et al., 2010), imaging techniques (Wagner et al., 2019) and quantification of different molecules (Durán-Toro et al., 2014; Nguyen et al., 2015), among others.

Bacterial biosynthesis of cadmium-based QDs has been extensively studied in the past few years through the biological production of both intra- and extracellular nanoparticles (Plaza et al., 2016; Ulloa et al., 2016; Yang et al., 2016; Oliva-Arancibia et al., 2017), as well as to study the development of other nanoparticles and the mechanisms associated with biosynthesis (Venegas et al., 2017). However, the mechanism involved in Cd-based QDs biosynthesis is still unknown. Overall, to carry out the biosynthesis of CdS nanoparticles, cadmium ion (Cd^{2+}) should be added into the system to react with sulfide anion (S^{2-}) provided exogenously or by the bacterial metabolism, in order to form the nanocrystal (Bai et al., 2009a; Gallardo et al., 2014; Yang et al., 2016).

Some bacteria are capable of releasing hydrogen sulfide (H_2S) as a strategy to trap exogenous cadmium (Cd) to form less toxic insoluble metal-sulfides (Holmes et al., 1997). This ability has been widely used in the biosynthesis of QDs during the last years (Bai et al., 2009b). In general, the biosynthesis of CdS QDs has been associated with sulfur-containing molecules such as glutathione, peptides, Cys and H_2S (Monrás et al., 2012; Yang et al., 2016). However, the role of other volatile sulfur compounds (VSCs) produced from bacterial metabolism in QDs biosynthesis, such as dimethylsulfide (DMS), dimethyldisulfide (DMDS) and methanethiol (MeSH) (Schulz and Dickschat, 2007), has not been studied yet.

Recently, intracellular biosynthesis of CdS QDs has been reported at low temperatures (15°C) using Antarctic bacteria from the *Pseudomonas* genus. Nanoparticles synthesis was performed in the presence of $CdCl_2$ without any additional sulfur sources. The mechanism of CdS formation was attributed to the production of sulfide from H_2S by Cys desulfhydrase in all strains tested except for *Pseudomonas fragi* GC01 strain (Gallardo et al., 2014). In this work, we study the link between the production of VSCs and the biosynthesis of CdS nanoparticles in *Pseudomonas fragi* GC01. We also carry out for the first time the biosynthesis of QDs in bacteria using Cys and Met as sole sulfur sources.

2.2 Material and Methods

2.2.1 Bacterial strains and culturing

Strains used in this work were *P. fragi* GC01 (Gallardo et al., 2014); *Pseudomonas deceptionensis* $M1^T$ wild type, *P. deceptionensis* $M1^T$ *megL*$^-$, *P. deceptionensis* $M1^T$ *mddA*$^-$ (Carrión et al., 2011, 2015). Bacterial strains were grown in Luria Bertani (LB;

complete) medium (Sambrook and Russell, 2001) for 24 h or in M9 (minimal) medium (Sambrook and Russell, 2001) for 48 h (stationary phase culture) at 28°C. *P. deceptionensis* $M1^T$ *megL* and *mddA* mutants were grown in media containing kanamycin (20 µg mL^{-1}) and spectinomycin (800 µg ml^{-1}), or gentamicin (5µg mL^{-1}), respectively.

2.2.2 Evaluation of CdS QDs biosynthesis

Nanoparticles biosynthesis by bacteria was performed following the protocol described by Monrás et al. (2012) and Gallardo et al. (2014). Briefly, bacteria were grown in M9 minimal medium supplemented with 0.25 mM of six different sulfur sources [sulfate ($MgSO_4$), sulfite (Na_2SO_3), thiosulfate ($Na_2O_3S_2$], sulfide (Na_2S), Met and Cys) for 48 h. Then, cultures were centrifuged at 10,000 rpm for 5 min (Himac CT15E centrifuge). Bacterial pellets were resuspended in $CdCl_2$ (10 µg mL^{-1}) and incubated at 28°C for another 48 h before assaying the production of nanoparticles. Nanoparticles formation was assessed using a short-wave UV-transilluminator at $\lambda_{excitation}$= 360 nm. Analysis were done with three biological replicates and samples with no $CdCl_2$ added were included as a control.

2.2.3 Sulfide detection assay

The production of H_2S was evaluated using lead acetate-soaked papers, as described by Shatalin et al. (2011). The assay was performed using 1 mL of bacterial cultures in microcentrifuge tubes and a lead acetate paper attached under the cap. Briefly, bacterial strains were grown on M9 minimal medium at 28°C until reaching an OD_{600}~ 0.8. Then, cultures were washed with fresh M9 medium with no sulfur sources. Bacterial pellets were resuspended and inoculated into M9 medium containing sulfate, sulfite, thiosulfate, sulfide, Met and Cys (0.5 mM) as sole sulfur sources in the presence or absence of $CdCl_2$ (10 µg mL^{-1}). Tubes were covered with a paper embedded in lead

acetate (100 mM) and incubated at 28°C for 2 h before detecting sulfides as described in Gallardo et al. (2014). Controls consisted of samples incubated with no sulfur sources.

2.2.4 Evaluation of extracellular biosynthesis of CdS QDs

The study of extracellular biosynthesis of nanoparticles was carried out following the protocol described by Monrás et al. (2012) and Gallardo et al. (2014) with some modifications. Briefly, cells were grown for 48 h in M9 medium at 28°C. Then, cultures were centrifuged at 10,000 rpm for 5 min (Himac CT15E centrifuge) and bacterial pellets were resuspended in fresh M9 medium supplemented with $CdCl_2$ (20 µg mL^{-1}) and a sulfur source such as Cys (0.1-2 mM), SO_4^{2-}, SO_3^{2-}, $S_2O_3^{2-}$ or Met (0.25-50 mM). After 0.5-2 h of incubation with Cys and 72 h with the others sulfur sources at 28°C, cells were centrifuged for 5 min at 10,000 rpm. Fluorescence of the supernatant was measured using a short-wave UV-transilluminator at $\lambda_{excitation}$= 360 nm. Cultures of bacterial strains were set up in triplicate and samples with no $CdCl_2$ were used as controls.

2.2.5 Purification of biosynthesized CdS nanoparticles

P. fragi GC01 was grown in M9 medium at 28°C in the presence of Cys (2 mM) or Met (40 mM) as sole sulfur sources to study the production of extracellular QDs. 10 mL of culture were taken after 1, 2 and 3 h incubation with Cys and after 72 h incubation with Met. Samples were then centrifuged 15 min at 6,000 rpm (PrO-Research K241R centrifuge) before collecting the fluorescent supernatants. Supernatants were filtered through 0.2 µm filters (BioLab) to remove cellular debris. Filtered supernatant was then concentrated to 100 µL using a 10 KDa membrane (Amicon). Concentrated nanoparticles suspension was lyophilized overnight and stored at 4°C until use.

2.2.6 Characterization of CdS nanoparticles

2.2.6.1 Absorption and fluorescence spectroscopy

Absorbance and fluorescence spectra of purified nanoparticles were determined with a multiplate reader Synergy H1 M (Biotek). Measurements were performed at room temperature and absorbance spectra were recorded in the range of 300 to 700 nm, whereas emission spectra were obtained using $\lambda_{excitation}$= 360 nm and recorded in the range of 390 to 700 nm (Gallardo et al., 2014; Plaza et al., 2016).

2.2.6.2 Quantum yield (QY) determination

The quantum yield (QY) of purified CdS QDs was determined following the protocol described by (Venegas et al., 2017; Bruna et al., 2019). Briefly, the fluorescence of 2 samples of QDs with different absorbances (between 0.01 and 0.1) was determined after excitation at 360 nm. The procedure was applied for yellow and red nanoparticles (obtained from Cys and Met, respectively) dissolved in water and as reference fluorescein dissolved in ethanol (QY = 0.97). Emission spectra were measured to obtain the integrated fluorescence intensity (IFI, is defined as the area of the fluorescence spectrum) and this value was plotted versus the absorbance of the solution. The slope of both curves (*m*) and the refractive index of the solvents (*n*) (water: 1.333 and ethanol: 1.335) were used to calculate the QY of CdS QDs considering fluorescein as reference (R). The following equation was used:

$$QY_{NPs} = QY_R[m_{NPs}/m_R][n^2{}_{NPs}/n^2{}_R]$$

2.2.6.3 Dynamic light scattering (DLS) measurements

The hydrodynamic size, zeta potential and polydispersity index (PDI, which is an indicative of size heterogeneity) were evaluated by dynamic light scattering (DLS) using

the Zetasizer Nano ZS (Malvern Instruments Co, UK). Polystyrene cuvettes with a path length of 10 mm at 25°C and a refraction index of 2.6 were used.

2.2.6.4 Atomic Force Microscopy (AFM)

Atomic force microscopy (AFM) images of nanoparticles were obtained using an AFM/SPM Series 5500 dynamics microscope (Agilent Technologies). Nanoparticles were measured using non-contact mode probe of 4 nm thickness, 125 μm in length, 30 μm frequency of 320 kHz resonance and a force constant of 42 N/m. Samples were 1/100 diluted and drop-casted over a silicon substrate before determining the average size of the nanoparticles at solid state using the WSxM 5.0 software, by automatically counting an average number of 40 particles per image for each CdS sample (Horcas et al., 2007).

2.2.6.5 Transmission Electron Microscopy (TEM)

The TEM analysis of nanoparticles was performed at the Center for the Development of Nanoscience and Nanotechnology (CEDENNA), using a HITACHI HT 7700 transmission electron microscope, operating with a Tungsten filament at an accelerating voltage of 120 kV, allowing a resolution of 0.2 nm. Samples (powder) were dispersed in distilled water using an ultrasonic bath and deposited on a copper TEM grid (200 mesh) coated with Formvar/carbon. Water was subsequently evaporated at room temperature.

2.2.6.6 Energy dispersive X-ray (EDX)

The elemental composition of the synthesized nanoparticles was determined with a scanning electron microscope (JSM-6010LA) operating with high vacuum, at an accelerating voltage of 20 kV and coupled to an energy-dispersive X-ray spectroscope (EDS, JEOL, JSM-6010LA).

2.2.6.7 X-ray diffraction (XRD)

X-ray diffraction (XRD) measurements were performed using a STADI-P (Stoe®, Darmstadt, Germany) diffractometer coupled to a Mythen 1K (Dectris®, Baden, Switzerland) detector that collected X-rays photons. Data were recorded at room temperature with powdered samples, in the 2θ range from 5.0° to 64.265°, 50 kV, 40 mA and using MoKα1 (λ = 0.7093 Å). Peaks were identified using published and standardized structures from Inorganic Crystal Structure Database (ICSD).

2.2.6.8 X-ray photoelectron spectroscopy (XPS)

X-ray photoelectron spectroscopy (XPS) measurements were performed using an X-ray photoelectron spectrometer (Thermo K-alpha spectromether, MA, USA) with a 72 W monochromated Al K-alpha^{+} source (E= 1486.6 eV) using 3000 eV, medium current, a spot size of 400 µm and 10 nm depth. Analyses were performed in two different points of powdered samples and the elemental composition was analysed using CasaXPS software.

2.2.7 Assays of microbial H_2S, MeSH, DMS and DMDS production

To measure H_2S, MeSH, DMS and DMDS production, *Pseudomonas* strains were grown overnight at 28°C in M9 minimal medium. Cultures were then adjusted to an OD_{600}=0.3 and diluted 10-fold into 2 mL vials containing 300 µL of M9 medium supplemented with 0.25, 0.5, 1, 2 and 4 mM sulfate, Cys and Met as sole sulfur sources. Samples were incubated at 28 °C for 48 h before measuring VSCs by gas chromatography using a flame photometric detector (Agilent 7890A GC fitted with a 7693 autosampler) and a HPINNOWax 30 m x 0.320 mm capillary column (Agilent Technologies J&W Scientific). An eight-point calibration curve of H_2S, MeSH, DMS and DMDS standards were used as described in Carrión et al. (2015). Protein content in the cells was determined

by the Bradford method (BioRad). Production of H_2S, MeSH, DMS and DMS was expressed as mmol per mg protein.

To estimate the production of VSCs under nanoparticles biosynthesis conditions, cells were adjusted to an OD_{600}=0.8 and inoculated into 300 µL of M9 medium supplemented with 2 mM sulfate, Cys or Met in the presence or absence of $CdCl_2$ (20 µg mL^{-1}). Samples were then incubated for 1, 24 and 48h at 28°C in 2 mL sealed vials before quantifying the VSCs produced by gas chromatography as above.

2.2.8 Data Analysis

Standard deviation (SD) of the results were expressed as mean (±). Statistical analysis of VSCs production was carried out using GraphPad Prism 6.0 (GraphPad Software, Inc.). Error bars represent SD (n=3). Student's t-test were performed considering $p < 0.05$. Statistical significance was indicated as follows: $*p < 0.05$, $**p < 0.01$ and $***p < 0.001$; ns, not significant.

2.3 Results

2.3.1 QDs biosynthesis and hydrogen sulfide production

P. fragi GC01 was able to use SO_4^{2-}, SO_3^{2-}, S^{2-}, $S_2O_3^{2-}$, Met and Cys as sole sulfur sources, although maximal growth was obtained with the former (data not shown). This suggests that these molecules could act as substrates to generate the S^{2-} required for the synthesis of CdS nanoparticles. To further investigate this hypothesis, the ability of *P. fragi* GC01 to biosynthesize CdS QDs from different S-containing molecules was evaluated. After 48 h exposure to biosynthetic conditions (0.25 mM sulfur source and 10 µg mL^{-1} $CdCl_2$), *P. fragi* GC01 cell pellets showed fluorescence when excited with UV

light (λ=360 nm) (Figure 1A). As previously reported, the generation of fluorescent pellets in cells exposed to Cd is an evidence of intracellular production of CdS QDs (Monrás et al., 2012; Gallardo et al., 2014; Plaza et al., 2016). A slightly fluorescent supernatant was only observed in presence of Cys, indicating that extracellular QDs biosynthesis occurred. Also, this result suggest that no VSCs involved in the extracellular production of CdS are generated by cells under the other conditions tested (Figure 1B).

In general, most biosynthesis methods described to date require sulfur-containing molecules with high affinity for Cd^{2+} such as antioxidant thiols or the VSC H_2S (Holmes et al., 1997;Bai et al., 2009; Monrás et al., 2012; Gallardo et al., 2014). However, as reported in our previous work, QDs biosynthesis by *P. fragi* GC01 on LB media was not directly related to the production of H_2S (Gallardo et al., 2014). Based on this, we studied the production of H_2S by *P. fragi* GC01 and obtained results revealed that no H_2S is generated when SO_4^{2-}, SO_3^{2-}, $S_2O_3^{2-}$, Met or Cys are used as sulfur sources (Figure 1C). As expected, H_2S was only observed when *P. fragi* GC01 cultures were exposed to S^{2-}, probably as consequence of the volatilization of sulfide from the medium as consequence of bacterial activity.

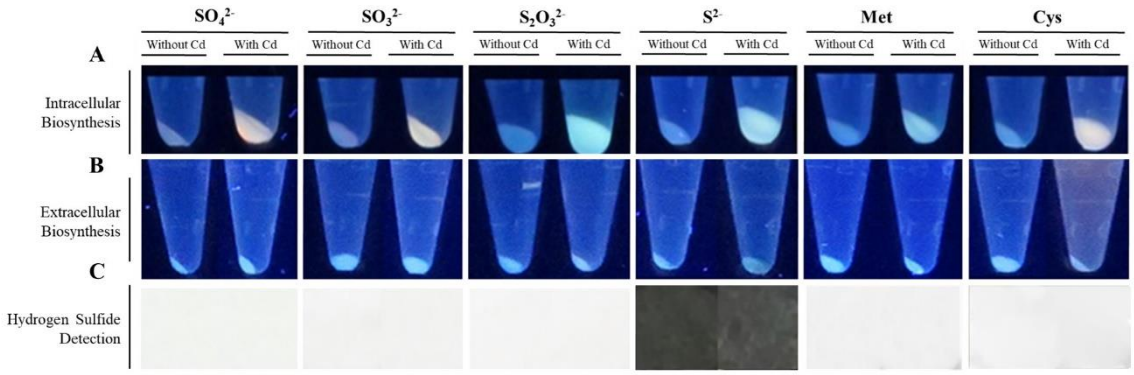

Figure 1. Biosynthesis of CdS QDs by *P. fragi* CG01 and hydrogen sulfide (H_2S) production in the presence of different sulfur sources at 28°C. (**A**) Fluorescence of

bacterial pellets exposed to biosynthesis conditions ($CdCl_2$ 10 µg mL^{-1}) using 0.25 mM SO_4^{2-}, SO_3^{2-}, $S_2O_3^{2-}$, S^{2-}, Met or Cys as sole sulfur sources after 48 h incubation. (**B**) Fluorescence of bacterial supernatant after UV light exposure. *P. fragi* CG01 was exposed to biosynthesis conditions with SO_4^{2-}, SO_3^{2-}, $S_2O_3^{2-}$, S^{2-}, Met or Cys as sole sulfur sources at 0.5 mM for 2 h. (**C**) Production of H_2S by *P. fragi* CG01 was observed as a dark precipitate on white papers treated with a lead acetate solution. Cells were grown with 0.5 mM of SO_4^{2-}, SO_3^{2-}, $S_2O_3^{2-}$, S^{2-}, Met or Cys as sole sulfur sources for 2 h in minimal medium, in the presence or absence of $CdCl_2$ (10 µg mL^{-1}).

2.3.2 Extracellular biosynthesis of CdS QDs

Based on the result obtained regarding the effect of Cys in the extracellular biosynthesis of CdS QDs by *P. fragi* GC01 (Figure 1B), we decided to evaluate new biosynthesis conditions. Extracellular biosynthesis of CdS QDs was observed in the presence of $CdCl_2$ (20 µg mL^{-1}) and Cys at concentrations ranging from 0.1 to 2 mM (Figure 2A). The intensity of the fluorescence in the supernatants indicated that the best condition for extracellular CdS QDs biosynthesis was 2 mM Cys and 20 µg mL^{-1} $CdCl_2$ (Figure 2A). Using this condition, we evaluated the biosynthesis of QDs by *P. fragi* GC01 at different times to study the generation of different emission colours, a unique characteristic of QDs associated with the time-dependent nanocrystal growth (Bruna et al., 2019; Ulloa et al., 2016; Venegas et al., 2017). Green, yellow and orange fluorescence colours were observed in culture supernatants of *P. fragi* GC01, confirming the extracellular generation of CdS QDs under this condition (Figure 2B).

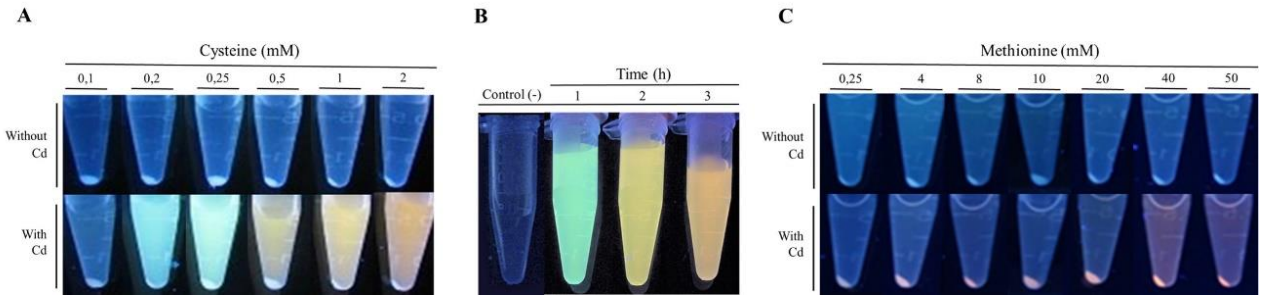

Figure 2. Fluorescence of *P. fragi* CG01 supernatants under biosynthesis conditions ($CdCl_2$ 20 µg mL^{-1}) after UV light exposure as indication of extracellular biosynthesis of Cds QDs. (**A**) Biosynthesis in minimal medium from various Cys concentrations in the presence or absence of $CdCl_2$ (20 µg mL^{-1}) after 2 h of incubation. (**B**) Fluorescence of bacterial supernatants of cells exposed to biosynthesis conditions (Cys 2 mM and $CdCl_2$ 20 µg mL^{-1}) at different incubation times. (**C**) Fluorescence of bacterial supernatant of *P. fragi* CG01 grown in minimal medium with various concentrations of Met in the presence or absence of $CdCl_2$ (20 µg mL^{-1}) for 72 h.

In addition, we evaluated the effect of SO_4^{2-}, SO_3^{2-}, $S_2O_3^{2-}$ or Met on the extracellular QDs biosynthesis by *P. fragi* GC01 in the presence of $CdCl_2$ (20 µg mL^{-1}) and using different concentrations of the S-sources (0.25-50 mM). Fluorescence was only observed in the supernatants of cultures incubated with 40 and 50 mM Met. Supernatants of these cultures were red after 72 h incubation (Figure 2C). However, fluorescent bacterial pellets were observed at all Met concentrations tested, suggesting the formation of intracellular QDs under these conditions (Figure 2C).

2.3.3 Characterization of biosynthesized CdS QDs

QDs produced in supernatants of *P. fragi* GC01 cultures exposed to Cys and Met were purified and characterized. Specifically, the stability (based on the zeta potential)

and the average hydrodynamic size of biosynthesized QDs was assessed by DLS. Biosynthesized QDs obtained with Cys had PDI values ranging from 0.50 to 0.53 and an average zeta potential (mean ± standard deviation) from -20.67 ± 0.64 mV to -15.70 ± 3.18, whereas nanoparticles synthesized using Met as sole sulfur source presented a PDI of 0.38 ± 0.04 and a zeta potential of -33.57 ± 2.76 mV. Moreover, the average nanocrystal size was below 36 nm in biosynthesis conditions with Cys (2 mM) and Met (40 mM) (Table 1).

Table 1. Particle size, PDI and Zeta potential of CdS QDs biosynthesized by *P. fragi* GC01 at different incubation times with cysteine (Cys) and after 72h incubation using methionine (Met) as sole sulfur source. Data are presented as mean ± standard deviation.

Nanoparticles	Particle Size (nm)	Polydispersity index (PDI)	Zeta Potential (mV)
Cys - 1h (green)	35.48 ± 4.96	0.53 ± 0.02	-15.70 ± 3.18
Cys - 2h (yellow)	24.40 ± 5.09	0.52 ± 0.01	-20.23 ± 3.94
Cys - 3h (orange)	27.39 ± 2.72	0.50 ± 0.05	-20.67 ± 0.64
Met - 72h (red)	27.71 ± 3.02	0.38 ± 0.04	-33.57 ± 2.76

In addition to the hydrodynamic size, a quantitative size analysis of the biosynthesized CdS QDs was implemented with atomic force microscopy (AFM) and transmission electron microscopy (TEM). The AFM topological images of nanoparticles synthesized with Cys and Met as sole sulfur source were analysed (Figure 3E, F). This technique allowed us to evaluate the average size of biosynthesized nanoparticles in solid-state. The average diameters of QDs produced in the presence of Cys were 28.45 ± 0.87 nm, 15.28 ± 1.26 nm and 17.04 ± 1.53 nm for green, yellow and orange nanoparticles respectively (Figure 3A, B, C), while the average diameter of QDs obtained with Met was

22.70 ± 0.73 nm (Figure 3D). The QDs with green fluorescence colour, corresponding to the nanoparticles obtained after 1 h of synthesis (Figure 3A) were larger than the rest of the QDs, despite being obtained in a shorter time of synthesis and their fluorescence colour corresponding to smaller nanoparticle sizes. This could be due to the high polydispersity index (PDI) of the biosynthesized nanoparticles (Table 1) probably as consequence of the organic cover, in addition to the low stability of the green nanoparticles, causing their agglomeration. TEM analysis of CdS nanoparticles revealed that the nanoparticles produced by *P. fragi* GC01 had a spherical-like morphology with a homogenous size distribution (Figure 4). TEM images determined that the average size of QDs produced in presence of Cys were 2.31 ± 0.51, 2.59 ± 0.71 and 2.59 ± 0.78 nm for green, yellow and orange fluorescent nanoparticles, respectively (Figure 4A, B, C). The diameter of QDs prepared with Met was ~ 16 nm, and showed the presence of planes, evincing the presence of a crystalline structure (Figure 4D). The small size of the nanoparticles obtained with Cys (~ 2 nm) did not show clear differences between green, yellow and orange nanoparticles. However, TEM analysis confirmed the formation of QD-type nanoparticles with a size below 20 nm (Rengers et al., 2019).

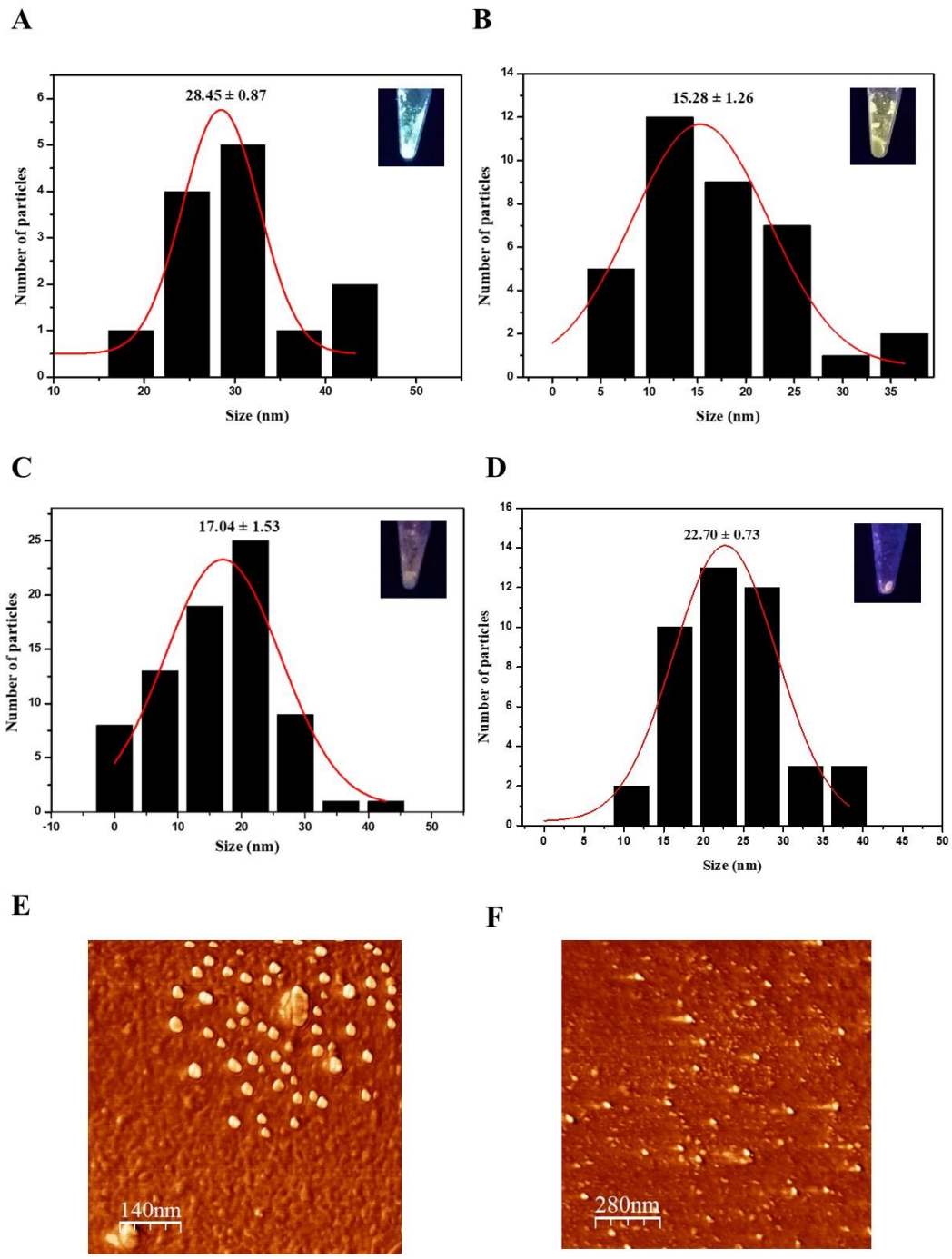

Figure 3. Characterization of CdS nanoparticles biosynthesized by *P. fragi* GC01 by AFM. AFM histogram of average solid-state size of nanoparticles synthesized from Cys showed (**A**) green, (**B**) yellow and (**C**) orange fluorescence. (**D**) AFM histogram of average solid-state size of nanoparticles synthesized with Met. 2D AFM topographical image of CdS nanoparticles synthesized with Cys for 3h (orange) (**E**) and Met after 72 h (**F**).

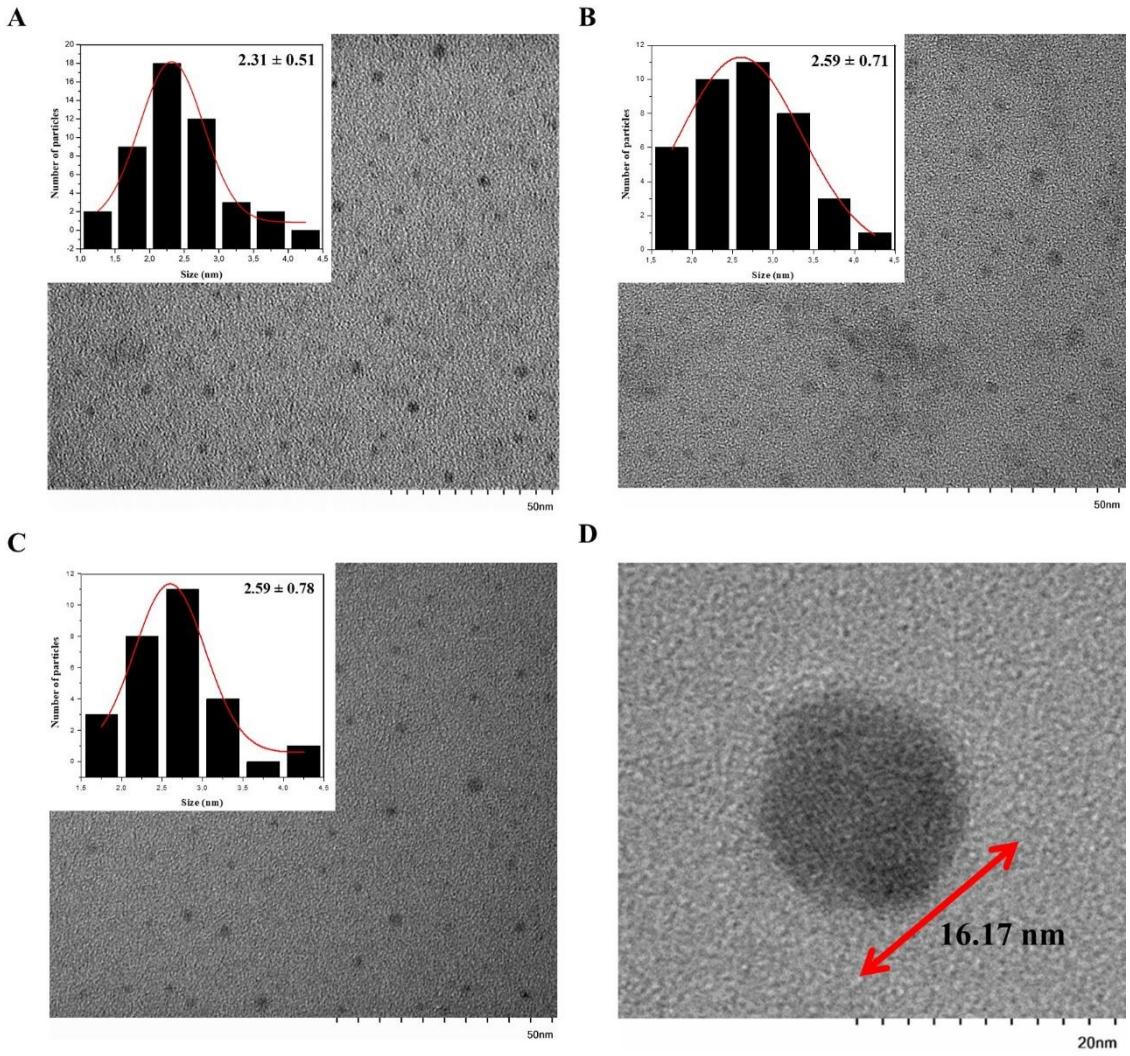

Figure 4. TEM image of CdS QDs biosynthesized with Cys or Met (inset: size histogram). QDs produced in presence of Cys and exhibiting (**A**) green (**B**) yellow and (**C**) orange fluorescence were evaluated. (**D**) CdS QDs biosynthesized with Met.

X-ray diffraction (XRD) measurements were performed to evaluate the crystal nature of CdS QDs. Figure 5A and 5B show the XRD patterns for CdS nanoparticles prepared with Cys and Met. Three characteristic peaks were observed at 12.85°, 21.06º and 32.69°, respectively (111, 220 and 311 planes, indexed as cubic CdS). Bai et al. (2009) obtained similar results for CdS nanoparticles synthesized by *Rhodobacter sphaeroides* and *Rhodopseudomonas palustris* (Bai et al., 2009b, 2009a). Additionally, defined peaks were observed for CdS nanoparticles obtained with Cys (Figure 5A).

Conversely, nanoparticles produced in the presence of Met displayed broader peaks, indicating defects in the crystal and a larger quantity of amorphous material, suggesting a thicker organic coating (Figure 5B). This could be consequence of high amounts of organic molecules attached to the nanoparticle surface, resulting in a crystal-amorphous interfacial effect (Muntaz Begum et al., 2016).

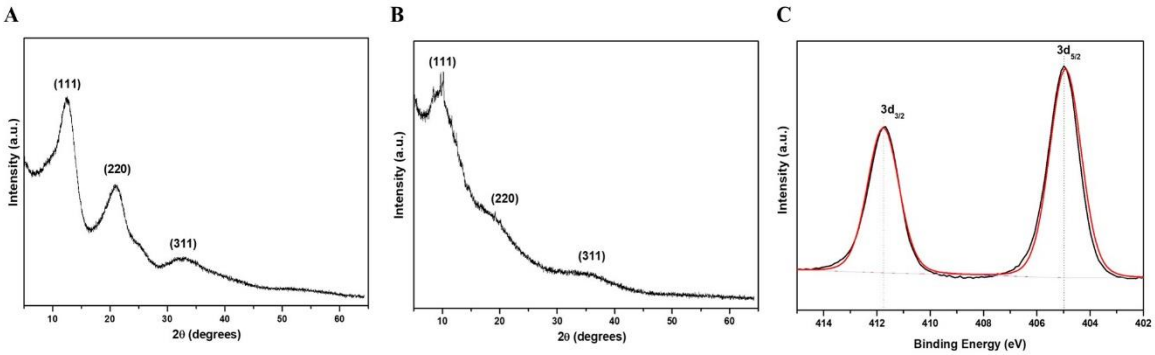

Figure 5. X-ray diffraction and X-ray photoelectron spectroscopy of QDs biosynthesized by *P. fragi* GC01. XRD pattern of CdS nanoparticles synthesized in cultures in the presence of (**A**) Cys and (**B**) Met as sole sulfur sources. (**C**) XPS spectra of Cd 3d region of CdS QDs obtained with Cys.

X-ray photoelectron spectroscopy (XPS) is a measurement of the surface of the sample, able to access only 10 nm depth. Spectra of CdS QDs produced from Cys and Met was evaluated with this technique. Survey spectra of CdS nanoparticles biosynthesized with Cys presented C 1s, Cd 3d, Na 1s, O 1s, P 2p and S 2p (Figure S1.1A). Cd 3d deconvoluted peaks (Figure 5C) indicated binding energies of 412 and 405 eV, corresponding to $Cd_{3/2}$ and $Cd_{5/2}$ as reported by Marusak et al., (2016) and Richards et al., (2016). Survey spectra of CdS obtained from Met contained similar elements, but it was not possible to identify Cd 3d peaks (Figure S1.1B). This is probably due to the

thick organic surface coating, which avoids Cd detection by XPS. Despite XPS did not allow the identification of Cd in QDs biosynthesized in presence of Met, XRD confirmed the formation of cubic CdS QDs and indicated the presence of amorphous coating on nanoparticles synthesised from Met (Figure 5B).

Spectroscopic properties of nanoparticles produced by *P. fragi* GC01 after 1 and 2 h of incubation under biosynthesis conditions with Cys (green and yellow nanoparticles, respectively) and after 72 h of incubation with Met (red nanoparticles), were evaluated. The absorbance spectra of the purified nanoparticles fractions showed a peak with maximum absorption at 360 nm for green nanoparticles, 370 nm for yellow nanoparticles and 380 nm for red nanoparticles (Figure 6A). This is in agreement with previous reports of biosynthesized CdS nanoparticles (Mi et al., 2011; Yang et al., 2015;Plaza et al., 2016; Bruna et al., 2019). Regarding the emission spectra of purified samples, emission peaks between 470-530 nm, 490-550 nm and 550-620 nm were determined for green, yellow and red nanoparticles respectively (Figure 6B). As expected, different emission spectra were observed for Cys green (1 h) and yellow (2 h) CdS QDs, with maximum fluorescence peaks at 500 and 530 nm, respectively (Figure 6B). Additionally, red nanoparticles (Met 72 h) showed an emission spectrum with maximum fluorescence peaks at 570 nm (Figure 6B). The quantum yields (QY) of the CdS QDs biosynthesized from Cys and Met was obtained by comparison with the QY of fluorescein in ethanol (standard). The quantum yield for the CdS QDs with Cys (2 h) and Met (72 h) were 21.04% and 7.81%, respectively.

The composition of biosynthesized nanoparticles was determined by EDS. QDs obtained after 3 h (orange) of biosynthesis with Cys (Figure S1.2) showed Cd and sulfur (S) elements signals. In addition, signals corresponding to oxygen (O) and carbon (C) were also detected, probably as part of the organic cover of QDs. It should be noted that

C signal could come from both the coating of the nanoparticle or from the carbon tape used in the SEM sample holder. This result was observed in all the nanoparticles biosynthesized in presence of Cys (Figure S1.2).

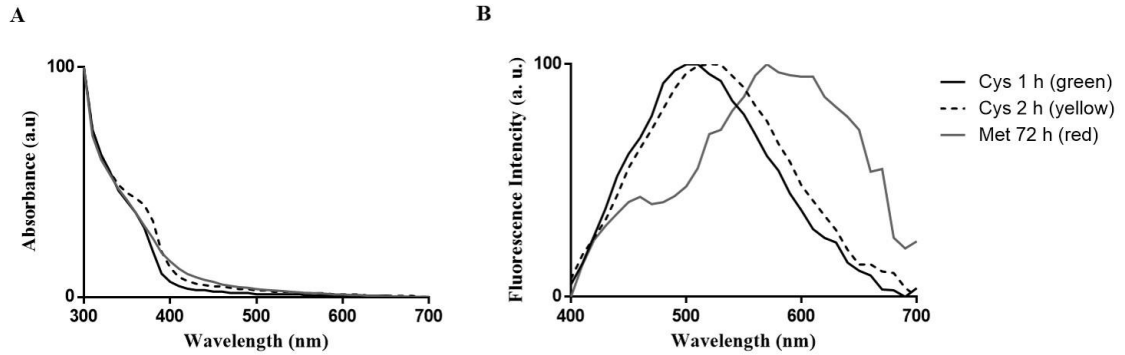

Figure 6. Optical properties of CdS QDs biosynthesized by *P. fragi* GC01. (**A**) UV-vis absorption spectra of purified QDs and (**B**) fluorescence emission spectra ($\lambda_{excitation}$= 360 nm).

2.3.4 Production of VSCs by *P. fragi* GC01

P. fragi GC01 was able to produce intracellular CdS QDs when grown on different sulfur compounds and extracellular QDs when Cys and Met were used as sole sulfur sources (see above). However, it was not possible to relate the formation of CdS nanoparticles to the production of H_2S under the conditions tested. Therefore, to elucidate the source of S^{-2} involved in QDs biosynthesis by *P. fragi* GC01, we analysed the VSCs produced by this strain. Specifically, the ability of *P. fragi* GC01 to release H_2S, MeSH, DMS and DMDS was evaluated when SO_4^{2-}, Cys or Met were used as sole sulfur source for bacterial growth and CdS biosynthesis. As shown in Figure 7A, *P. fragi* GC01 produced H_2S, MeSH and DMS in the presence of SO_4^{2-}, Cys and Met, with concentrations of MeSH between 2 to 600-fold and 6 to 28-fold higher than those of H_2S and DMS, respectively. Moreover, cells grown with sulfate or Cys produced low levels

of VSCs even at high concentrations of substrate (below 42 mmol per mg protein) (Figures 7A). Finally, maximal formation of DMS and MeSH was observed when Met was used as sole sulfur source (190 and 5400 mmol per mg protein) and this was the only condition in which DMDS was detected (Figure 7A).

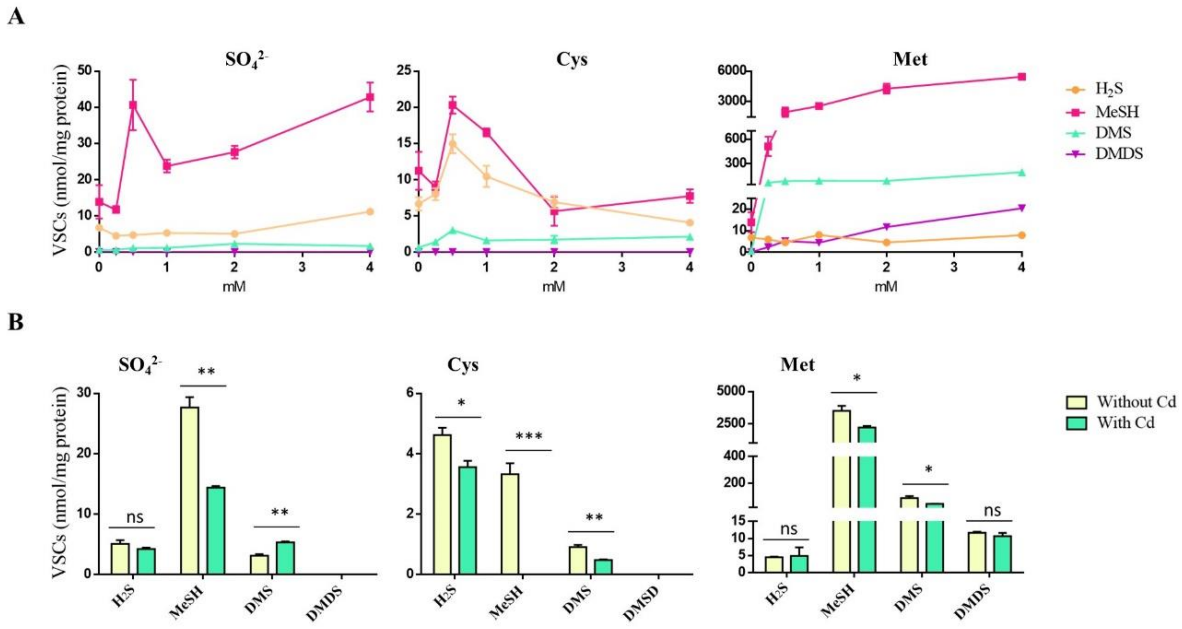

Figure 7. VSCs produced by *P. fragi* GC01 from SO_4^{2-}, Cys and Met under biosynthesis conditions (**A**) VSCs production from sulfur sources with concentrations ranging from 0 to 4 mM after 48 h of incubation. (**B**) VSCs production under biosynthesis conditions with different sulfur sources in the presence or absence of $CdCl_2$ (20 µg mL^{-1}) after 48 h. Results represent the average of three biological replicates with their respective standard deviations. Student's t-test ($P<0.05$): Comparison between treatments with and without cadmium (Cd). Statistically significant differences are shown as: ***$P < 0.001$, **$P < 0.01$, *$P < 0.05$.

The production of VSCs by *P. fragi* GC01 under QDs biosynthesis conditions (presence of sulfur source 2 mM and 20 µg mL^{-1} $CdCl_2$) after 48 h of incubation was also

tested (Figure 7B). This selection was based on the ability to biosynthesize extracellular QDs when this strain was supplemented with Cys (2 mM) after 1 h, and intracellular biosynthesis from Met and SO_4^{2-} (2 mM) after 48 h. Low levels of H_2S were determined in all sulfur sources analysed, and a decrease in H_2S was observed after Cd-exposure (biosynthesis conditions) when Cys was used as sulfur source (Figure 7B). MeSH production from all sulfur compounds decreased in presence of Cd, suggesting that this gas could be a source of S^{2-} that interacts with Cd^{2+}. In addition, DMS levels decreased in incubations with Cd and the sulfur sources Cys or Met. Finally, there were no statistically significant differences (ns, $P > 0.05$) in DMDS production were determined between treatments with and without Cd (Figure 7B). These results suggest that H_2S and MeSH are involved in the generation of CdS QDs providing directly or indirectly the S^{2-} that interacts with Cd^{2+} to form the nanocrystal seed.

2.3.5 VSCs catabolic pathways associated to biosynthesis of CdS QDs in *Pseudomonas deceptionensis*

P. deceptionensis $M1^T$ was used to study the possible relationship between nanoparticles biosynthesis and VSCs catabolism, since its genome has been sequenced and the pathways of DMS and MeSH production elucidated (Carrión et al., 2015). Specifically, Carrión et al. (2015) showed that MeSH was synthesized in this strain from Met in a reaction catalysed by methionine gamma lyase (encoded by *megL*). In turn, MeSH was converted into DMS via a methyltransferase termed MddA. *P. deceptionensis* $M1^T$ wild type, *P. deceptionensis* $M1^T$ *megL*$^-$ (unable to produce MeSH from Met) and *P. deceptionensis* $M1^T$ *mddA*$^-$ (unable to synthesize DMS from MeSH) (Carrión et al., 2015) were used to study the production of extra- and intracellular nanoparticles in the presence of Cys or Met, using the same conditions as in *P. fragi* GC01 (Cys or Met 2 mM and $CdCl_2$ 20 μg mL^{-1}). Extracellular biosynthesis was detected in the three *P. deceptionensis*

M1^T strains after 1 h incubation with Cys (Figure S1.3A). As expected, all the strains produced H_2S, although lower concentrations were observed in the presence of Cd^{2+} (Figure S1.3B). These results suggest that QDs production is mediated by H_2S as it has been reported in other bacterial strains (Bai et al., 2009a; Ulloa et al., 2016; Bruna et al., 2019). Finally, *P. deceptionensis* M1^T produced higher levels of H_2S than *P. fragi* GC01 (Figure S1.3B and Figure S1.3), a phenomenon that could be explained by the presence of Cys desulfhydrase, which converts Cys into H_2S.

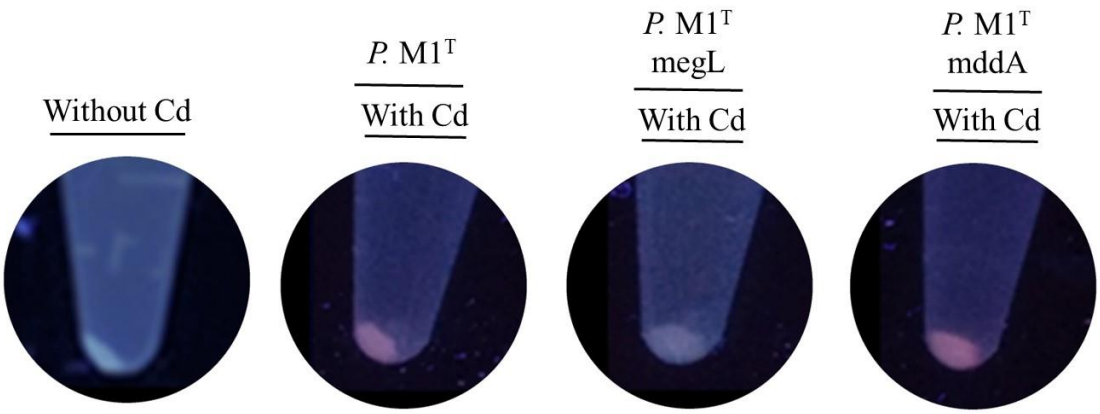

Figure 8. Biosynthesis of CdS QDs by *P. deceptionensis* M1^T strains in the presence of Met as sole sulfur source. Fluorescence of supernatants of *P. deceptionensis* M1^T strains under biosynthesis conditions after UV light exposure. Bacterial strains were grown in M9 medium with 2mM Met, in presence or absence of $CdCl_2$ 20 µg mL^{-1} for 48 h.

The results shown in Figure 8 suggest that QDs biosynthesis from Met is mainly associated to the production of MeSH in *P. deceptionensis* M1^T wild type and *mddA*$^-$ strains. In support of this hypothesis, *P. deceptionensis* M1^T *megL*$^-$, which does not produce MeSH from Met (Carrión et al., 2015), did not generate fluorescent nanoparticles or pellets under biosynthesis conditions (Figure 8). Finally, *P. deceptionensis* M1^T *mddA*$^-$, although does not synthetize DMS, was able to produce CdS QDs in the presence of Met, discarding DMS as a substrate for nanoparticle biosynthesis (Figure 8).

2.4 Discussion

The use of bacteria as cell factories to produce nanoparticles with great economic and technological value has increased in the past few years as a safe and eco-friendly alternative, but it also provides the possibility to manufacture nanoparticles with new properties and applications. In a previous work, we reported the use of different Antarctic *Pseudomonas* spp., resistant to oxidative stress, to biosynthesize CdS QDs (Gallardo et al., 2014). The synthesis of CdS QDs was intracellular and it was performed at low temperatures (15°C). However, it was not possible to associate the CdS nanoparticles biosynthesis in *P. fragi* GC01 to the use of sulfur-containing molecules with affinity to Cd as precursor to their biosynthesis, such as antioxidant thiols and volatile sulfur compounds as H_2S (Holmes et al., 1997;Bai et al., 2009; Monrás et al., 2012; Gallardo et al., 2014). Consequently, we decided to study the ability of *P. fragi* GC01 to use different sulfur sources to grow, to biosynthesize CdS QDs and to produce VSCs.

In this work, we study the link between CdS QDs biosynthesis and production of VSCs from different sulfur sources, focusing on Cys and Met, in *P. fragi* GC01. We showed that this strain can grow on a wide variety of sulfur sources such as sulfate, sulfite, sulfide, thiosulfate, Met and Cys, as well as produce intracellular nanoparticles from them. Sulfur is an essential element for cell growth, but it can only be assimilated as S^{2-} in its fully reduced state. The sulfur required by bacteria can be obtained in both inorganic and organic forms (Kertesz, 2001). Inorganic sulfate is the most abundant sulfur source in the environment and the main metabolic pathway by which bacteria assimilate this element (Kertesz, 2001). Sulfate assimilation occurs by active transportation of the substrate into the cell by an ABC-type transporter and is subsequently reduced to S^{2-} before being assimilated into organic material (Kertesz, 2000, 2004). However, bacteria can also use other inorganic sulfur sources to grow such as sulfite, thiosulfate and sulfide.

Sulfite and sulfide can enter the sulfate assimilation pathway, where sulfite is reduced to sulfide by the enzyme sulfite reductase (Kredich, 2008). Moreover, thiosulfate is incorporated into *Pseudomonas* cells through an ABC-type transporter for sulfate/thiosulfate (Kertesz, 2004) and can be assimilated after being reduced to sulfide by the enzyme thiosulfate reductase (Barton et al., 2017). In addition, Cys can be assimilated directly by bacteria via a transsulfuration pathway with subsequent formation of Met, or can be used by cysteine desulfhydrase to produce sulfide (Awano et al., 2003, 2005). Finally, Met can be used as sole sulfur source by some bacteria. Met may be provided to the cells by desulfurization to yield inorganic sulfate or by a reverse transsulfuration pathway, which converts Met to Cys. This pathway has been reported in bacteria from the *Pseudomonas* genus (Vermeij and Kertesz, 1999).

In the study of the intracellular biosynthesis of CdS nanoparticles from different sulfur sources by *P. fragi* GC01, Cd^{+2} was exogenously provided as a substrate, with bacterial metabolism being responsible for providing the S^{-2} needed for the formation of CdS QDs. However, several metabolic pathways can be involved in the synthesis of CdS QDs through the generation of S^{-2}, due to its incorporation into organic material as the final product of sulfur assimilation metabolism in bacteria (Kertesz, 2001, 2004; Awano et al., 2005; Kredich, 2008; Barton et al., 2017). No H_2S was produced by *P. fragi* GC01 at detectable levels under any condition tested. Although H_2S could be formed at concentrations below of detection limit, it is also possible that the absence of this VSC in *P. fragi* GC01 samples could be due to the lack or reduced activity of enzymes involved in the reduction of sulfur compounds to sulfide.

Conversely, extracellular biosynthesis of CdS QDs was only observed when Cys and Met were used as sole sulfur sources. The nanoparticles obtained with Cys showed several fluorescent colours of the supernatants (between green and orange) depending on

the incubation time and Cys concentrations. This optical property is a unique and characteristic phenomenon of QDs, which emit different colours of fluorescence according to the nanocrystal size (Yang et al., 2016; Ulloa et al., 2018; Bruna et al., 2019). Nevertheless, the optical properties of fluorescence emission also can be affected by the surface defects decorating the nanoparticles as has been reported by Bruna et al. (2019) in the biosynthesis of QDs of CdS by halophilic bacteria. Additionally, bacterial supernatants incubated with Met showed red fluorescence, the colour of which did not vary over time. This observation strongly suggests that the nanoparticles produced by the extracellular biosynthesis of CdS QDs, when using Met as the sole sulfur source, could have different properties from the nanoparticles produced from Cys either because the S^{2-} as precursor of the QDs biosynthesis could be provided by different bacterial metabolic pathways or because other reduced sulfur anions are involved in CdS QDs biosynthesis when interacting with Cd.

Therefore, in this study we have established that *P. fragi* GC01 biosynthesize CdS QDs from Cys and Met through several characterization methods. CdS nanoparticles produced by this Antarctic strain showed a zeta potential value (lower than -20 mV) indicative of high stability in aqueous solutions, with nanocrystals produced with Met being the most stable (Kuznetsova and Rempel, 2015). The average size of the nanoparticles produced with Cys (~ 2 nm) and Met (~ 16 nm), determined from TEM images, were consistent with the size of QDs biosynthesized by other microorganisms (Bruna et al., 2019; Wang et al., 2018; Al-Shalabi and Doran, 2016; Tandon and Vats, 2016; Wu et al., 2015; Syed and Ahmad, 2013; Chen et al., 2009; Khachatryan et al., 2009). TEM as a technique for characterizing nanomaterials enables the visualization of the shape and size of the nanoparticles by providing direct images of nanomaterials at a spatial resolution (Lina et al., 2014). The results obtained with TEM showed mainly the

diameter of the core (Kale et al., 2013), which explains the great discrepancy in the particle sizes observed between TEM (size < 17 nm), AFM (size in the range of 15 -29 nm) and DLS (size in the range of 24 -36 nm), because the latter two techniques might be considering the organic layer of the nanoparticles as well as presenting a greater aggregation of particles in the samples. In this context, the average hydrodynamic size of the nanoparticles estimated by DLS was larger than in AFM. DLS is based on the particle behavior in aqueous medium and hydrodynamic size is measured through Brownian motion, which considers both the size of the particle and the solvation layer, resulting in larger average diameters. On the other hand, AFM is commonly used to determine particle size distribution in solid state by the interaction between the sample and tip, where the tip is either repelled or attracted. Thus, AFM average diameter tends to present lower values when compared to DLS, as it represents only the particle size and does not consider the solvating layer (Hoo et al., 2008). The elemental analysis, the crystalline shape and surface composition of the nanoparticles by EDS, XRD and XPS confirm the formation of CdS QDs. Specifically, EDS analysis of the nanoparticles obtained from Cys showed signals associated to Cd and S elements, while the XRD taken from the nanoparticles synthesized from Cys and Met as sole sulfur source, indicated the formation of cubic nanocrystals of CdS, which are related to the diffraction of the crystalline planes (111), (220) and (311). The same XRD pattern has been reported for the CdS QDs obtained via chemical (Waly et al., 2017; Bharti et al., 2018; Wang et al., 2018) and biological synthesis (Sankhla et al., 2016; Chakraborty et al., 2018). XPS analysis was developed in the 1960 by Siegbanh's research group and, since then, it has been widely used to determine the chemical composition and state of elements present on a sample surface (Siegbahn et al., 1967). To perform the measurements, an external X-ray beam is injected, commonly reaching 10 nm depth on the sample. The incident X-ray is able to eject

electrons from core levels (1s, 2s, 2p…) and these photoelectrons have characteristic Kinect energies, which enables the differentiation of each element and their respective chemical state (Baer and Engelhard, 2010). In this work, the XPS analysis was carried out to study the surface composition of the nanocrystals. The XPS analysis of the surface composition of the nanocrystals produced with Cys and Met, presented signals in the C 1s, Cd 3d, Na 1s, O 1s, P 2p and S 2p region. The presence of N and S suggest that Cys and Met are part of the organic coating of the QDs surface, indicating that these sulfur compounds could be stabilising the QDs. The Cd 3d spectrum deconvoluted peaks indicated binding energies of 412 and 405 eV, corresponding to $Cd_{3/2}$ and $Cd_{5/2}$ respectively (Marusak et al., 2016; Richards et al., 2016). Furthermore, the intensity ratio of $Cd_{3/2}$ and $Cd_{5/2}$ peaks was 2:3, confirming that Cd was obtained in the state of Cd^{2+}, which is in accordance to what it has been previously reported for CdS QDs (Bag et al., 2017). It was not possible to identify the Cd 3d peaks in the spectra of CdS QDs produced using Met, despite similar elements have been observed on the surface composition of the nanocrystals. This could be due to the different organic compounds of a thick (> 10 nm) surface coating of the nanoparticle produced with Met, whereby, the Cd may not be detected in this technique. Additionally, the presence of an amorphous coating on the nanoparticles obtained with Met was also determined by XRD (Muntaz Begum et al., 2016), technique that confirmed the formation of cubic CdS QDs.

The absorbance spectra of green and yellow CdS nanoparticles produced with Cys and red nanoparticles from Met synthesized by *P. fragi* GC01 showed peaks at 360, 370 nm and 380, respectively. This is in agreement with the typical characteristic of CdS QDs, a plasmon resonance absorption with maximum absorption below 400 nm (Liu et al., 2014), in comparison with the absorption of bulk CdS nanoparticles at 515 nm (Song et al., 2014). The corresponding fluorescence emission peaks were observed at 500, 530 and

570 nm for green, yellow and red nanoparticles, respectively. Both peaks (absorbance and fluorescence) of QDs obtained from Cys progressively shifted to longer wavelengths over time, changing from green (1 h) to yellow (2 h) fluorescence colour. This phenomenon can be explained by the different sizes of the purified nanoparticles (Yang et al., 2015;Dunleavy et al., 2016). The absorbance and fluorescence properties are in agreement with previous reports of biological synthesis of CdS nanoparticles, were the nanoparticles display maximal absorbance peaks between 360-380 nm and fluorescence emission peaks between 470-600 nm (Gallardo et al., 2014; Yang et al., 2015; Dunleavy et al., 2016; Plaza et al., 2016; Ulloa et al., 2016; Venegas et al., 2017; Glatstein et al., 2018). In addition, the quantum yield for both nanoparticles solutions obtained from Cys (yellow) and Met (red) were of 21.04% and 7.81%, respectively. Interestingly, a high quantum yield (21.04%) was determined in QDs produced from Cys (Venegas et al., 2017; Bruna et al., 2019) in comparison to those generated from biosynthesis with Met. These results could be due to the size differences observed beween nanoparticles where the nanoparticles obtained from Cys (yellow) have a size of ~ 2 nm and the nanoparticles from Met (red) have a size of ~ 16 nm. Nevertheless, quantum yield (7.81%) determined in QDs produced from Met are high when compared other reported biological syntheses (Yang et al., 2015; Jang et al., 2015; Al-Shalabi and Doran, 2016).

In this study, we have also shown that *P. fragi* GC01 can produce H_2S, MeSH and DMS in presence of SO_4^{2-}, Cys and Met. However, DMDS was only detected when Met was used as sole sulfur source. It has been reported that many bacterial strains from different environments can release VSCs such as H_2S, MeSH, DMS, DMDS among others, as a result of a sulfur assimilation process involved in the synthesis of amino acids or from biological degradation of sulfur-containing compounds (Lomans et al., 2002; Schulz and Dickschat, 2007; Korpi et al., 2009). Specifically, Met yielded the highest

concentrations of MeSH and DMS, although generated low concentrations of DMDS and H_2S. MeSH is the main VSCs released by *P. fragi* GC01 from all sulfur sources tested. Met has been described as a major precursor of VSCs biosynthesis, especially of MeSH (Vermeij and Kertesz, 1999; Lu et al., 2013; Carrión et al., 2015), which, in turn, is a precursor of DMS and DMDS (Lu et al., 2013). The formation of MeSH from Met is catalyzed by methionine ɣ-lyase (Vermeij and Kertesz, 1999). Additionally, MeSH can be produced by methylation of H_2S in a reaction catalyzed by a thiol S-methyltransferase enzyme. On the other hand, the production of DMS by methylation of MeSH is mediated by the methyltransferase MddA, which uses S-adenosyl-L-methionine (Ado-Met) as methyl donor (Carrión et al., 2015). However, DMDS can be produced by chemical oxidation of MeSH (Chin and Lindsay, 1994; Lu et al., 2013). Besides, Cys has been described as the main precursor of H_2S, through a reaction catalyzed mainly by Cys desulfhydrase (Awano et al., 2003, 2005). Additionally, Cys can be incorporated into the cell directly via trans-sulfuration to form Met, which in turn is the precursor of the rest of the volatiles detected (Vermeij and Kertesz, 1999). When SO_4^{2-} is used as sole sulfur source, it is reduced to sulfide (S^{-2}), which leads to the production of Cys and Met (Kertesz, 2004).

VSCs production by *P. fragi* GC01 under biosynthesis conditions (presence of Cd^{+2}) with Cys and Met was tested. The main results obtained showed a significant statistical decrease of H_2S between the treatment with and without Cd in presence of Cys ($P < 0.05$). By the other hand, the production of MeSH significatively decreased when Cd^{+2} ($CdCl_2$) was added in presence of all sulfur sources tested ($P< 0.05$). Although the production of several VSCs has been reported in bacteria, only H_2S has been associated with the biosynthesis of CdS nanoparticles (Bai et al., 2009a; Gallardo et al., 2014; Yang et al., 2016). The production of VSCs by *P. fragi* GC01 under biosynthesis conditions

showed higher H_2S and MeSH production from Cys and Met. In addition, a statistically significant reduction of both VSCs ($P < 0.05$) was observed when samples were treated with Cd. Decreased H_2S production in the Cd treatment suggests that the production of QDs is mediated by H_2S, as it has been previously reported in other bacteria (Bai et al., 2009a; Yang et al., 2015). In general, different authors have suggested that the mechanism of cadmium-based nanoparticles formation was the generation of H_2S (as sulfide source) from Cys in a reaction mediated by Cys desulfhydrase (Bai et al., 2009a; Holmes et al., 1997) or cystathionine γ-lyase (Dunleavy et al., 2016). Both enzymes catalyze the formation of pyruvate, ammonia and hydrogen sulfide from Cys. Therefore, the fluorescence in the bacterial supernatant indicated extracellular CdS QDs formation by the reaction of Cd^{2+} added into the system with S^{2-} provided by the bacterial metabolism, likely through the H_2S production as a result of enzymatic degradation of Cys (Bai et al., 2009a; Yang et al., 2016). In addition to be a sulfur source, the amino acid Cys could also act as a capping agent in CdS nanoparticles formation (Dunleavy et al., 2016).

The importance of Met in biosynthesis of CdS QDs and the role of VSCs catabolic pathways was studied using different strains of *P. deceptionensis* $M1^T$. Carrión et al. (2015) described a novel pathway of DMS production from MeSH, which in turn is a product of Met catabolism. Intracellular biosynthesis of CdS QDs was observed in all *P. deceptionensis* $M1^T$ strains except for *P. deceptionensis* $M1^T$ *megL*$^-$, which cannot form MeSH from Met. In addition, the fact that *deceptionensis* $M1^T$ *mddA*$^-$ was able to synthesize nanoparticles, discards DMS as a substrate in this process, since this strain cannot produce DMS from MeSH. These results strongly suggest that MeSH could act as a source of S^{2-} to synthesize CdS QDs when Met is added to the medium as sole sulfur source.

2.5 Conclusion

In conclusion, here we establish that *P. fragi* GC01 is able to biosynthesize extracellular CdS QDs in the presence of the amino acids Cys and Met. The bioproduction of these nanoparticles is linked to the ability of this strain to form the volatile sulfur compounds H_2S and MeSH from Cys and Met, respectively. Both VSCs produced by *P. fragi* GC01 act as a source of S^{2-} in the biosynthesis of CdS QDs. Interestingly, the biosynthesis of Cd-based nanoparticles from Met has not been previously described, nor the participation of volatile organic compounds such as MeSH in the biosynthesis process. Therefore, this study constitutes the first report correlating the production of the VSC MeSH and the biosynthesis of CdS QDs.

Conflict of Interest

The authors declare that this research was conducted in the absence of any commercial or financial relationships that could be construed as a potential conflict of interest.

Author Contributions

CG-B, JP-D, and AQ: conceived and designed the study; CG-B: performed the experiments; JCP: contributed to performed the experiments of characterization of nanoparticles; JCP, ABS, ND and OR; analyzed the data and discussion regarding the characterization of nanoparticles. OC and JDT; designed, analyzed the data and discussion regarding the Volatile Sulfur Compounds. CG-B, JP-D and AQ: analyzed the data and prepared the manuscript. All authors commented on or contributed to the manuscript.

Funding

This work was supported by CONICYT scholarship 21151066 (CG-B), Fondecyt 1151255 (JMP-D), Fondecyt 1181697, INACH DT_05_16 (CG-B, AQ), INACH RT-25_16 (JMP-D), FAPESP (2018/08194-2 and 2018/02832-7) and CNPq (404815/2018-9). Funding from the Natural Environment Research Council (NE/M004449) supported OC and JDT work.

Acknowledgments

We thank Dr. Elena Mercade from University of Barcelona for kindly providing *Pseudomonas deceptionensis* $M1^T$ wild type strain.

CHAPTER III

Genomics Insights on Pseudomonas sp. CG01: an Antarctic Cadmium Resistant Strain Capable to Biosynthesize CdS Nanoparticles using Methionine as S-source

PUBLISHED

Gallardo-Benavente C., Campo-Giraldo J.L., Castro-Severyn J., Quiroz A. and Pérez-Donoso J.M. 2021. Genomics Insights on *Pseudomonas* sp. CG01: an Antarctic Cadmium Resistant Strain Capable to Biosynthesize CdS Nanoparticles using Methionine as S-source. Genes (MDPI). 12: 187. doi: 10.3390/genes12020187

Genomics Insights on *Pseudomonas* sp. CG01: an Antarctic Cadmium Resistant Strain Capable to Biosynthesize CdS Nanoparticles using Methionine as S-source

Carla Gallardo-Benavente[1,2], Jessica L. Campo-Giraldo[3], Juan Castro-Severyn[4], Andrés Quiroz[2,5]* and José M. Pérez-Donoso [3*]

[1] Programa de Doctorado en Ciencias de Recursos Naturales, Universidad de La Frontera, Temuco, Chile.

[2] Centro de Excelencia en Investigación Biotecnológica Aplicada al Medio Ambiente (CIBAMA), Facultad de Ingeniería y Ciencias, Universidad de La Frontera, Temuco, Chile.

[3] BioNanotechnology and Microbiology Lab, Center for Bioinformatics and Integrative Biology, Facultad de Ciencias de la Vida, Universidad Andres Bello, Santiago, Chile.

[4] Laboratorio de Microbiología Aplicada y Extremófilos, Facultad de Ingeniería y Ciencias Geológicas, Universidad Católica del Norte, Antofagasta, Chile.

[5] Departamento de Ciencias Químicas y Recursos Naturales, Facultad de Ingeniería y Ciencias, Universidad de La Frontera, Temuco, Chile.

* Correspondence: andres.quiroz@ufrontera.cl (A.Q.); jose.perez@unab.cl (J.M.P.-D.)

Abstract

Here, we present the draft genome sequence of *Pseudomonas* sp. GC01, a cadmium-resistant Antarctic bacterium capable of biosynthesizing CdS fluorescent nanoparticles (quantum dots, QDs) employing a unique mechanism involving the production of methanethiol (MeSH) from methionine (Met). To explore the molecular/metabolic components involved in QDs biosynthesis, we conducted a comparative genomic analysis, searching for the genes related to cadmium resistance and sulfur metabolic pathways. The genome of *Pseudomonas* sp. GC01 has a 4,706,645 bp size with a 58.61% G+C content. *Pseudomonas* sp. GC01 possesses five genes related to cadmium transport/resistance, with three P-type ATPases (*cadA*, *zntA*, and *pbrA*) involved in Cd-secretion that could contribute to the extracellular biosynthesis of CdS QDs. Furthermore, it exhibits genes involved in sulfate assimilation, cysteine/methionine synthesis, and volatile sulfur compounds catabolic pathways. Regarding MeSH production from Met, *Pseudomonas* sp. GC01 lacks the genes *E4.4.1.11* and *megL* for MeSH generation. Interestingly, despite the absence of these genes, *Pseudomonas* sp. GC01 produces high levels of MeSH. This is probably associated with the *metC* gene that also produces MeSH from Met in bacteria. This work is the first report of the potential genes involved in Cd resistance, sulfur metabolism, and the process of MeSH-dependent CdS QDs bioproduction in *Pseudomonas* spp. strains.

Keywords: Antarctic bacteria; nanoparticle biosynthesis; comparative genomics; volatile sulfur compounds.

3.1 Introduction

Antarctica is one of the most extreme ecosystems for the development of life on earth (Cary et al., 2010). The harsh conditions that characterize this environment include; low temperatures, high dehydration rates, high radiation, and low nutrients availability (Wasley et al., 2006). However, many microorganisms have adapted to colonize this environment by developing unique strategies to survive under these conditions. Because of this, the Antarctic continent is of great interest as a source of biodiversity and, therefore, of new biotechnological and bioactive compounds, such as enzymes, proteins, and secondary metabolites (Nichols et al., 2002; Romoli et al., 2011; Papaleo et al., 2012). In this context, the use of Antarctic microorganisms as bio-factories for the production of metal-based nanocrystals or quantum dots (QDs) has been explored during the last years (Gallardo et al., 2014; Plaza et al., 2016; Gallardo-Benavente et al., 2019).

QDs are fluorescent semiconductor nanoparticles generally composed of CdS, CdSe, ZnS, ZnTe, CdTe, InP, $CuInS_2$, or GaAs, with size below 20 nm (Mal et al., 2016; Jadhav et al., 2017; McHugh et al., 2018; Rengers et al., 2019). These nanoparticles exhibit outstanding characteristics, including broad absorption, size-dependent emission color, narrow emission profile, resistance to photobleaching, strong luminescence, and long luminescent lifetimes (Alivisatos, 1996; Zhou and Ghosh, 2007; Rengers et al., 2019). Remarkable properties of QDs are associated with the size and composition of nanocrystals (McHugh et al., 2018; Rengers et al., 2019). They can be effectively tapped for several applications like imaging techniques (Wagner et al., 2019), solar cells (Nozik et al., 2010; Muthalif et al., 2019), optoelectronics (Faraon et al., 2007), and quantification of different molecules (Durán-Toro et al., 2014; Nguyen et al., 2015), among others.

The biosynthesis or biological production of QDs using microorganisms has emerged as an eco-friendly, cost effective, and highly biocompatible alternative (Monrás et al., 2012; Qin et al., 2018). Bacterial biosynthesis of cadmium-based QDs has been extensively studied during the last years because of their simplicity and the distinctive optical properties of the nanoparticles produced (Plaza et al., 2016; Ulloa et al., 2016; Yang et al., 2016; Oliva-Arancibia et al., 2017). Most biosynthesis methods described to date have been associated with sulfur-containing molecules such as peptides, antioxidant thiols, and hydrogen sulfide (H_2S). In general, H_2S has been reported as a source of sulfide anion (S^{2-}) that interacts with cadmium ion (Cd^{2+}) for the formation of CdS QDs (Holmes et al., 1997; Bai et al., 2009b; Monrás et al., 2012; Yang et al., 2016). Nevertheless, despite the knowledge generated during the last years, the mechanism involved in CdS nanoparticle biosynthesis is still unclear.

Pseudomonas is a genus of bacteria known for its metabolic versatility and capacity to inhabit a wide range of environments, including the Antarctica (Kim and Park, 2014; Peix et al., 2018; Ali et al. 2019). Recent research has reported that Antarctic bacteria from the *Pseudomonas* genus can biosynthesize CdS nanoparticles at low temperatures (15 ºC) (Gallardo et al., 2014). *Pseudomonas sp.* GC01, previously reported as *Pseudomonas fragi* GC01 (Gallardo et al., 2014), is a psychrotolerant bacterial strain isolated from Deception Island (South Shetland archipelago, Antarctica), highly resistant to cadmium (Minimal inhibitory concentration [MIC] 1.8 mM CdCl2), and with the ability to biosynthesize CdS QDs (Gallardo et al., 2014; Gallardo-Benavente et al., 2019). *Pseudomonas* sp. GC01 strain can biosynthesize QDs inside cells in the presence of sulfate, sulfite, thiosulfate, cysteine (Cys), and methionine (Met) as sole sulfur sources. On the other hand, extracellular biosynthesis of CdS QDs only occurs in the presence of Cys and Met. Interestingly, this bacterium biosynthesizes CdS QDs through a novel

mechanism that use methanethiol (MeSH) instead of H_2S as a sulfur source for nanocrystal formation (Gallardo-Benavente et al., 2019). In this work, we studied the genome of *Pseudomonas* sp. GC01 to understand the molecular and metabolic components involved in their unique mechanism to biosynthesize CdS QDs through a comparative genomic analysis.

3.2 Material and methods

3.2.1 Bacterial isolation and growth conditions

The *Pseudomonas* sp. GC01 strain used in this work was isolated from a soil sample obtained from Deception Island in the South Shetland archipelago, Antarctica (S62◦58006.2" W60◦42032.5"), during the 48th Chilean Antarctic Expedition (ECA) organized by the Chilean Antarctic Institute (INACH), and previously identified as *Pseudomonas fragi* GC01 (Gallardo et al., 2014). The cells were grown in Luria Bertani (LB) medium (Sambrook and Russell, 2001) at 15°C.

3.2.2 DNA extraction, sequencing and assembly

DNA was isolated with the Genomic DNA kit (UltraClean Microbial DNA Isolation Kit, Mo Bio Laboratories, Inc, Carlsbad, CA, USA) according to the manufacturer's instructions. Following, genomic libraries were constructed using the NanoTru-Seq DNA kit (for a pair-ended with an insert size average of 420pb). Next, 1.6 pM of the libraries were loaded and the run was performed in a MiSeq platform (Illumina). Resulting reads were filtered and trimmed by using Trimmomatic v0.30 (Bolger AM, 2014), with filters of quality (Q<30), length (<100), ambiguities (0Ns), and adapters were cut. Moreover, the filtered reads were de-novo assembled using the SPAdes v3.7 software (Gurevich A, *et al*, 2012). Hence, assembly quality and

completeness/contamination were evaluated using the Quast v5.0.2 (Gurevich et al., 2013) and CheckM v1.1.2 (Parks, 2015) softwares, respectively. The complete genome sequence of *P. fragi* strain GC01 has been deposited in GenBank under the accession number JABEMH000000000.1 (BioProject: PRJNA629082).

3.2.3 Genome functional description

Functional assignations of the assembled genome were made through annotation with Prokka v1.13.3 (Seemann, 2014) and EggNOG Mapper v2.0.1 (Huerta-Cepas et al., 2017) software's. EggNOG orthologues prediction was inferred with the diamond mapping strategy and the orthologues selected was restricted to one to one annotation. Chromosome topology was drawn using DNAPlotter v18.0.0 (Carver et al., 2009). Moreover, the Clusters of orthologous groups (COG) classification of *Pseudomonas* sp. CG01 predicted proteins was visualized through the ggplot2 R package (Wickham, 2009).

3.2.4 *Pseudomonas* genomic dataset

A total of 28 *Pseudomonas* strains (including *Pseudomonas* sp. CG01) were used for comparative analyses. The other 27 genomes were extracted from the GenBank (Supplementary Table S2.1), selected trying to capture: considerable diversity, cold environment origin, and the presence of interest phenotypic capacities (as production of volatile sulphur compounds). All 28 genomes were re-annotated with Prokka v1.13.3 (Seemann, 2014) and EggNOG mapper v2.0.1 (Huerta-Cepas et al., 2017) to have a comparable set.

3.2.5 Genetic relationships and Pan-genome analysis

For whole-genome comparisons, average nucleotide identity (ANI) was calculated for the dataset, in an all against all pairwise manner using pyani (Python3 module: Pritchard, 2016), with a BLASTn approach (Altschul et al., 1990). The results were

visualized using pheatmap v1.0.12 R packages (Kolde, 2015). Moreover, the pan genome was calculated, defining the compartments by clustering the proteins families into ortholog groups based on their sequence similarity using GET_HOMOLOGUES (Contreras-Moreira and Vinuesa, 2013) with orthoMCL v1.4 (Li et al., 2003) algorithm. The core genome was composed by the protein clusters present in ≥ 26 (of the 28) genomes. The accessory genome was composed by those protein clusters present in ≤ 3 genomes and the clusters present in between 4 and 25 genomes were classified as disposable genome. Moreover, starting with the alignment of the core-genome clusters, a phylogenetic reconstruction was calculated using the PARS program from the PHYLIP v3.6 package to produce a parsimony tree, which was visualized using FigTree v1.4.3.

3.2.6 Phenotype Gene Search

To identify metal resistance/tolerance genes (especially bivalent cations) and their distribution among the genomes set, a BLASTp approach was used. In addition, the BacMet: Metal Resistance Experimental Database v2.0 (Pal et al., 2014) was targeted with the 28 *Pseudomonas* genomes, considering e-value ($<1E^{-03}$), query coverage (>75%), and identity (>70%) filters. Besides, a second database of Cadmium Resistance Genes Database was constructed for this research-based in literature evidence (Supplementary Table S2.2). On the other hand, the genes related to the interest pathways were extracted from each genome using the KEGG identifiers (from the EggNOG annotations). Following, sulfur metabolism (map00920) and cysteine/methionine metabolism (ko00270) were converted to KEGG molecular networks using KEGG Mapper (Kanehisa, 2019). Finally, results were visualized using the ggplot2 R package (Wickham, 2009).

3.3 Results and Discussion

3.3.1 Genomic features of Antarctic *Pseudomonas* sp. GC01

The draft genome sequence of *Pseudomonas* sp. GC01 was obtained by Illumina sequencing and the assembly was deposited in GenBank (accession number JABEMH000000000.1). The size of *Pseudomonas* sp. GC01 genome was 4,706,645 bp with a guanine-cytosine (GC) content of 58.6%. The genome annotation yielded 4875 predicted coding sequences (CDSs, including 2411 hypothetical proteins), 49 transference RNA (tRNA), and three ribosomal RNA (rRNA) genes on 2004 contigs (N50: 3572 bp; Figure 1a). The functional classification of CDSs was performed based on clusters of orthologous groups of proteins (COGs) (Tatusov et al., 2000). From the total number of CDSs (4875) found in *Pseudomonas* sp. GC01, 3961 (81.3%) of them were classified in COGs functional categories, of which 721 were functionally unknown (COG S) (Figure 1b); leaving 914 that could not be classified. The largest COG categories were Transcription (COG K) with 366 CDSs corresponding to 9.2% of the total, followed by Amino acid transport, and metabolism (COG E), Inorganic ion transport (COG P) and metabolism, and Cell wall/membrane/envelope biogenesis (COG M) with 8.8% (350 CDSs), 7.9% (316 CDSs) and 6.9% (274 CDSs) respectively (Figure 1b).

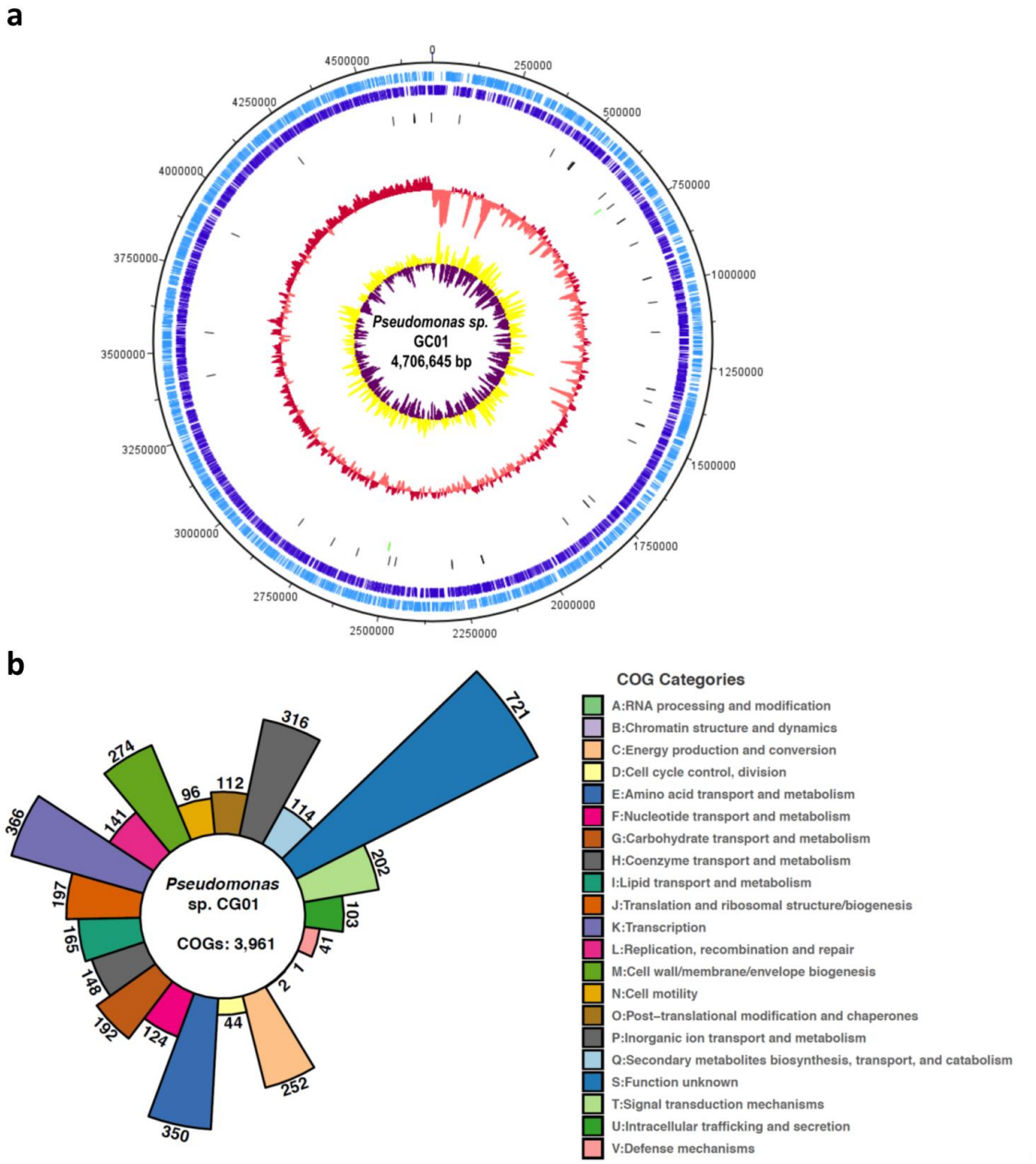

Figure 1. Genome characteristics of *Pseudomonas* sp. GC01. (**a**) Complete chromosome map of *Pseudomonas* sp. GC01. The chromosome map comprises six circles. The dark-blue and light-blue circles show the positions of protein-coding genes on the plus and minus strands. The black bars on the third circle represent tRNA genes. The green bars on the fourth circle represent rRNA genes. The pink/red circle shows the GC content. The purple/yellow circle shows the GC skew. (**b**) Distribution of COG categories on the

Pseudomonas sp. GC01 predicted proteins. The figure shows the number of CDSs assigned in each COG category depicted by color.

3.3.2 Genetic relationships and Pan-genome analysis

Comparative genome analysis of *Pseudomonas* sp. GC01 was performed in relation to 27 *Pseudomonas* genome sequences available in GenBank (Supplementary Table S2.1). The selection criteria of the *Pseudomonas* strains were mainly cold environment origin and Blast sequence similarity with *Pseudomonas* sp. GC01. *Pseudomonas* strains with interest phenotypic characteristics such as VSC production (*P. deceptionensis* species; Carrion et al., 2015; Gallardo-Benavente et al., 2019) and the reference strain *P. aeruginosa* PAO1 (Stover et al., 2000; Klockgether et al., 2010) were also included in the study.

Genome similarity of the 28 *Pseudomonas* strains studied was determined by average nucleotide identity (ANI) analysis (Pritchard et al., 2016). The ANI values ranged from 75.3% to 99.9%, indicating high diversity between the entire genomes set evaluated (Figure 2). A 99% sequence identity was determined between *Pseudomonas* sp. GC01, *Pseudomonas* sp. Lz4W (Pandiyan and Ray, 2013), and *P. fragi* P121 (Yanzhen et al., 2016), suggesting that these strains belong to the same species. However, it is interesting that the *P. fragi* P121 strain did not group with the other two *P. fragi* strains included in the dataset, only sharing 85% identity with both strains. Moreover, the *Pseudomonas* sp. GC01 also closely resembles *Pseudomonas* sp. L.10.10 (See-Too et al., 2016) with a 91% sequence identity, followed by an 85% sequence identity to *P. fragi* DBC (Singha et al., 2017) and two strains of *P. deceptionensis* LMG25555 and DSM26521 (Carrión et al., 2011; von Neubeck et al., 2016). Interestingly, the strains with the higher similarity to *Pseudomonas* sp. GC01 were isolated from cold environments, such as the Arctic (*P. fragi* P121; Yanzhen et al., 2016) and Antarctica (*Pseudomonas* sp. Lz4W, *Pseudomonas*

sp. L.10.10, and *P. deceptionensis* LMG25555; Carrión et al., 2011; Pandiyan and Ray, 2013; See-Too et al., 2016). The *P. aeruginosa* strains were also the most divergent and ancestral branch among the set.

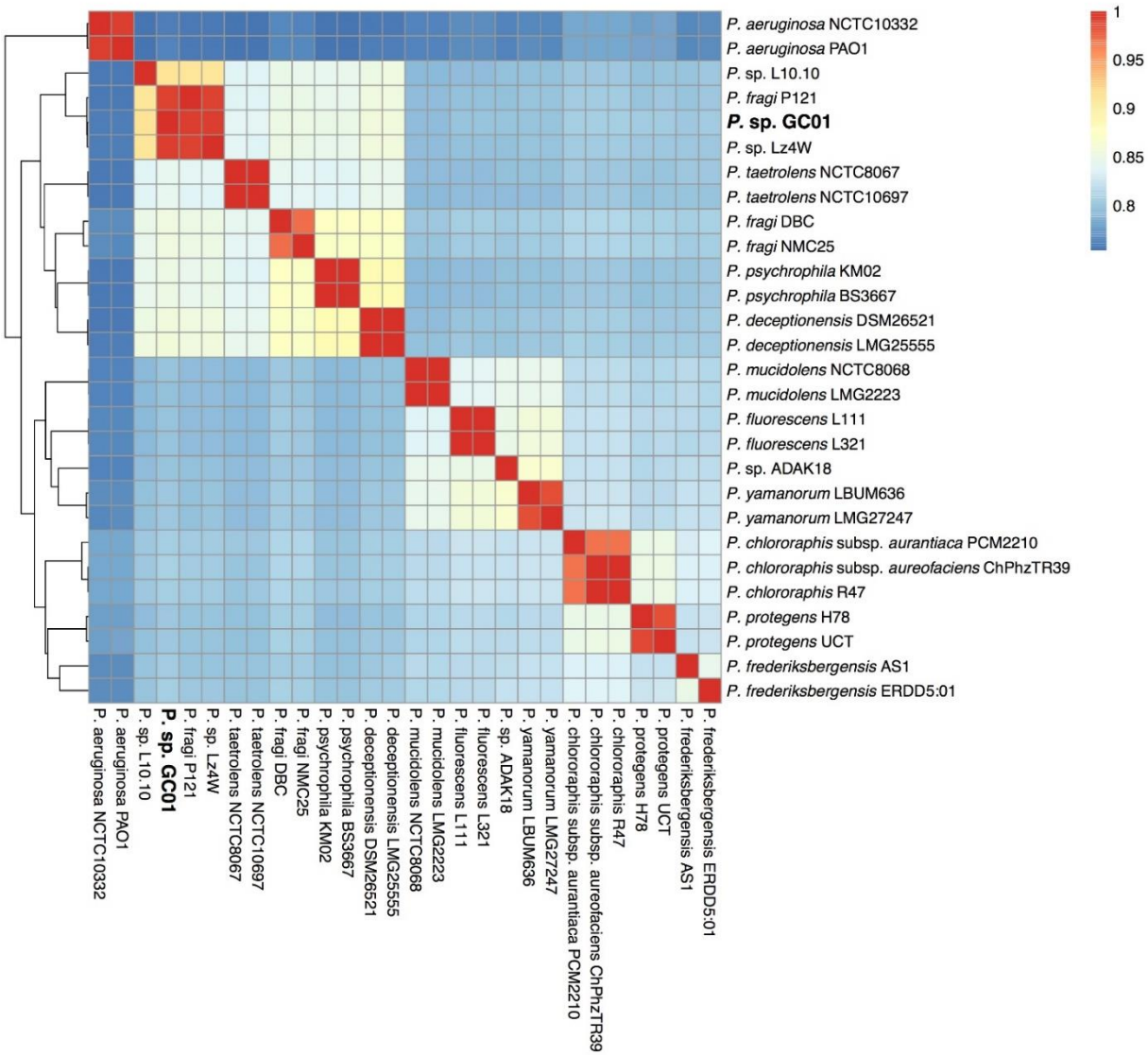

Figure 2. Heatmap displaying relationships (hierarchical clustering) between the 28 *Pseudomonas* strains based on ANI analysis. The color gradients show the percentage of identity shared by each pair of genomes, from lowest (blue) to highest (red).

The phylogenomic results further confirms the segregation of the *Pseudomonas* strains in several divergent modules (Figure 3a), where *P. aeruginosa* strains are the most distant and ancient of the set. The *Pseudomonas sp.* GC01 strain shares a clade with the *P. fragi* P121, *P. sp.* Lz4W and *P. sp.* L.10.10 strains, inside a branch mostly composed by strains from cold environments (Pandiyan and Ray, 2013; See-Too et al., 2016; Yanzhen et al., 2016). A Pan-genome analysis was performed to determine if the phenotypic differences could arise from the genotypic diversity between the *Pseudomonas* set. The pan-genome was composed of 17,751 clusters with only 2,024 clusters (11.4%) belonging to the core-genome compartment (Figure 3b), a result that supports the high diversity previously established between these 28 genomes. Further, considering an average of 4,933 proteins coded in each genome of the 28 strains, the core compartment (2,024 clusters) represent approximately 42% of the total genome (Supplementary Table S2.3). While the accessory genome size ranged from 180 to 2,736 clusters among the strains (Figure 3b). Particularly, the accessory genome of *Pseudomonas* sp. GC01 is composed by 271 clusters, 24 of them exclusively found on this strain (22 hypothetical proteins and two possible related to stress response: the SOS response associated protein UmuD and a FAD-dependent oxidoreductase). Moreover, our data shows that there is a significant fraction of the *Pseudomonas* sp. GC01 genome which we cannot discard as the possible origin of the particular capacities displayed by the strain. Therefore, with the improvement of bioinformatic tools and databases enrichment these mysteries will be cleared up over time (da Costa et al., 2018).

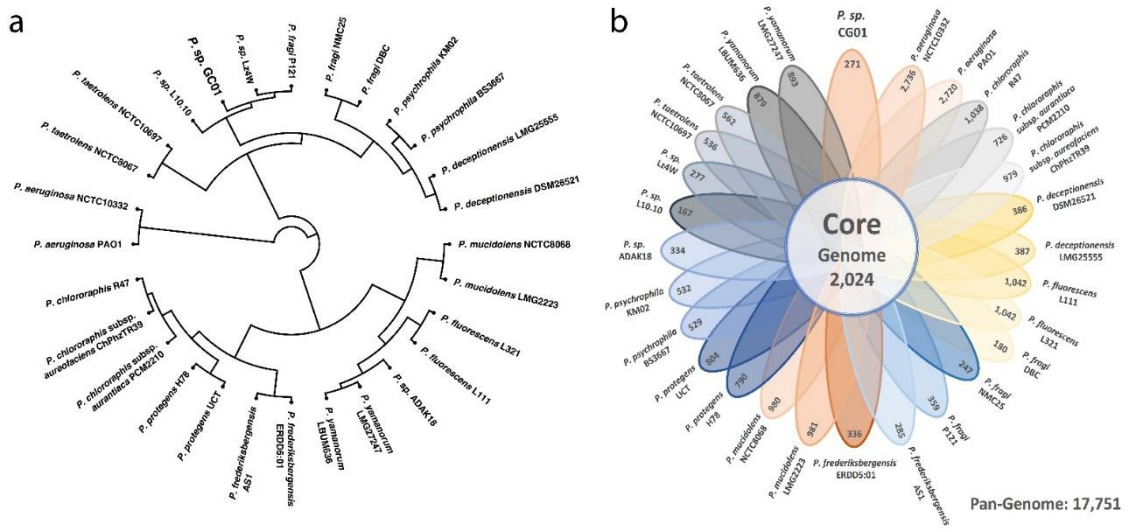

Figure 3. Phylogeny and Pan-genome of 28 *Pseudomonas* strains. (**a**) Circular phylogenetic tree showing the relationships between all *Pseudomonas* strains inference based on Core-genome sequences alignment. (**b**) Flower diagram representing the amount of core and accessory clusters for each *Pseudomonas* strain considered in the Pan-genome.

3.3.3 Comparative overview of metal-resistance genes on *Pseudomonas* strains

Cadmium is a heavy metal with no cellular role and highly toxic for most organisms. Cadmium toxicity is associated with oxidative stress and damage to different cellular biomolecules such as lipids, proteins, and nucleic acids (Naz et al., 2005; Khan et al., 2015; Abbas et al., 2018; Abdelbary et al., 2019; Qin et al., 2019). *Pseudomonas* sp. GC01 is a Cd-resistance (1.8 mM $CdCl_2$) strain that biosynthesize CdS QDs when exposed to this metal (Gallardo et al., 2014; Gallardo-Benavente et al., 2019). However, the genes involved in Cd^{+2} tolerance/response and the implication of them in the biosynthesis of nanoparticles are still unknown. Based on these, we performed a bioinformatic search of metal resistance genes focusing on Cd-resistance markers in all 28 *Pseudomonas* genomes, using the BacMet database (Pal et al., 2014) and the UniProt entries for a more specific search.

Pseudomonas genomes revealed 72 genes involved in the resistance to multidrug, oxidative stress and metal(loid), among others (Figure 4). 47 genes are involved in the uptake, tolerance, or detoxification of metal(loid)s such as arsenic (As), antimony (Sb), zinc (Zn), iron (Fe), copper (Cu), magnesium (Mg), manganese (Mn), chromium (Cr), tellurium (Te), selenium (Se), silver (Ag), cobalt (Co), lead (Pb), mercury (Hg), nickel (Ni), and Cd (Figure 4). Four of these genes, *actP*, *copR*, *oscA*, and *ruvB*, were present in all *Pseudomonas* strains, while other five genes; *arsB*, *cadR*, *recG*, *sodA*, and *sodB*, were absent only in one or two strains of the dataset (Figure 4). *P. aeruginosa* PAO1 (*fpvA* and *PA0320*), *P. protegens* UCT (*merA*, *merD*, *merE*, *merP*, *merR*, *merT* and *pitA*) and *Pseudomonas* sp. GC01 (*mgtA*) presented exclusive metal(loid) resistance genes (Figure 4), according to the BacMet database.

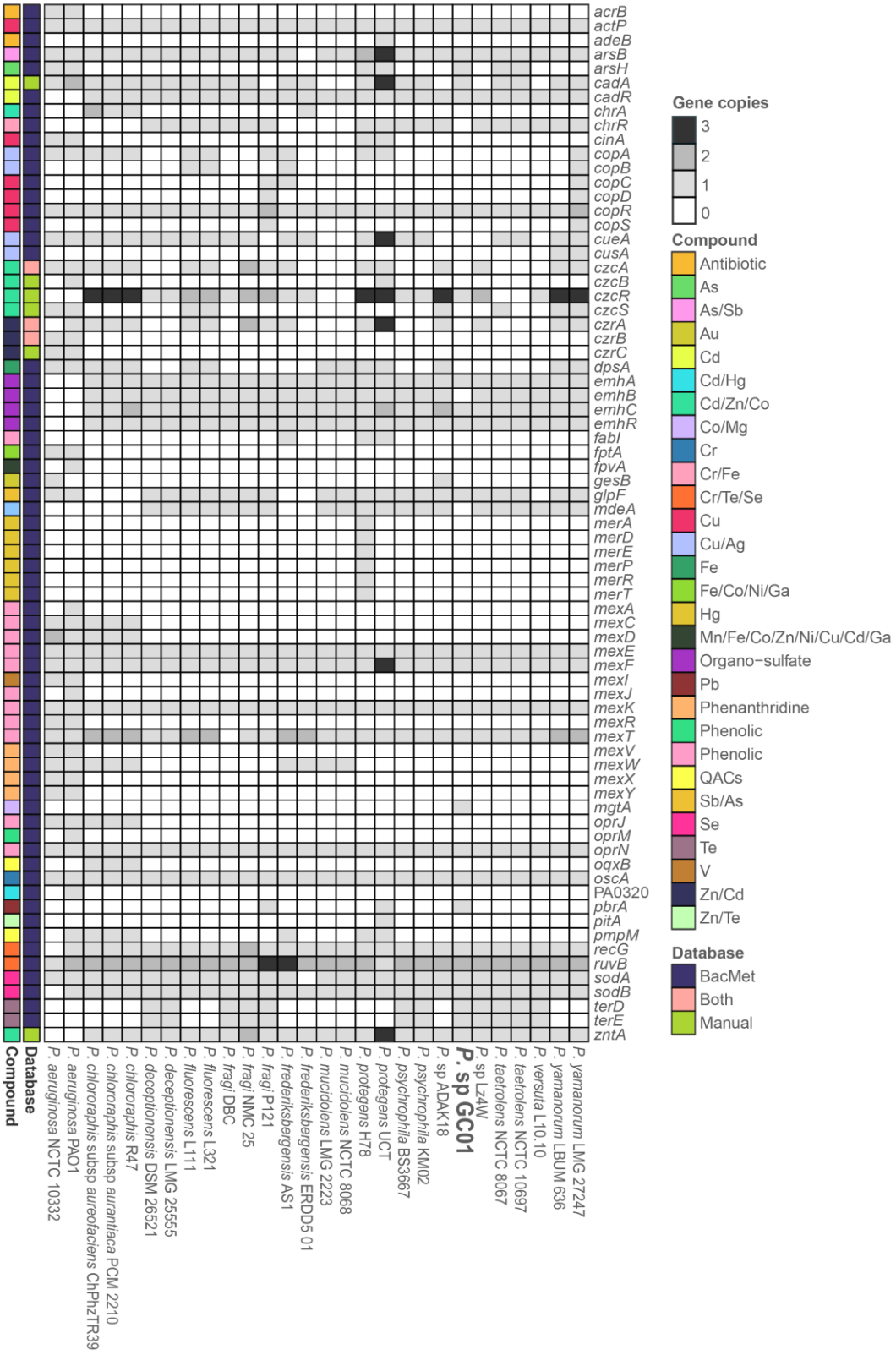

Figure 4. Heatmap of the metal-resistance genes present on the 28 *Pseudomonas* genomes. The scale shows the copy number of each gene in the corresponding genome, the metal(loid)/compound associated with the gene, and the database used.

In general, the analysis of the 28 *Pseudomonas* strains indicated the presence of at least one gene related to cadmium in each genome, and a total of thirteen genes when all genomes were considered (*cadA*, *zntA*, *pbrA*, *cadR*, *czcR*, *czcS*, *czcA*, *czcB*, *czrA*, *czrB*, *czrC*, *fpvA*, and *PA0320*; Figure 4, 5). Most of these genes correspond to classic genomic determinants involved in cadmium response (Wang and Crowley, 2005; Abdelbary et al., 2019) that code for bivalent cation transport pumps and regulatory systems (Figure 5) (Stafford et al., 1999; Nies, 2016; Qin et al., 2019).

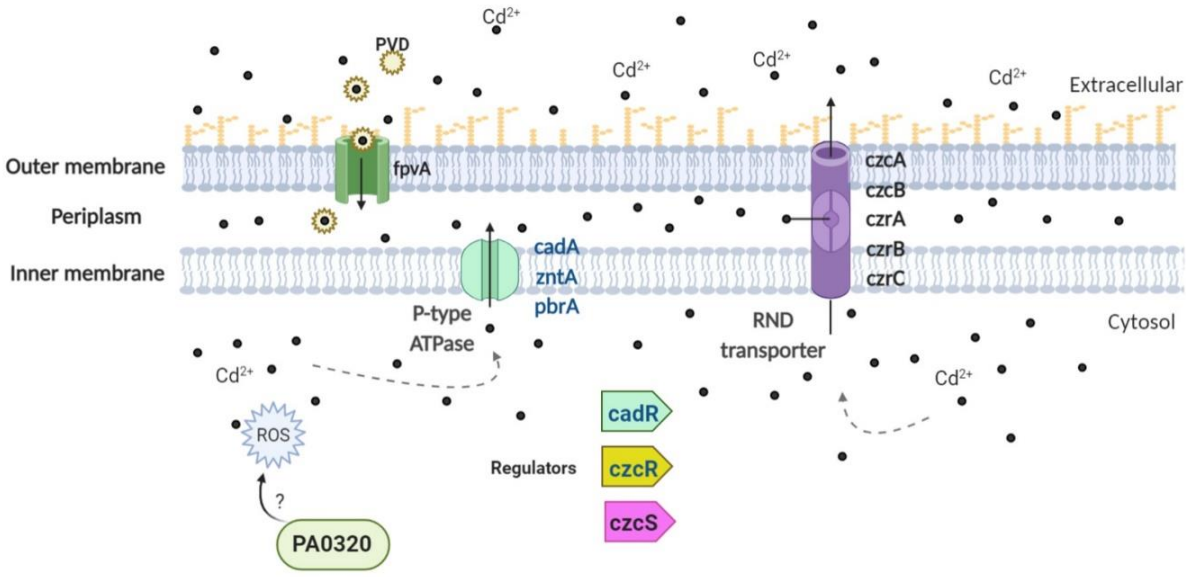

Figure 5. Schematic representation of the cadmium-resistance mechanisms based on the *Pseudomonas* genomes results. Proteins names in blue are those found in the genome of *Pseudomonas* sp. GC01.

Five genes associated with Cd-response were determined in the genome of *Pseudomonas* sp. GC01 (Figures 4, 5). Three of these code for the PIB2-type ATPases (TC 3.A.3) *cadA* (Cd^{2+} and Zn^{2+}), *zntA* (Zn^{2+}, Cd^{2+}, and Pb^{2+}), and *pbrA* (Pb^{2+}, Zn^{2+}, and Cd^{2+}), which are primarily involved in cadmium, zinc, and lead transport from the cytoplasm to the periplasm (Scherer and Nies, 2009; Nies, 2016; Vidhyaparkavi et al.,

2017; Qin et al., 2019; Mazhar et al., 2020) (Figure 5). The other two genes, *cadR* and *czcR*, code for regulatory elements involved in metal-resistance (Figure 5). *cadR* encodes a cadmium-induced transcriptional regulatory protein involved in Cd^{2+} resistance in several bacteria, including *Pseudomonas* strains (Permina et al., 2006; Prabhakaran et al., 2018; Cayron et al., 2020). While *CzcR* has been described as a DNA binding heavy metal response regulator, part of the *czcRS* two-component system, involved in Cd^{2+}, Zn^{2+}, and Co^{2+} resistance (Perron et al., 2004; Liu et al., 2015; Pal et al., 2017; Orellana-Saez et al., 2019, Mazhar et al., 2020). The five genes present in *Pseudomonas* sp. GC01 were found in most *Pseudomonas* strains; *cadA* and *czcR* in 22 strains, *zntA* and *cadR* in 26 strains, and *pbrA* only in 3 strains (Figure 4).

Regarding the Cd^{2+} resistance genes *czcA*, *czcB*, *czcS*, *czrA*, *czrB*, *czrC*, *fpvA*, and *PA0320*, none of them was found in the genome of *Pseudomonas* sp. GC01 (Figure 4). *czcA* and *czcB* (Cd^{2+}, Zn^{2+}, and Co^{2+}), as well as *czrA*, *czrB*, and *czrC* (Cd^{2+}, and Zn^{2+}), are members of the RND family (Resistance Nodulation and cell Division, TC_2.A.6.3) of heavy metal efflux, that are involved in the export of Cd^{+2} from the periplasm to the extracellular space (Hassan et al., 1999; Hu and Zhao, 2007; Valencia et al., 2013; Chong et al., 2016; Chellaiah, 2018; Abdelbary et al., 2019). The *czc* family is one of the best characterized RND efflux outer membrane proteins involved in Cd^{2+} resistance present in many Gram-negative bacteria including *Pseudomonas* (Perron et al., 2004; Liu et al., 2015; Khan et al., 2015; Choudhary and Sar, 2016; Pal et al., 2017). However, *czcA* and *czcB* were absent in 12 and 26 *Pseudomonas* genomes, respectively, including *Pseudomonas* sp. GC01 (Figure 4). The genes involved in the *czr* efflux system were absent in 13 (*czrA*) and 26 (*czrB*, and *czrC*) *Pseudomonas* strains (Figure 4). Additionally, the regulatory gene *czcS* (part of the two-component-regulatory systems *czcRS*) was present in 8 *Pseudomonas* strains (Figure 4). This gene encodes a heavy metal sensor

histidine kinase involved in Cd^{2+}, Zn^{2+}, and Co^{2+} homeostasis in bacteria (Liu et al., 2015; Mazhar et al., 2020). On the other hand, the gene *PA0320* has been associated with Cd^{2+} resistance by favoring the tolerance to reactive oxygen species (ROS; Fukushima et al., 2012). The *fpvA* gene (Fe^{3+}, Mn^{2+}, Co^{2+}, Zn^{2+}, Ni^{2+}, Cu^{2+}, and Cd^{2+}) codes for an outer membrane transporter and receptor of the siderophore pyoverdine (PVD), involved in iron uptake with a broad specificity for PVD–metal complexes in *P. aeruginosa* (Braud et al., 2009; Hannauer et al., 2012). These last two genes were only found in *P. aeruginosa* PAO1 (Figure 4).

According to the results obtained, the absence of *czcA*, *czcB*, *czrA*, *czrB*, and *czrC* in *Pseudomonas* sp. GC01 denies the possibility of their participation in the Cd^{2+} transport process required for the extracellular biosynthesis of CdS. However, *Pseudomonas* sp. GC01 contains other genes involved in the cadmium response (Figure 4) that could participate in the biosynthesis of CdS QDs. *Pseudomonas* sp. GC01 *cadA*, *zntA*, and *pbrA* genes are candidates for Cd^{2+} efflux, favoring the extracellular interaction of metal ions with sulfur-containing molecules such as H_2S or MeSH to form the CdS nanoparticles. These genes represent three potential targets probably involved in CdS nanoparticle formation in *Pseudomonas* sp. GC01. However, the most novel characteristic of CdS biosynthesis in this bacterium is their capacity to synthesize nanoparticles in presence of different sulfur sources, particularly Met.

3.3.4 Comparative analysis of genes involved in Sulfur metabolism

Since the *Pseudomonas* sp. GC01 can biosynthesize CdS QDs from several sulfur sources, and sulfur is a vital element in the formation of these nanoparticles, we searched for genes involved in sulfur metabolic pathways. To carry out this, we use data available in the KEGG database related to sulfur metabolism (map00920) and cysteine/methionine metabolism (ko00270). A set of 91 genes were found in the 28 *Pseudomonas* genomes,

39 belonging to sulfur metabolism, 52 to cysteine/methionine metabolism, and seven shared in both metabolisms (Figure 6). The genome sequences revealed the presence of numerous common genes encoding proteins related to sulfur transport, sulfate/sulfur assimilation, Cys and Met synthesis/degradation, and VSCs catabolic pathways, among others. These results are consistent with the ability of bacteria of the *Pseudomonas* genus to use a wide variety of organic and inorganic sulfur sources to growth (Vermeij and Kertesz, 1999; Kertesz, 2004).

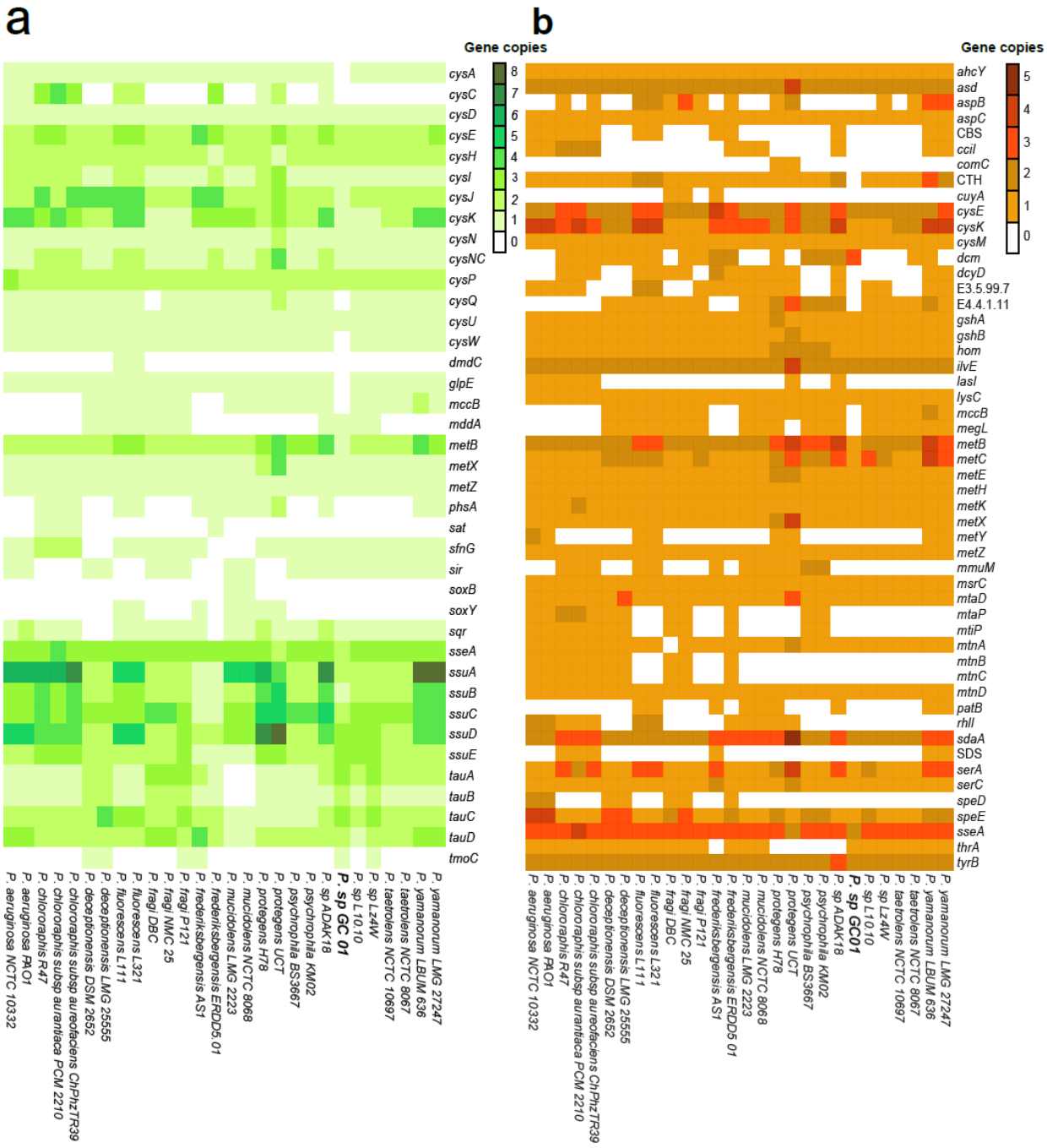

Figure 6. Heatmap of the sulfur metabolic genes present in the 28 *Pseudomonas* genomes analyzed. (**a**) Sulfur metabolism genes. (**b**) Cysteine and methionine metabolism genes. The heat scale shows the copy number of each gene in the corresponding genome.

Sulfur is an essential element required for cell growth in all bacteria (Kertesz, 2001). It is also an essential component in CdS nanoparticle biosynthesis (Holmes et al., 1997; Bai et al., 2009a; Gallardo et al., 2014; Yang et al., 2016). The *Pseudomonas* sp.

GC01 strain can use several sulfur sources such as sulfate, sulfite, thiosulfate, Cys, and Met to grow and biosynthesize CdS QDs (Gallardo-Benavente et al., 2019). However, the extracellular biosynthesis mechanism of CdS nanoparticles has been linked to the ability of this strain to release H_2S and MeSH in the presence of Cys and Met, respectively (Gallardo-Benavente et al., 2019).

Sulfate assimilation in bacteria proceeds by a sequence of similar reactions involving the uptake and activation of sulfate, followed by stepwise reduction to sulfide (Kertesz, 2000, 2004). The *Pseudomonas* genome sequences revealed that sulfate assimilation begins with the active uptake of sulfate by ABC-type transport for sulfate/thiosulfate (encoded by *cysA* [EC: 3.6.3.25], *cysP*, *cysU*, and *cysW* in all strains, and by *cysP* and *cysU* in *Pseudomonas* sp. GC01) (Figure 7). Subsequently, sulfate is transformed to adenosine-5′-phosphosulphate (APS) catalyzed by ATP sulfurylase (EC: 2.7.7.4) encoded by *cysN*, *cysD,* and *cysNC* in the *Pseudomonas* strains (Kertesz, 2004), and *sat* genes, which were present only in four strains (Figure 6a). Then APS can be reduced to sulfite directly through APS reductase *cysH* (EC: 1.8.4.10, present in all strains), or indirectly via 3′-phosphoadenosine-5′-phosphosulfate (PAPS) that uses APS kinase *cysC* (EC: 2.7.1.25), followed by PAPS reductase (*cysH*, EC: 1.8.4.8, found in 11 *Pseudomonas* strains) (Figure 6a). Obtained sulfite is then reduced to generate sulfide by sulfite reductase encoded by *cysI*, *cysJ* (EC: 1.8.1.2), and *sir* (EC: 1.8.7.1, found in 19 strains including *Pseudomonas* sp. GC01), before being assimilated into organic material (Figure 6a, 7**)** (Kertesz, 2004; Kredich, 2008; Seiflein and Lawrence, 2001).

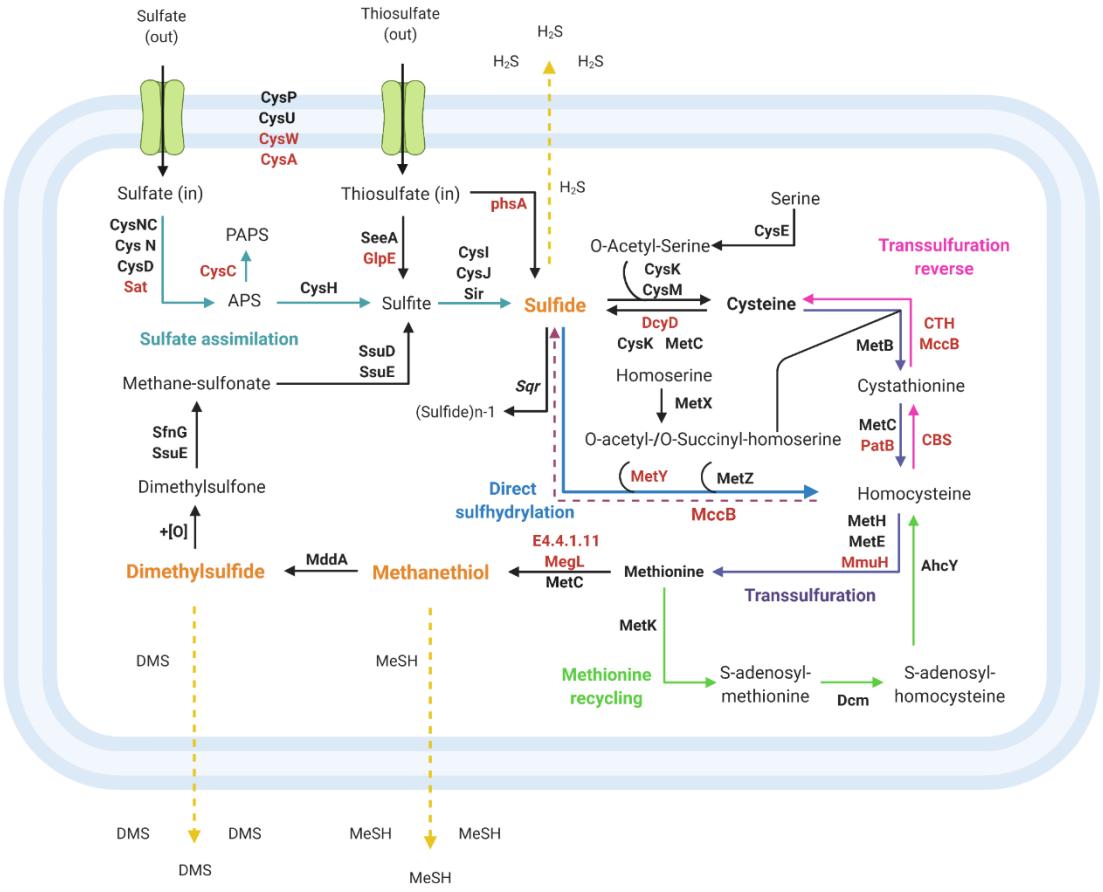

Figure 7. Sulfur metabolic pathways present in the genome of *Pseudomonas* sp. GC01. The schematic representation of protein identified in the genome of *Pseudomonas* sp. GC01 involved in sulfur assimilation, cysteine and methionine synthesis, and volatile sulfur compounds catabolic pathways. Protein names in red were not found in this strain but present in other *Pseudomonas* strains.

Regarding the use of sulfite and thiosulfate as inorganic sulfur sources by bacteria, sulfite can enter the sulfate assimilation pathway, where sulfite is reduced to sulfide by the enzyme sulfite reductase *cysI*, *cysJ*, and *sir* (Kredich, 2008). Thiosulfate can be incorporated through ABC-type transporters (sulfate/thiosulfate, described above) and reduced to sulfite by thiosulfate sulfurtransferase (EC: 2.8.1.1; Kawano et al., 2017) encoded by *seeA* and *glpE* (the latter absent only in *Pseudomonas* sp. GC01) before being assimilated as sulfide via the sulfate assimilation pathway (Figure 6a, 7). Additionally,

14 strains of *Pseudomonas* (not including *Pseudomonas* sp. GC01) contain in their genomes the thiosulfate reductase enzyme (*phsA*, EC: 1.8.5.5) that catalyzes the reduction of thiosulfate to sulfide (Figure 6a, 7; Clark and Barrett, 1987; Stoffels et al., 2012). The sulfide generated by the different inorganic sulfur sources is incorporated into cells as cysteine by the action of the enzymes cysteine synthase *cysk* and *cysM* (EC: 2.5.1.47 and EC: 2.5.1.144;Lewis et al., 2013) that catalyzes the addition of sulfide into O-acetyl-serine (Figure 6a-b, 7). Cys then works as the sulfur group donor, either directly or indirectly, for the synthesis of all other sulfur-bearing molecules in the cell, such as thiamine, glutathione, coenzyme A, and Met (Seiflein and Lawrence, 2001; Wada and Takagi, 2006).

Some bacteria belonging to the *Pseudomonas* genus can assimilate sulfur from reduced sulfur molecules such as the amino acids Cys and Met (Vermeij and Kertesz 1999). Generally, this metabolism is associated with internal recycling processes developed by bacteria to maximize available nutrients (Seiflein and Lawrence, 2006). Cys as a sole sulfur source can be assimilated directly via the transsulfuration pathway that converts Cys to Met (Figure 7**;** Vermeij and Kertesz, 1999; Wüthrich et al., 2018). This pathway was observed in all *Pseudomonas* genomes analyzed and produces homocysteine by the action of cystathionine gamma-synthetase (*metB*, EC: 2.5.1.48) and cystathionine beta-lyase (EC: 4.4.1.13) encoded by *metC* and *patB* (in 9 strains; Figure 6b) (Zdych et al., 1995; Auger et al., 2005; Miyamoto et al., 2018). Subsequently, homocysteine is methylated to produce Met by methionine synthases encoded by *metE* or *metH* (EC: 2.1.1.14 or EC: 2.1.1.13; Alaminos and Ramos, 2001) present in all strains, and by homocysteine S-methyltransferase (*mmuH*, EC: 2.1.1.13; Li et al., 2016) determined in 12 *Pseudomonas* strains (Figure 6b, 7).

On the other hand, Cys also may break down to release sulfide in bacteria through the enzyme cysteine desulfhydrase (EC: 4.4.1.15; Awano et al., 2003, 2005; Yu et al., 2007; Oguri et al., 2012). The gene encoding this enzyme (*dcyD*) was found in 16 strains, not including *P. aeruginosa*, *P. deceptionensis*, *Pseudomonas* sp. Lz4W, *Pseudomonas fragi* P121, and *Pseudomonas* sp. GC01 strains, among others (Figure 6b). Low H_2S production in the presence of Cys and other sulfur sources had been reported in *Pseudomonas* sp. GC01 by Gallardo-Benavente et al., (2019). This report is concordant with the absence of *dcyD* in this strain. Along with the presence of the enzyme sulfide: quinine oxidoreductase encoded by *sqr* (EC: 1.8.5.4, present in 15 strains; Figure 6a), whose function is to oxidize sulfide to polysulfide or sulfite and thiosulfate in heterotrophic bacteria as *P. aeruginosa* PAO1 (Xia et al., 2017), diminishing the sulfide released by bacteria. Therefore, the *dcyD* absence in *Pseudomonas* sp. GC01 suggests that sulfide production from Cys may be catalyzed by enzymes with lower cysteine desulfhydrase activity present in their genome as cysteine synthases (*cysK*) and cystathionine beta-lyase (*metC*) (Figure 7; Awano et al., 2003, 2005).

The sulfide produced by the sulfate assimilation pathway or by Cys degradation can be used by *Pseudomonas* strains to yield Met through both transsulfuration (described above) and direct sulfhydrylation pathways. Direct sulfhydrylation pathway has been described as the main Met synthesis pathway in *Pseudomonas* genus (Kertesz, 2004), and the critical gene (*metZ*) was present in all genomes analyzed (Figure 6b, 7). Previous to Met formation, this pathway involves the direct formation of homocysteine catalyzed by the enzyme O-succinylhomoserine sulfhydrylase (*metZ*, EC:2.5.1.-) using O-succinyl-homoserine as substrate (Figure 6b), or the synthesis of homocysteine using O-acetyl-homoserine and sulfide (present in 8 strains) catalyzed by the O-acetyl-L-homoserine sulfhydrolase (*metY*, EC: 2.5.1.49) (Vermeij and Kertesz, 1999; Alaminos and Ramos,

2001; Kertesz, 2004; Perumal et al., 2008; Shim et al., 2016; Wüthrich et al., 2018; Kulikova et al., 2019).

Regarding the metabolic pathways associated with Met as a sole sulfur source for bacterial growth, the *Pseudomonas* genomes showed two metabolic pathways that allow conversion of this amino acid to Cys for cell growth. In the first pathway, Met may be desulfurized to produce sulfite entering in the synthetic pathway of Cys through the sulfate assimilation (Vermeij and Kertesz 1999). The formation of MeSH from Met degradation catalyzed by enzyme methionine gamma-lyase (EC: 4.4.1.11) has been reported in *Pseudomonas* (Fukumoto et al., 2012; Carrion et al., 2015; El-Sayed et al., 2017). The genes coding for this enzyme, *megL* and *EC4.4.1.11*, were found in 19 and 20 of the *Pseudomonas* genomes analyzed, respectively (Figure 6b). Despite the ability of *Pseudomonas* sp. GC01 to produce high concentrations of MeSH from Met, these genes were absent in their genome (Gallardo-Benavente et al., 2019). This result suggests that MeSH production in *Pseudomonas* sp. GC01 is catalyzed by an enzyme different from methionine gamma-lyase. In this context, the enzyme cystathionine beta-lyase (*metC*) has been described in some bacteria with the ability to produce MeSH from Met (Dias and Weimer, 1998; Lee et al., 2007; Schulz and Dickschat, 2007; Veselova et al., 2019) and is presented as the principal candidate to carry out this function in the *Pseudomonas* sp. GC01 (Figure 7). Once MeSH is formed, this sulfur volatile is methylated by the enzyme methanethiol S-methyltransferase (*mddA*, EC: 2.1.1.334) to produce dimethylsulfide (DMS) (Carrión et al., 2015), and then DMS is oxidized to dimethylsulfone (Endoh et al., 2003). Dimethylsulfone is converted to methane-sulfonate and sulfite by the action of the enzymes dimethylsulfone monooxygenase (*sfnG*, EC: 1.14.14.35), FMN reductase (*ssuE*, EC 1.5.1.38), and alkanesulfonate monooxygenase (*ssuD*, EC: 1.14.14.5; Endoh et al., 2003). Finally, sulfite produced can enter the sulfate assimilation pathway for Cys

biosynthesis (Figure 7) (Vermeij and Kertesz, 1999; Endoh et al., 2003). Two key members of Met desulfurization to sulfite are *mddA* and *sfnG* genes, which were absent in 17 and 5 *Pseudomonas* strains analyzed, respectively (Figure 6a). Therefore, this result showed the presence of this pathway in 9 bacterial strains, including *Pseudomonas* sp. GC01 (Figure 6a, 7).

The second pathway that converts Met to Cys in bacteria involves methionine recycling and homocysteine conversion to Cys by reverse transsulfuration or sulfide formation (Figure 7; Vermeij and Kertesz 1999; Kertesz, 2004, Hullo et al., 2007). In general, Met is used by S-adenosylmethionine synthase (*metK*, EC: 2.5.1.16), present in all genomes, for the synthesis of the universal methyl donor S-adenosyl-methionine (SAM) (Kertesz, 2004; Wüthrich et al., 2018). Subsequently, SAM is regenerated or recycled to Met via the formation of homocysteine by the action of methyltransferases (encoded by *dmc* [EC: 2.1.1.37, cytosine-specific methyltransferases] in 18 strains) and homocysteine adenosylhomocysteine *ahcY* (EC: 3.3.1.1) (Figure 6b, 7). Then, Cys is formed by the reverse transsulfuration pathway via cystathionine by the enzymes cystathionine beta-synthase (*CBS*, EC: 4.2.1.22) and cystathionine gamma-lyase (*CTH* or *mccB*, EC: 4.4.1.1) in 12 strains (Figure 6b, 7). While in 17 *Pseudomonas* strains, homocysteine desulfhydrase *mccB* (EC: 4.4.1.2) produces sulfide from homocysteine, which enters the Cys biosynthesis pathway via sulfate assimilation route (Figure 7). *Pseudomonas* sp. GC01 lacks *CBS*, *CTH*, and *mccB* genes, suggesting that Met is used as a sulfur source in this bacterium by Met desulfurization pathway via Dimethylsulfone. However, we cannot discard that other still unknown genes or pathways could be involved in this prosses.

In general, no significant discrepancies were observed between the 28 *Pseudomonas* genomes analyzed. From a total of 84 genes observed, 33 genes were

absent in some of the bacterial strains (Figure 6), probably due to the genomic diversity between the strains (Figures 2, 3). Nevertheless, sulfur is an essential element for bacterial growth. Therefore, sulfur metabolism pathways are remarkably similar between different organisms (Kertesz, 2001, 2004). Bacterial assimilation of sulfur into organic molecules is varied, and the sulfur metabolic pathways depend on the sulfur source used and the genomic potential of each bacteria. The genes involved in sulfate assimilation pathways, transsulfuration, direct sulfhydrylation, methionine salvage, reverse transsulfuration, VSCs catabolic pathways, among others described in this work, were found in the *Pseudomonas* strains analyzed (Figure 7).

Extracellular biosynthesis of CdS QDs in bacteria has been mainly associated with H_2S (Bai et al., 2009a; Yang et al., 2016) and recently has been linked with MeSH production in *Pseudomonas* sp. GC01 (Gallardo-Benavente et al., 2019). When Cys is used as sulfur source, the mechanism of CdS nanoparticles involves H_2S generation (as sulfide source) mediated by cysteine desulfhydrase (*dcyD*) or cystathionine gamma-lyase (*CTH* or *mccB*) (Holmes et al., 1997; Bai et al., 2009a; Dunleavy et al., 2016). Interestingly, *Pseudomonas* sp. GC01 biosynthesizes CdS nanoparticles from Cys, despite lacking these genes. Therefore, it is believed that *cysK* (cysteine synthases) and *metC* (cystathionine beta-lyase) would participate in H_2S production in this strain.

Regarding the CdS QD biosynthesis associated with the production of MeSH in bacteria, Gallardo-Benavente et al. (2019) proposed a relationship between CdS nanoparticle biosynthesis and MeSH production in *Pseudomonas* sp. GC01, which also was linked to the activity of methionine gamma-lyase in *P. deceptionensis* M^{1T} (Gallardo-Benavente et al., 2019). However, *megL* and *EC4.4.1.11* genes that encodes this enzyme are absent in *Pseudomonas* sp. GC01 genome. This is puzzling particularly considering the high MeSH production and the ability to produce CdS QDs in presence of Met

previously reported in this strain (Gallardo-Benavente et al., 2019). Accordingly, once again, *metC* appears as the main candidate to carry out this function due to their ability to produce MeSH from Met in bacteria (Dias and Weimer, 1998; Lee et al., 2007; Schulz and Dickschat, 2007; Veselova et al., 2019).

3.4 Conclusion

Our findings confirm the presence of three Cd efflux P-type ATPases transporters (*cadA*, *zntA*, and *pbrA*) in the genome of *Pseudomonas* sp. GC01. The identification of these Cd^{2+} transport genes provides evidence about the detoxification mechanisms of cadmium in this strain which could contribute to the extracellular biosynthesis of CdS QDs (Figure 8).

The absence of *megL* and *EC4.4.1.11* in *Pseudomonas* sp. GC01 genome discarded a role for the enzyme methionine gamma-lyase in the MeSH-dependent biosynthesis of QDs CdS. However, the *metC* gene (coding for cystathionine beta-lyase) involved in the transsulfuration pathway is the main candidate to produce MeSH from Met during the extracellular biosynthesis of CdS QDs in *Pseudomonas* sp. GC01 (Figure 8). In addition, H_2S generation from Cys during the extracellular biosynthesis of CdS nanoparticles is most probably linked to *cysK* (cysteine synthases) and *metC* in *Pseudomonas* sp. GC01, since this strain lacks the gene *dcyD* coding for a cysteine desulfhydrase (Figure 8).

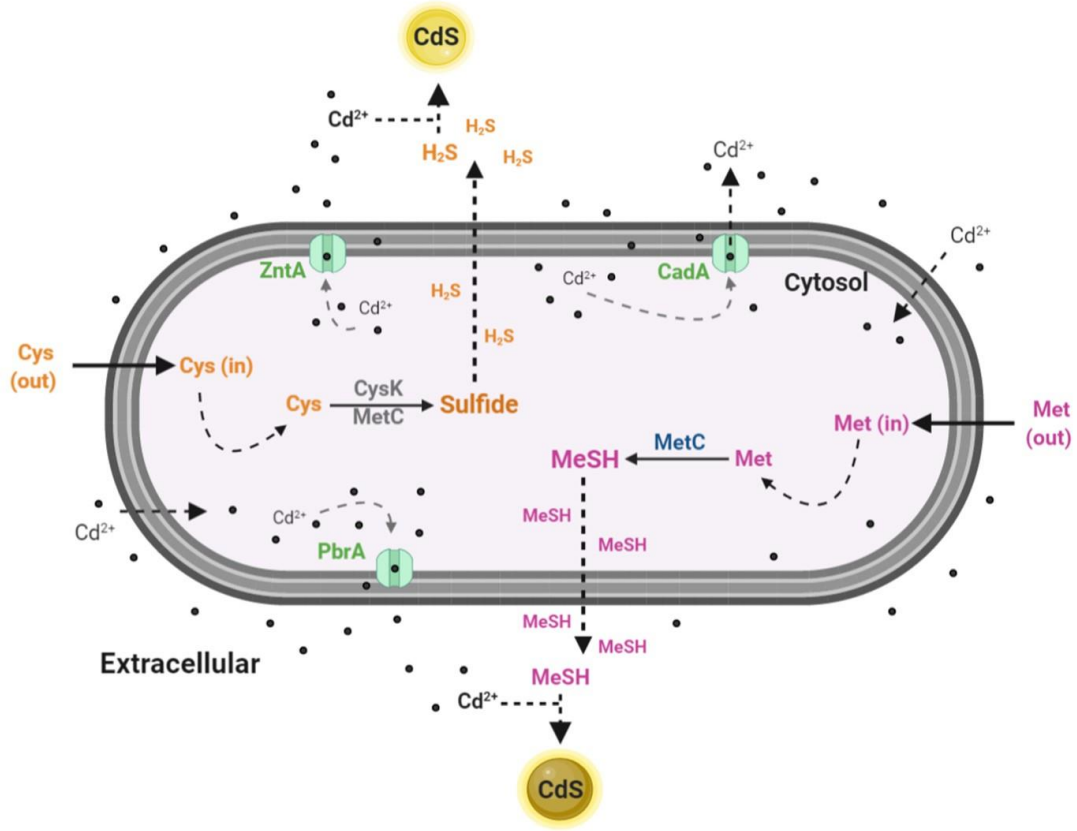

Figure 8. Schematic representation of the CdS QDs biosynthesis by *Pseudomonas* sp. GC01. The figure shows the proteins present in the *Pseudomonas* sp. GC01 genome involved in the biosynthesis of CdS nanoparticles when Cys (CysK and MetC) or Met (MetC) was used as the sulfur source as well as the Cd^{2+} efflux pumps CadA, ZntA, and PbrA.

Altogether, the results presented in this study constitute valuable information regarding the potential molecular mechanism involved in bacterial biosynthesis of CdS QDs based on H_2S and MeSH generation, two processes scarcely known to date. Therefore, this genomic study constitutes the first report about genes potentially involved in CdS QDs bioproduction in *Pseudomonas* sp. strains and the first molecular approach to a bacterial mechanism of Cd-resistance and MeSH production in the Antarctic strain *Pseudomonas* sp. GC01.

Supplementary Materials

The following are available online at https://www.mdpi.com/2073-4425/12/2/187/s1, Table S1: Accession numbers and data for the selected 28 *Pseudomonas* strains genomes, Table S2: Cadmium-resistance Genes Database described in the literature to *Pseudomonas*, Table S3: Genes Classification for each strain in the pangenome compartments.

Author Contributions

Conceptualization, CG-B, JP-D, and AQ; conceived and designed the study, JLC-G and JC-S; carried out all the bioinformatics, CG-B, JLC-G and JC-S; analyzed the data, CG-B: wrote the first manuscript draft. All authors commented, contributed, edited the manuscript and approved the final version.

Funding

This research was supported by Erika Elcira Donoso Lopez, CONICYT scholarship 21151066 (CG-B), Fondecyt 1200870 (JMP-D), Fondecyt 1181697 (QA), INACH DT_05_16 (CG-B, AQ), INACH RT-25_16 (JMP-D), CONICYT scholarship 21171644 (JLCG) and Universidad Católica del Norte 2020 Postdoctoral Fellowship (JC-S).

Acknowledgments

In the loving memory of Claudio Vásquez Guzmán, an excellent friend, mentor, and scientist, but a better human being. Thanks for all the adventures and for showing us the beauty of science and friendship.

Conflicts of Interest

The authors declare that this research was conducted in the absence of any commercial or financial relationships that could be construed as a potential conflict of interest.

CHAPTER IV

General discussion, concluding remarks and future directions

4. General discussion, concluding remarks and future directions

4.1 General discussion

Biosynthesis o biological synthesis of CdS QDs using bacteria has been a topic of increasing interest in the past few years due to represent a simple, safe, inexpensive, and environmentally friendly alternative to manufacture nanocrystals with new properties and applications (Ulloa et al., 2016, 2018; Prasad et al., 2016; Sekar and Parvathi, 2019; Bruna et al., 2019 Iravani, and Varma, 2020; Khan and Lee, 2020). In general, using bacteria as cell factories to generate CdS QDs involves the action of biomolecules to reduce, stabilize, and capping agents (Monrás et al., 2012; Sankhla et al., 2016; Ma et al., 2020). However, cell behavior and the mechanism involved in the biosynthesis process have still not been determined. Despite this, most CdS biosynthesis methods described to date have been associated with the use of sulfur-containing molecules with affinity to Cd, such as peptides, thiols, and volatile sulfur compounds as H_2S (Holmes et al., 1997; Bai et al., 2009; Monrás et al., 2012; Gallardo et al., 2014). In previous work, we reported intracellular biosynthesis of CdS QDs at low temperatures (15°C) of different Antarctic *Pseudomonas* spp. Psychrotolerant, resistant to oxidative stress and cadmium (Gallardo et al., 2014). Nevertheless, it was not possible to establish a relation between CdS nanoparticles generation with sulfur-containing molecules with affinity to Cd as a substrate to CdS QDs biosynthesis in *Pseudomonas* sp. GC01 (Holmes et al., 1997; Bai et al., 2009; Monrás et al., 2012; Gallardo et al., 2014). Consequently, firstly we studied the ability of *Pseudomonas* sp. GC01 to use various sulfur sources to grow, biosynthesize CdS QDs, and produce volatile sulfur compounds (VSCs) (Chapter II).

Our outcomes demonstrated that *Pseudomonas* sp. GC01 grows on a wide variety of sulfur sources such as sulfate, sulfite, sulfide, thiosulfate, Cys, and Met, and

biosynthesize CdS QDs from them. However, extracellular biosynthesis of nanoparticles was only observed when Cys and Met were used as sole sulfur sources. The Met supernatants showed red fluorescence, the color of which did not switch over time. In contrast, the supernatants obtained with Cys showed different fluorescent colors (between green and orange) depending on Cys concentrations and the incubation time (Figure 2A, B, Chapter II). This optical property is a phenomenon unique and characteristic of QDs, which emit different fluorescence (different colours) depending on the nanoparticle size (Yang et al., 2016; Ulloa et al., 2018; Bruna et al., 2019). However, the fluorescence emission also can be affected by the surface defects of QDs (Bruna et al., 2019). The CdS nanoparticles produced showed high stability in aqueous solutions with a zeta potential value lower than -20 mV, where nanocrystals produced from Met being the most stable (Kuznetsova and Rempel, 2015). The electron microscopy images determined an average size of the CdS QDs produced with Cys (~ 2 nm) and Met (~ 16 nm). This result agrees with the reported of the size of QDs biosynthesized (Bruna et al., 2019; Wang et al., 2018; Al-Shalabi and Doran, 2016; Tandon and Vats, 2016; Wu et al., 2015; Syed and Ahmad, 2013; Chen et al., 2009; Khachatryan et al., 2009). Energy dispersive X-ray (EDX), X-ray diffraction (XRD), and X-ray photoelectron spectroscopy (XPS) analysis confirmed the formation of cubic nanocrystals of CdS with an organic layer (Waly et al., 2017; Bharti et al., 2018; Wang et al., 2018; Chakraborty et al., 2018; Sankhla et al., 2016; Muntaz Begum et al., 2016; Richards et al., 2016; Bag et al., 2017). Furthermore, the presence of N and S in the XPS analysis suggests that QDs surface are composite by Cys and Met as part of the organic coating, indicating that these amino acids could be stabilizing the nanocrystals.

The absorbance and fluorescence properties of QDs produced with Cys (green and yellow), and Met (red) are in agreement with previous reports of nanoparticles

biosynthesized, were the CdS QDs display maximal absorbance peaks between 360-380 nm and fluorescence emission peaks between 470-600 nm (Gallardo et al., 2014; Yang et al., 2015; Dunleavy et al., 2016; Plaza et al., 2016; Ulloa et al., 2016; Venegas et al., 2017; Glatstein et al., 2018). CdS QDs biosynthesized with Cys (yellow) present higher quantum yield (QY) than biosynthesized with from Met (red), with 21.04% and 7.81%, respectively (Venegas et al., 2017; Bruna et al., 2019). This result is probably due to the size differences observed between nanoparticles (~ 2 and 16 nm). Nevertheless, QY determined in QDs based on Met still are high compared to other biosynthesis reported (Yang et al., 2015; Jang et al., 2015; Al-Shalabi and Doran, 2016). The differences observed in the nanoparticle characterization between QDs produces with Cys and Met strongly suggest that nanoparticles produced by the extracellular biosynthesis of CdS QDs using Met having different properties from the nanoparticles produced by Cys. It is probably a result of the different sulfur sources used as sulfide precursors and the organic coating of the nanoparticles.

The analysis of VSCs revealed that *Pseudomonas* sp. GC01 produces H_2S, MeSH, and DMS in the presence of sulfate, Cys, and Met. At the same time, DMDS was only detected when Met was used as the sole sulfur source. Interestingly, MeSH is the main VSCs released by *Pseudomonas* sp. GC01 from all sulfur sources tested in contrast with H_2S, which presented a low production in all treatments. The release of VSCs such as H_2S, MeSH, DMS, and DMDS has been informed in bacteria from different environments, as a result of sulfur assimilation for synthesis of amino acids Cys and Met or by the degradation of sulfur-containing compounds (Lomans et al., 2002; Schulz and Dickschat, 2007; Korpi et al., 2009). Amino acid Met been described as the main precursor of VSCs biosynthesis due to acts as a substrate for MeSH production, which in turn, is a precursor of DMS and DMDS (Vermeij and Kertesz, 1999; Lu et al., 2013;

Carrión et al., 2015). While the amino acid Cys acts substrate in bacterial H_2S production (Yang et al., 2015; Dunleavy et al., 2016).

As expected, the VSCs production by *Pseudomonas* sp. GC01 under biosynthesis conditions (presence of Cd^{+2}) with Cys and Met showed a higher production of H_2S and MeSH, respectively, in comparison to the other volatiles. Besides, a reduction ($P < 0.05$) of both VSCs was observed when samples were treated with Cd, strongly suggesting the use of these volatile compounds as S-source for the generation of CdS QDs when Cys or Met is used as a substrate. In support of this, different authors have suggested the generation of H_2S (as sulfide source) from Cys as a mechanism of cadmium-based nanocrystals formation in a reaction catalyzed by Cysteine desulfhydrase or cystathionine γ-lyase (Bai et al., 2009a; Holmes et al., 1997; Yang et al., 2015; Dunleavy et al., 2016). Also, the amino acid Cys has been suggested for acting as a capping agent in CdS QDs formation (Dunleavy et al., 2016). Nevertheless, the role of the MeSH as a sulfide source or Met as a sulfur substrate in the biosynthesis of CdS QDs has not been informed yet.

Therefore, the role of the volatile MeSH and DMS on CdS QDs biosynthesis from Met was evaluated in two mutants of the Antarctic strain *Pseudomonas deceptionensis* $M1^T$: megL- (unable to produce MeSH from Met) and mddA- (unable to generate DMS from MeSH) (Carrión et al., 2015). Our outcomes showed a positive biosynthesis of nanoparticles from mddA- strain discarding the role of DMS as a synthesis substrate. Surprisingly, the megL- strain was unable to biosynthesize CdS QDs. This finding strongly suggests that MeSH could act as a source of S^{2-} to synthesize CdS QDs when Met is used as a sulfur source (Figure 8, Chapter II).

Finally, to understand the molecular and metabolic components involved in the biosynthesis of CdS QDs described above, the genome analysis of *Pseudomonas* sp.

GC01 by comparative genomics was performed (Chapter III). *Pseudomonas* sp. GC01 is a Cd-resistance strain (1.8 mM $CdCl_2$) that biosynthesizes CdS QDs when exposed to this metal (Gallardo et al., 2014). Based on this premise, cadmium-resistance genes were searched in their genome. The results showed the presence of genes *cadR*, and *czcR* which encode for regulatory elements implicate in metal-resistance, the transcriptional regulatory protein CadR associated to Cd^{2+} resistance and DNA binding heavy metal response regulator protein CzcR involved in Cd^{2+}, Zn^{2+}, and Co^{2+} resistance (Perron et al., 2004; Permina et al., 2006; Liu et al., 2015; Pal et al., 2017; Prabhakaran et al., 2018; Orellana-Saez et al., 2019; Cayron et al., 2020; Mazhar et al., 2020). Besides, three genes code for the PIB2-type ATPases *cadA*, *zntA*, and *pbrA*, primarily implicated in cadmium, zinc, and lead transport from the cytoplasm to the periplasm was found (Scherer and Nies, 2009; Nies, 2016; Vidhyaparkavi et al., 2017; Qin et al., 2019; Mazhar et al., 2020). Our outcomes demonstrated that the genome of *Pseudomonas* sp. GC01 contains five genes potentially involved in cadmium-resistance, including three Cd^{2+} efflux proteins that could act as cellular detoxification mechanisms. Additionally, the capacity to produce extracellular CdS QDs displayed by *Pseudomonas* sp. GC01 could be favored the extracellular interaction of Cd^{2+} with H_2S or MeSH released in biosynthesis conditions to form the CdS nanocrystals.

Regarding genes involved in sulfur metabolism present in the genome of *Pseudomonas* ps. GC01, the results revealed numerous genes related to the assimilation of sulfate, sulfite, and thiosulfate (Figure 6 and 7, Chapter III). These genes are associated mainly with the sulfate assimilation pathway in *Pseudomonas* sp. GC01, which involves the uptake and activation of sulfate, followed by stepwise reduction to S^{2-}, before being assimilated into organic material (Kertesz, 2000, 2004; Kredich, 2008; Seiflein and Lawrence, 2001), generating H_2S from sulfite is the last step of this pathway, which

involved enzymes sulfite reductase (Kertesz, 2000, 2004; Kredich, 2008). Three sulfite reductase encoded by *cysI*, *cysJ* (EC: 1.8.1.2), and *sir* (EC: 1.8.7.1) were found in *Pseudomonas* sp. GC01. Besides, a thiosulfate sulfurtransferase (EC: 2.8.1.1; Kawano et al., 2017) encoded by *seeA* reducing thiosulfate to sulfite before entering the sulfate assimilation pathway. Sulfur is an essential element for cell growth, but it can only be assimilated as S^{2-} in its fully reduced state. Therefore, inorganic sulfur assimilation implicates the cellular generation of H_2S before their incorporation into organic material. Accordingly, *Pseudomonas* sp. GC01 could use the H_2S produced as the substrate to intracellular biosynthesis of CdS QDs when sulfate, sulfite, and thiosulfate was used as the sole sulfur source.

On the other hand, our results showed that *Pseudomonas* sp. GC01 uses the amino acids Cys and Met as a sulfur source to grow and extracellular biosynthesis of CdS QDs. The use of these amino acids by bacteria has been associated with internal recycling processes to maximize available nutrients (Seiflein and Lawrence 2006). Cys as a sole sulfur source can be assimilated directly via the transsulfuration pathway that converts Cys to Met (Vermeij and Kertesz, 1999; Wüthrich et al., 2018), or break down to release sulfide (H_2S) through the enzyme cysteine desulfhydrase (EC: 4.4.1.15) (Awano et al., 2003, 2005; Oguri et al., 2012). The sulfide produced by Cys degradation (or by sulfate assimilation pathway) can yield Met through direct sulfhydrylation pathway, which has been described as the main Met synthesis route in bacteria of the *Pseudomonas* genus (Kertesz, 2004). Both pathways (transsulfuration pathways and direct sulfhydrylation pathways) present in the genome of *Pseudomonas* sp. GC01 (Figure 7, Chapter III). Expectedly, due to low H_2S production from Cys in *Pseudomonas* sp. GC01, the enzyme cysteine desulfhydrase (encode by *dcyD*), was absent from their genome. This result suggests that other enzymes with lower cysteine desulfhydrase activity as cysteine

synthases (EC: 2.5.1.47, *cysK*) and cystathionine beta-lyase (EC: 4.4.1.13, *metC*) present in the genome of *Pseudomonas* sp. GC01 could generate sulfide from Cys (Awano et al., 2003, 2005). As mentioned above, extracellular biosynthesis of CdS QDs in bacteria has been mainly associated with H_2S production from Cys by the action of enzymes cysteine desulfhydrase (*dcyD*) or cystathionine gamma-lyase (EC: 4.4.1.1, *CTH* or *mccB*) (Bai et al., 2009a; Yang et al., 2016). Interestingly, *Pseudomonas* sp. GC01 biosynthesizes QDs of CdS from Cys, despite the lack of these genes. Therefore, one attractive via of sulfide generation for the biosynthesis of CdS nanoparticles based on Cys are the enzymes cysteine synthases (*cysK*) and cystathionine beta-lyase (*MetC*). In support of this, recently, cystathionine beta-lyase has been associated with H_2S production from Cys and precipitation of CdS nanoparticles (Ma et al., 2020).

Regarding the use of Met as a sole sulfur source for bacterial growth, the genome results of *Pseudomonas* sp. GC01 showed the absence of genes involved in the reverse transsulfuration pathway to the conversion of Met to Cys via cystathionine by the enzymes cystathionine beta-synthase (EC: 4.2.1.22, *CBS*) and cystathionine gamma-lyase (EC: 4.4.1.1, CTH or mccB) (Vermeij and Kertesz 1999; Kertesz, 2004). However, key members of the Met desulfurization pathway, the genes *mddA*, and *sfnG*, were present in *Pseudomonas* sp. GC01. In this pathway, Met may be desulfurized to produce sulfite entering the synthetic pathway of Cys through the sulfate assimilation (Vermeij and Kertesz 1999).

Besides, the use of Met as a sulfur source to extracellular biosynthesis of CdS QDs via MeSH production has been determined in this study. The MeSH generation from Met desulfurization by enzyme methionine gamma-lyase (EC: 4.4.1.11) has been reported in *Pseudomonas* strains (Fukumoto et al., 2012; Carrion et al., 2015; El-Sayed et al., 2017). Unexpectedly the genes *megL* and *EC4.4.1.11* that encode methionine gamma-lyase were

absent in the genome of *Pseudomonas* sp. GC01, despite the ability of this strain to produce high concentrations of MeSH from Met. However, the enzyme cystathionine beta-lyase (*metC*, present in *Pseudomonas* sp. GC01 genome) has been described with the ability to produce MeSH from Met (Dias and Weimer, 1998; Lee et al., 2007; Schulz and Dickschat, 2007; Veselova et al., 2019) (Figure 8). Based on these results, once again, the gene *metC* emerges as a potential candidate involved in extracellular biosynthesis of Cd QDs, in this case, due to their ability to generate MeSH from Met in bacteria.

4.2 Concluding remarks and future directions

-Our findings confirm that *Pseudomonas* sp. GC01 is capable of biosynthesize extracellular CdS QDs in the presence of the amino acids Cys and Met. Furthermore, this production of nanocrystals was associated with the ability of *Pseudomonas* sp. GC01 to form the volatile sulfur compounds H_2S and MeSH as a source of S^{2-} for the CdS biosynthesis from Cys and Met, respectively. Our nanoparticle bio-production approach by volatile sulfur compounds provides the first evidence about el use of a volatile organic compound such as MeSH produced from Met in the CdS QDs biosynthesis process.

-Our research also confirms the presence of three P-type ATPases transporters, *cadA*, *zntA*, and *pbrA*, in the genome of *Pseudomonas* sp. GC01. Identifying these metal transport genes provides evidence about the tools of detoxification used by this strain under Cd-stress. Besides, metal ion efflux as a potential mechanism of cadmium-resistance could contribute to the extracellular biosynthesis of CdS QDs in *Pseudomonas* sp. GC01.

-The role of enzymes methionine gamma-lyase (*megL* and *EC4.4.1.11*) and cysteine desulfhydrase (*dcyD*) in the extracellular biosynthesis of CdS nanoparticles based on MeSH and H_2S was discarded due to the absence of the genes that encode these enzymes in the genome of *Pseudomonas* sp. GC01.

-The gene *metC* (cystathionine beta-lyase) is presented as the main candidate to produces both H_2S and MeSH as S^{2-} sources to the extracellular biosynthesis of CdS QDs when Cys and Met were used as sole sulfur sources in *Pseudomonas* sp. GC01 (Figure 8, chapter III).

This Thesis project not only contributes to extend the understanding of the biosynthesis of nanoparticles based on cadmium by identifying new molecules involved in their process synthesis and potential mechanisms associated with these, but also the development of new methods to biosynthesize cadmium semiconductor nanoparticles using microorganisms. Future assessments of this investigation are to test the ability of enzyme cystathionine beta-lyase to volatile sulfur compounds produce, and CdS nanocrystal generation under an approach biomimetic. Besides, our results provide a good model of metal-detoxification through the bacterial precipitation of cadmium into CdS QDs to be used in bioremediation. Further in-depth studies are needed to elucidate the mechanisms involved in the biosynthesis process due to the complex cellular interactions. The knowledge of the genetic and metabolisms of biomolecules associated with biosynthesis of nanoparticles would allow us to develop new protocols for nanoparticles with different properties and applications.

References

Abbas, S. Z., Rafatullah, M., Hossain, K., Ismail, N., Tajarudin, H. A., and Abdul Khalil, H. P. S. (2018). A review on mechanism and fu-ture perspectives of cadmium-resistant bacteria. *Int. J. Environ. Sci. Technol*. 15, 243–262. doi:10. 1007/s13762-017-1400-5

Abdelbary, S., Elgamal, M. S., and Farrag, A. (2019). "Trends in Heavy Metals Tolerance and Uptake by *Pseudomonas aeruginosa*", in *Pseudomonas Aeruginosa*-An Armory Within, eds., Sriramulu D. *IntechOpen*. doi:10.5772/intechopen.85875

Alaminos, M., and Ramos, J. L. (2001). The methionine biosynthetic pathway from homoserine in *Pseudomonas putida* involves the *metW, metX, metZ, metH* and *metE* gene products. *Arch. Microbiol*. 176, 151-154. doi:https://doi.org/10.1007/s002030100293

Al-Shalabi, Z., and Doran, P. M. (2016). Biosynthesis of fluorescent CdS nanocrystals with semiconductor properties: Comparison of microbial and plant production systems. *J. Biotechnol*. 223, 13–23. doi:10.1016/j.jbiotec.2016.02.018.

Ali, J., Hameed, A., Ahmed, S., and Ali, M. I. (2016). Role of catalytic protein and stabilizing agents in transformation of Ag ions to nanoparticles by *Pseudomonas aeruginosa*. *IET Nanobiotechnology* 10, 295–300. doi:10.1049/iet-nbt.2015.0093.

Ali, P., Shah, A. A., Hasan, F., Cai, H., Sosa, A., and Chen, F. (2019). Draft Genome Sequence of a Cold-Adapted *Pseudomonas* sp. Strain, BGI-2, Isolated from the Ice of Batura Glacier, Pakistan. *Microbiol. Resour. Announc*. 8, e00320-19. doi:10.1128/MRA.00320-19

Alivisatos, A. P. (1996). Perspectives on the Physical Chemistry of Semiconductor Nanocrystals. *J. Phys. Chem*. 100, 13226–13239. doi:https://doi.org/10.1021/jp9535506

Altschul, S., Gish, W., Miller, W., Myers, E., and Lipman, D. (1990). Basic local alignment search tool. *J. Mol. Biol*. 215, 403-410. doi:https://doi.org/10.1016/S0022-2836(05)80360-2

Ashengroph, M., Khaledi, A., and Bolbanabad, E. M. (2020). Extracellular biosynthesis of cadmium sulphide quantum dot using cell-free extract of *Pseudomonas chlororaphis* CHR05 and its antibacterial activity. *Process Biochem.* 89, 63-70. doi:https://doi.org/10.1016/j.procbio.2019.10.028

Auger, S., Gomez, M. P., Danchin, A., and Martin-Verstraete, I. (2005). The PatB protein of *Bacillus subtilis* is a CS-lyase. *Biochimie.* 87, 231-238. doi:https://doi.org/10.1016/j.biochi.2004.09.007

Awano, N., Wada, M., Kohdoh, A., Oikawa, T., Takagi, H., and Nakamori, S. (2003). Effect of cysteine desulfhydrase gene disruption on L-cysteine overproduction in *Escherichia coli*. *Appl. Microbiol. Biotechnol*. 62, 239–243. doi:10.1007/s00253-003-1262-2.

Awano, N., Wada, M., Mori, H., Nakamori, S., and Takari, H. (2005). Identification and functional analysis of *Escherichia coli* cysteine desulfhydrases. *Society* 71, 4149–4152. doi:10.1128/AEM.71.7.4149.

Ayano, H., Kuroda, M., Soda, S., and Ike, M. (2015). Effects of culture conditions of *Pseudomonas aeruginosa* strain RB on the synthesis of CdSe nanoparticles. *J. Biosci. Bioeng*. 119, 440–445. doi:10.1016/j.jbiosc.2014.09.021.

Baer, D. R., and Engelhard, M. H. (2010). XPS analysis of nanostructured materials and biological surfaces. *J. Electron Spectros. Relat. Phenomena* 178–179, 415–432. doi:10.1016/j.elspec.2009.09.003.

Bag, P. P., Wang, X. S., Sahoo, P., Xiong, J., and Cao, R. (2017). Efficient photocatalytic hydrogen evolution under visible light by ternary composite CdS@NU-1000/RGO. *Catal. Sci. Technol.* 7, 5113–5119. doi:10.1039/c7cy01254c.

Bai, H. J., Zhang, Z. M., Guo, Y., and Yang, G. E. (2009a). Biosynthesis of cadmium sulfide nanoparticles by photosynthetic bacteria *Rhodopseudomonas palustris*. *Coll. Surfaces B Biointer.* 70, 142–146. doi:10.1016/j.colsurfb.2008.12.025.

Bai, H., Zhang, Z., Guo, Y., and Jia, W. (2009b). Biological synthesis of size-controlled cadmium sulfide nanoparticles using immobilized Rhodobacter sphaeroides. Nanoscale Res. Lett. 4, 717–723. doi:10.1007/s11671-009-9303-0.

Bajorowicz, B., Kobylański, M. P., Gołąbiewska, A., Nadolna, J., Zaleska-Medynska, A., and Malankowska, A. (2018). Quantum dot-decorated semiconductor micro-and nanoparticles: A review of their synthesis, characterization and application in photocatalysis. *Adv. Colloid Interface Sci.* 256, 352-372. doi:https://doi.org/10.1016/j.cis.2018.02.003

Barton, L. L., Ritz, N. L., Fauque, G. D., and Lin, H. C. (2017). Sulfur cycling and the intestinal microbiome. *Dig. Dis. Sci.* 62, 2241–2257. doi:10.1016/j.asoc.2017.08.004.

Bharti, D. B., Bharati, A. V., and Wankhade, A. V. (2018). Synthesis, characterization and optical property investigation of CdS nanoparticles. *Luminescence* 33, 1445–1449. doi:10.1002/bio.3572.

Bolger, A. M., Lohse, M., and Usadel, B. (2014). Trimmomatic: a flexible trimmer for Illumina sequence data. *Bioinformatics* 30, 2114-2120. doi:https://doi.org/10.1093/bioinformatics/btu170

Braud, A., Hoegy, F., Jezequel, K., Lebeau, T., and Schalk, I. J. (2009). New insights into the metal specificity of the *Pseudomonas aeruginosa* pyoverdine–iron uptake pathway. *Environ. Microbiol*. 11, 1079-1091. doi:https://doi.org/10.1111/j.1462-2920.2008.01838.x

Bruna, N., Collao, B., Tello, A., Caravantes, P., Díaz-Silva, N., Monrás, J. P., et al. (2019). Synthesis of salt-stable fluorescent nanoparticles (quantum dots) by polyextremophile halophilic bacteria. *Sci. Rep*. 9, 1953. doi:10.1038/s41598-018-38330-8.

Carrión, O., Curson, A. R. J., Kumaresan, D., Fu, Y., Lang, A. S., Mercadé, E., et al. (2015). A novel pathway producing dimethylsulphide in bacteria is widespread in soil environments. *Nat. Commun*. 6, 6579. doi:10.1038/ncomms7579.

Carrión, O., Miñana-Galbis, D., Montes, M. J., and Mercadé, E. (2011). *Pseudomonas deceptionensis* sp. nov., a psychrotolerant bacterium from the antarctic. *Int. J. Syst. Evol. Microbiol*. 61, 2401–2405. doi:10.1099/ijs.0.024919-0.

Carver, T., Thomson, N., Bleasby, A., Berriman, M., and Parkhill, J. (2009). DNAPlotter: circular and linear interactive genome visuali-zation. *Bioinformatics* 25, 119-120. doi:https://doi.org/10.1093/bioinformatics/btn578

Cary, S. C., McDonald, I. R., Barrett, J. E., and Cowan, D. A. (2010). On the rocks: the microbiology of Antarctic dry valley soils. *Nat Rev Microbiol*. 8, 129–138. doi:10.1038/nrmicro2281

Cayron, J., Effantin, G., Prudent, E., and Rodrigue, A. (2020). Original sequence divergence among *Pseudomonas putida* CadRs drive specificity. *Res. Microbiol*. 171, 21-27. doi:https://doi.org/10.1016/j.resmic.2019.11.001

Chakraborty, J., Mallick, S., Raj, R., and Das, S. (2018). Functionalization of extracellular polymers of *Pseudomonas aeruginosa* N6P6 for synthesis of CdS nanoparticles and cadmium bioadsorption. *J. Polym. Environ*. 26, 3097–3108. doi:10.1007/s10924-018-1195-6.

Chellaiah, E. R. (2018). Cadmium (heavy metals) bioremediation by *Pseudomonas aeruginosa*: a minireview. *Appl. Water Sci*. 8, 154. doi: https://doi.org/10.1007/s13201-018-0796-5

Chen, Y. L., Tuan, H. Y., Tien, C. W., Lo, W. H., Liang, H. C., and Hu, Y. C. (2009). Augmented biosynthesis of cadmium sulfide nanoparticles by genetically engineered *Escherichia coli*. *Biotechnol. Prog*. 25, 1260–1266. doi:10.1002/btpr.199.

Chin, H. W., and Lindsay, R. C. (1994). Ascorbate and transition-metal mediation of methanethiol oxidation to dimethyl disulfide and dimethyl trisulfide. *Food Chem*. 49, 387–392. doi:10.1016/0308-8146(94)90009-4.

Chong, T. M., Yin, W. F., Chen, J. W., Mondy, S., Grandclément, C., Faure, D., Dessaux, Y., and Chan, K. G. (2016). Comprehensive genomic and phenotypic metal resistance profile of *Pseudomonas putida* strain S13. 1.2 isolated from a vineyard soil. *AMB Expr*. 6, 95. doi:https://doi.org/10.1186/s13568-016-0269-x

Choudhary, S., and Sar, P. (2016). Real-time PCR based analysis of metal resistance genes in metal resistant *Pseudomonas aeruginosa* strain J007. *J. Basic Microbiol*. 56, 688-697. doi:https://doi.org/10.1002/jobm.201500364

Clark, M. A., and Barrett, E. L. (1987). The *phs* gene and hydrogen sulfide production by *Salmonella typhimurium*. *J. Bacteriol*. 169, 2391-2397. doi:10.1128/jb.169.6.2391-2397.1987

Contreras-Moreira, B., and Vinuesa, P. (2013). GET_HOMOLOGUES, a versatile software package for scalable and robust microbial pangenome analysis. *Appl. Environ. Microbiol*. 79, 7696-7701. doi: 10.1128/AEM.02411-13

Cotta, M. A. (2020). Quantum Dots and Their Applications: What Lies Ahead?. *ACS Appl. Nano Mater*. 3, 4920-4924. doi: 10.1021/acsanm.0c01386

da Costa, W. L. O., Araujo, C. L. D. A., Dias, L. M., Pereira, L. C. D. S., Alves, J. T. C., Araújo, F. A., et al. (2018). Functional annotation of hypothetical proteins from the *Exiguobacterium antarcticum* strain B7 reveals proteins involved in adaptation to extreme environments, including high arsenic resistance. *PloS one* 13, e0198965. doi: https://doi.org/10.1371/journal.pone.0198965

Dias, B., and Weimer, B. (1998). Conversion of methionine to thiols by *lactococci*, *lactobacilli*, and *brevibacteria*. *Appl. Environ. Microbiol*. 64, 3320-3326. doi:10.1128/AEM.64.9.3320-3326.1998

Dunleavy, R., Lu, L., Kiely, C. J., McIntosh, S., and Berger, B. W. (2016). Single-enzyme biomineralization of cadmium sulfide nanocrystals with controlled optical properties. *Proc. Natl. Acad. Sci*. 113, 5275–5280. doi:10.1073/pnas.1523633113.

Durán-Toro, V., Gran-scheuch, A., Órdenes-aenishanslins, N., Monrás, J. P., and Saona, L. A. (2014). Quantum dot-based assay for Cu^{2+} quantification in bacterial cell culture. *Anal. Biochem. J*. 450, 30–36. doi:10.1016/j.ab.2014.01.001.

El-Sayed, A. S., Ruff, L. E., Ghany, S. E. A., Ali, G. S., and Esener, S. (2017). Molecular and spectroscopic characterization of Asper-gillus flavipes and *Pseudomonas putida* L-Methionine γ-Lyase in vitro. *Appl. Biochem. Biotechnol*. 181, 1513-1532. doi:https://doi.org/10.1007/s12010-016-2299-x

Endoh, T., Kasuga, K., Horinouchi, M., Yoshida, T., Habe, H., Nojiri, H., et al. (2003). Characterization and identification of genes essential for dimethyl sulfide utilization in *Pseudomonas putida* strain DS1. *Appl. Microbiol. Biotechnol*. 62, 83-91. doi:https://doi.org/10.1007/s00253-003-1233-7

Faraon, A., Englund, D., Fushman, I., Stoltz, N., and Petroff, P. (2007). Local quantum dot tuning on photonic crystal chips. *Appl. Phys. Lett*. 90, 213110.

doi: https://doi.org/10.1063/1.2742789

Fontes, A., and Santos, B. S. (2020). "Applications in Biology ", in Quantum Dots. Springer.

Fukumoto, M., Kudou, D., Murano, S., Shiba, T., Sato, D., Tamura, T., et al. (2012). The role of amino acid residues in the active site of L-methionine γ-lyase from *Pseudomonas putida*. *Biosci. Biotechnol. Biochem*. 76, 1275-1284. doi:https://doi.org/10.1271/bbb.110906

Fukushima, K., Dubey, S. K., and Suzuki, S. (2012). YgiW homologous gene from *Pseudomonas aeruginosa* 25W is responsible for tributyltin resistance. *J. Gen. Appl. Microbiol*. 58, 283-289. doi:https://doi.org/10.2323/jgam.58.283

Gallardo, C., Monrás, J. P., Plaza, D. O., Collao, B., Saona, L. A., Durán-Toro, V., et al. (2014). Low-temperature biosynthesis of fluorescent semiconductor nanoparticles (CdS) by oxidative stress resistant Antarctic bacteria. *J. Biotechnol*. 187, 108–115. doi:10.1016/j.jbiotec.2014.07.017.

Gallardo-Benavente, C. D., Carrión, O., Todd, J. D., Pieretti, J., Seabra, A., Duran, N., et al. (2019). Biosynthesis of CdS quantum dots mediated by volatile sulfur compounds

released by antarctic *Pseudomonas fragi*. *Front. Microbiol*. 10, 1866. doi:https://doi.org/10.3389/fmicb.2019.01866

Glatstein, D. A., Bruna, N., Gallardo-Benavente, C., Bravo, D., Carro Pérez, M. E., Francisca, F. M., et al. (2018). Arsenic and cadmium bioremediation by antarctic bacteria capable of biosynthesizing CdS fluorescent nanoparticles. *J. Environ. Eng*. 144, 04017107. doi:10.1061/(ASCE)EE.1943-7870.0001293.

Gholami, Z., Dadmehr, M., Jelodar, N. B., Hosseini, M., and Parizi, A. P. (2020). One-pot biosynthesis of CdS quantum dots through in vitro regeneration of hairy roots of *Rhaphanus sativus* L. and their apoptosis effect on MCF-7 and AGS cancerous human cell lines. *Mater. Res. Express* 7, 015056. doi: 10.1088/2053-1591/ab66ea

Gour, A., and Jain, N. K. (2019). Advances in green synthesis of nanoparticles. *Artif. Cells Nanomed. Biotechnol*. 47, 844-851. doi:https://doi.org/10.1080/21691401.2019.1577878

Gurevich, A., Saveliev, V., Vyahhi, N., and Tesler, G. (2013). QUAST: quality assessment tool for genome assemblies. *Bioinformatics* 29, 1072-1075. doi:https://doi.org/10.1093/bioinformatics/btt086

Hannauer, M., Braud, A., Hoegy, F., Ronot, P., Boos, A., and Schalk, I. J. (2012). The PvdRT-OpmQ efflux pump controls the metal selec-tivity of the iron uptake pathway mediated by the siderophore pyoverdine in *Pseudomonas aeruginosa*. *Environ. Microbiol*. 14, 1696-1708. doi:https://doi.org/10.1111/j.1462-2920.2011.02674.x

Hassan, M., van der Lelie, D., Springael, D., Römling, U., Ahmed, N., Mergeay, M. (1999). Identification of a gene cluster, czr, involved in cadmium and zinc resistance in *Pseudomonas aeruginosa*. *Gene* 238, 417-425. doi:https://doi.org/10.1016/S0378-1119(99)00349-2

Holmes, J. D., Richardson, D. J., Saed, S., Evans-Gowing, R., Russell, D. A., and Sodeau, J. R. (1997). Cadmium-specific formation of metal sulfide Q-particles. *Microbiology* 143, 2521–2530. doi:10.1099/00221287-143-8-2521.

Hoo, C. M., Starostin, N., West, P., and Mecartney, M. L. (2008). A comparison of atomic force microscopy (AFM) and dynamic light scattering (DLS) methods to characterize nanoparticle size distributions. *J. Nanoparticle Res*. 10, 89–96. doi:10.1007/s11051-008-9435-7.

Horcas, I., Fernández, R., Gómez-Herrero, J., and Baro, A. M. (2007). WSXM : A software for scanning probe microscopy and a tool for nanotechnology. *Rev. Sci. Instrum*. 78, 013705. doi:https://doi.org/10.1063/1.2432410.

Hu, N., and Zhao, B. (2007). Key genes involved in heavy-metal resistance in *Pseudomonas putida* CD2. *FEMS Microbiol. Lett*. 267(1), 17-22. doi:https://doi.org/10.1111/j.1574-6968.2006.00505.x

Hullo, M. F., Auger, S., Soutourina, O., Barzu, O., Yvon, M., Danchin, A., et al. (2007). Conversion of methionine to cysteine in *Bacillus subtilis* and its regulation. *J. Bacteriol*. 189, 187-197. doi:10.1128/JB.01273-06

Huerta-Cepas, J., Forslund, K., Coelho, L. P., Szklarczyk, D., Jensen, L. J., Von Mering, C., et al. (2017). Fast genome-wide functional annotation through orthology assignment by eggNOG-mapper. *Mol. Biol. Evol.* 34, 2115-2122. doi: https://doi.org/10.1093/molbev/msx148

Iravani, S., and Varma, R. S. (2020). Bacteria in Heavy Metal Remediation and Nanoparticle Biosynthesis. *ACS Sustain. Chem. Eng.* 8, 5395-5409. doi:https://doi.org/10.1021/acssuschemeng.0c00292

Jadhav, P., Bhand, G. R., Mohite, K. C., and Chaure, N. B. (2017). CdS quantum dots synthesized by low-cost wet chemical technique. *AIP Conf. Proc*. 1832, 1–3. doi:10.1063/1.4980379.

Jang, G. G., Jacobs, C. B., Ivanov, I. N., Joshi, P. C., Meyer, H. M., Kidder, M., et al. (2015). In situ capping for size control of monochalcogenide (ZnS, CdS and SnS) nanocrystals produced by anaerobic metal-reducing bacteria. *Nanotechnology* 26. doi:10.1088/0957-4484/26/32/325602.

Jo, J. H., Singh, P., Kim, Y. J., Wang, C., Mathiyalagan, R., Jin, C. G., et al. (2016). *Pseudomonas deceptionensis* DC5-mediated synthesis of extracellular silver nanoparticles. *Artif. Cells, Nanomedicine Biotechnol*. 44, 1576–1581. doi:10.3109/21691401.2015.1068792.

Joonu, J., and Averal, H. I. (2016). Heavy metal resistant CZC genes identification in *Bacillus cereus*, *Enterobacter asburiae* and *Pseudomonas aeruginosa* isolated from BHEL industry, Tamilnadu. *J. Microbiol. Biotechnol*. 5, 27-31. doi: https://doi.org/10.3389/fmicb.2019.01154

Khan, S. A., and Lee, C. S. (2020). "Green Biological Synthesis of Nanoparticles and Their Biomedical Applications", in Applications of Nanotechnology for Green Synthesis. (Cham: Springer). doi:https://doi.org/10.1007/978-3-030-44176-0_10

Kale, A., Bao, Y., Zhou, Z., and Prevelige, P. E. (2013). Directed self-assembly of CdS quantum dots on bacteriophage P22 coat protein templates. *Nanotechnology* 24, 045603. doi:10.1088/0957-4484/24/4/045603.

Kanehisa, M. and Sato, Y. (2019). KEGG Mapper for inferring cellular functions from protein sequences. *Protein Sci*. 29, 28-35. doi:https://doi.org/10.1002/pro.3711

Karimi, F., Rajabi, H. R., and Kavoshi, L. (2019). Rapid sonochemical water-based synthesis of functionalized zinc sulfide quantum dots: study of capping agent effect on photocatalytic activity. *Ultrason. Sonochem. 57*, 139-146.

doi: https://doi.org/10.1016/j.ultsonch.2019.05.019

Kawano, Y., Onishi, F., Shiroyama, M., Miura, M., Tanaka, N., Oshiro, S., et al. (2017). Improved fermentative L-cysteine overproduction by enhancing a newly identified thiosulfate assimilation pathway in *Escherichia coli*. *Appl. Microbiol. Biotechnol*. 101, 6879-6889. doi:https://doi.org/10.1007/s00253-017-8420-4

Kertesz, M. A. (2000). Riding the sulfur cycle - Metabolism of sulfonates and sulfate esters in Gram-negative bacteria. *FEMS Microbiol. Rev*. 24, 135–175. doi:10.1016/S0168-6445(99)00033-9.

Kertesz, M. A. (2001). Bacterial transporters for sulfate and organosulfur compounds. Res. Microbiol. 152, 279–290. doi:10.1016/S0923-2508(01)01199-8.

Kertesz, M. A. (2004). Metabolism of sulphur-containing organic compounds. Pseudomonas, Vol 3 Biosynth. Macromol. Mol. Metab. 3, 323–357. doi:10.1007/978-1-4419-9088-4_12.

Khachatryan, G., Khachatryan, K., Stobinski, L., Tomasik, P., Fiedorowicz, M., and Lin, H. M. (2009). CdS and ZnS quantum dots embedded in hyaluronic acid films. *J. Alloys Compd*. 481, 402–406. doi:10.1016/j.jallcom.2009.03.011.

Khan, Z., Nisar, M. A., Hussain, S. Z., Arshad, M. N. and Rehman, A. (2015). Cadmium resistance mechanism in *Escherichia coli* P4 and its potential use to bioremediate environmental cadmium. *Appl. Microbiol. Biotechnol*. 99, 10745–10757.

doi:10.1007/s00253-015-6901-x

Kim, J., and Park, W. (2014). Oxidative stress response in *Pseudomonas putida*. *Appl. Microbiol. Biotechnol*. 98, 6933-6946. doi: https://doi.org/10.1007/s00253-014-5883-4

Klockgether, J., Munder, A., Neugebauer, J., Davenport, C. F., Stanke, F., Larbig, K. D., et al. (2010). Genome diversity of *Pseudomonas aeruginosa* PAO1 laboratory strains. *J. Bacteriol*. 192, 1113-1121. doi: 10.1128/JB.01515-09

Kolde, R. Pheatmap: Pretty Heatmaps. R Package Version 1.0.8. Available online: https://CRAN.R- pro-ject.org/package=pheatmap (accessed on May, 2020).

Korpi, A., Järnberg, J., and Pasanen, A. (2009). Microbial volatile organic compounds. *Crit. Rev. Toxicol*. 39, 139–193. doi:10.1080/10408440802291497.

Kredich, N. M. (2008). Biosynthesis of Cysteine. *EcoSal Plus* 3, 1–30.

doi:10.1128/ecosalplus.3.6.1.11.

Kulikova, V. V., Revtovich, S. V., Bazhulina, N. P., Anufrieva, N. V., Kotlov, M. I., Koval, V. S., et al. (2019). Identification of O-acetylhomoserine sulfhydrylase, a putative enzyme responsible for methionine biosynthesis in *Clostridioides difficile*: Gene cloning and biochemical characterizations. *IUBMB life* 71, 1815-1823. doi:https://doi.org/10.1002/iub.2139

Kumar, C. G., and Mamidyala, S. K. (2011). Extracellular synthesis of silver nanoparticles using culture supernatant of *Pseudomonas aeruginosa*. *Coll. Surfaces B Biointer*. 84, 462–466. doi:10.1016/j.colsurfb.2011.01.042.

Kuznetsova, Y. V., and Rempel, A. A. (2015). Size and zeta potential of CdS nanoparticles in stable aqueous solution of EDTA and NaCl. *Inorg. Mater*. 51, 215–219. doi:10.1134/S0020168515020119.

Lee, W. J., Banavara, D. S., Hughes, J. E., Christiansen, J. K., Steele, J. L., Broadbent, J. R., et al. (2007). Role of cystathionine β-lyase in catabolism of amino acids to sulfur volatiles by genetic variants of *Lactobacillus helveticus* CNRZ 32. *Appl. Environ. Microbiol*. 73, 3034-3039. doi:10.1128/AEM.02290-06

Lee, S.W., Glickmann, E., and Cooksey, D.A. (2001). Chromosomal locus for cadmium resistance in *Pseudomonas putida* consisting of a cadmium-transporting ATPase and a MerR family response regulator. *Appl. Environ. Microbiol*. 67, 1437-1444.
doi: 10.1128/AEM.67.4.1437-1444.2001

Lewis, T. A., Glassing, A., Harper, J., and Franklin, M. J. (2013). Role for ferredoxin: NAD(P)H oxidoreductase (FprA) in sulfate assimi-lation and siderophore biosynthesis in *Pseudomonads*. *J. Bacteriol*. 195, 3876-3887. doi:10.1128/JB.00528-13

Li, L., Stoeckert, C. J., Roos, D. S. (2003). OrthoMCL: identification of ortholog groups for eukaryotic genomes. *Gen. Res*. 13, 2178-2189. doi:http://www.genome.org/cgi/doi/10.1101/gr.1224503.

Li, K., Li, G., Bradbury, L. M., Hanson, A. D., and Bruner, S. D. (2016). Crystal structure of the homocysteine methyltransferase MmuM from *Escherichia coli*. *Biochem. J*. 473, 277-284. doi:https://doi.org/10.1042/BJ20150980

Liu, P., Chen, X., Huang, Q., and Chen, W. (2015). The role of CzcRS two-component systems in the heavy metal resistance of *Pseudomonas putida* X4. *Int. J. Mol. Sci*. 16, 17005-17017. doi: https://doi.org/10.3390/ijms160817005

Lina, P.-C., Lina, S., Paul C., W., and Rajagopalan, S. (2014). Techniques for physicochemical characterization of nanomaterials. *Biotechnol. Adv*. 31, 711–726. doi:10.1038/mp.2011.182.doi.

Liu, S., Wang, X., Pang, S., Na, W., Yan, X., and Su, X. (2014). Fluorescence detection of adenosine-5 0 -triphosphate and alkaline phosphatase based on the generation of CdS quantum dots. *Anal. Chim. Acta* 827, 103–110. doi:10.1016/j.aca.2014.04.027.

Lomans, B. P., Drift, C. Van Der, Pol, A., and Camp, H. J. M. O. Den (2002). Microbial cycling of volatile organic sulfur compounds. *C. Cell. Mol. Life Sci*. 59, 575–588.

Lu, X., Fan, C., He, W., Deng, J., and Yin, H. (2013). Sulfur-containing amino acid methionine as the precursor of volatile organic sulfur compounds in algea-induced black bloom. *J. Environ. Sci.* (China) 25, 33–43. doi:10.1016/S1001-0742(12)60019-9.

Ma, N., Sha, Z., and Sun, C. (2020). Formation of cadmium sulfide nanoparticles mediates cadmium resistance and light utilization of the deep-sea bacterium *Idiomarina* sp. OT37-5b. *Environ. Microbiol.* doi:https://doi.org/10.1111/1462-2920.15205

Mahle, R., Kumbhakar, P., Pramanik, A., Kumbhakar, P., Sahoo, S., Mukherjee, R., et al. (2020). Probing the bacterial detoxification of cadmium to form cadmium sulfide quantum dots and the underlying mechanism. *Mater. Adv.* 1, 1168-1175. doi: 10.1039/D0MA00105H

Mal, J., Nancharaiah, Y. V., Van Hullebusch, E. D., and Lens, P. N. L. (2016). Metal chalcogenide quantum dots: Biotechnological synthesis and applications. *RSC Adv*. 6, 41477–41495. doi:10.1039/c6ra08447h.

Marusak, K. E., Feng, Y., Eben, C. F., Payne, S. T., Cao, Y., You, L., et al. (2016). Cadmium sulphide quantum dots with tunable electronic properties by bacterial precipitation. *RSC Adv*. 6, 76158–76166. doi:10.1039/c6ra13835g.

McHugh, K. J., Jing, L., Behrens, A. M., Jayawardena, S., Tang, W., Gao, M., et al. (2018). Biocompatible Semiconductor Quantum Dots as Cancer Imaging Agents. *Adv. Mater*. 30, 1–18. doi:10.1002/adma.201706356.

Mi, C., Wang, Y., Zhang, J., Huang, H., Xu, L., Wang, S., et al. (2011). Biosynthesis and characterization of CdS quantum dots in genetically engineered *Escherichia coli*. *J. Biotechnol*. 153, 125–132. doi:10.1016/j.jbiotec.2011.03.014.

Miyamoto, T., Katane, M., Saitoh, Y., Sekine, M., and Homma, H. (2018). Cystathionine β-lyase is involved in d-amino acid metabolism. *Biochem. J*. 475, 1397-1410.

doi:https://doi.org/10.1042/BCJ20180039

Monrás, J. P., Díaz, V., Bravo, D., Montes, R. A., Chasteen, T. G., Osorio-Román, I. O., et al. (2012). Enhanced glutathione content allows the in vivo synthesis of fluorescent CdTe nanoparticles by *Escherichia coli*. *PLoS One* 7, 1–10. doi:10.1371/journal.pone.0048657.

Mazhar, S. H., Herzberg, M., Ben Fekih, I., Zhang, C., Bello, S.K., Li, Y. P., et al. (2020). Comparative Insights Into the Complete Genome Sequence of Highly Metal Resistant Cupriavidus metallidurans Strain BS1 Iso-lated From a Gold–Copper Mine. *Front. Microbiol*. 11, 47. doi: https://doi.org/10.3389/fmicb.2020.00047

Muntaz Begum, S. K., Ravindranadh, K., Ravikumar, R. V. S. S. N., and Rao, M. C. (2016). Spectroscopic studies on PVA capped ZnSe nanoparticles. Optoelectron. Adv. Mater. Rapid Commun. 10, 889–892.

Muthalif, M. P. A., Sunesh, C. D., and Choe, Y. (2019). Enhanced light absorption and charge recombination control in quantum dot sensitized solar cells using tin doped

cadmium sulfide quantum dots. J. Colloid Interface Sci. 534, 291–300. doi:10.1016/j.jcis.2018.09.035.

Naz, N., Young, H. K., Ahmed, N., Gadd, G. M. (2005). Cadmium accumulation and DNA homology with metal resistance genes in sulfate-reducing bacteria. *Appl. Environ. Microbiol*. 71, 4610-4618. doi:10.1128/AEM.71.8.4610-4618.2005

Nguyen, N. H., Duong, T. G., Hoang, V. N., Pham, N. T., Dao, T. C., and Pham, T. N. (2015). Synthesis and application of quantum dots-based biosensor. Adv. Nat. Sci. Nanosci. Nanotechnol. 6, 15015. doi:10.1088/2043-6262/6/1/015015.

Nichols, D. S., Sanderson, K., Buia, A., Van de Kamp, J., Holloway, P., Bowman, J. P., et al. (2002). "Bioprospecting and biotechnology in Antarctica", in The Antarctic: past, present and future. Antarctic CRC research report 28, eds., Jabour-Green, J., and Haward, M. Hobart, pp. 85-103.

Nies, D. H. (2016). The biological chemistry of the transition metal "transportome" of *Cupriavidus metallidurans*. *Metallomics* 8, 481-507. doi:10.1039/C5MT00320B

Nozik, A. J., Beard, M. C., Luther, J. M., Law, M., Ellingson, R. J., and Johnson, J. C. (2010). Semiconductor quantum dots and quantum dot arrays and applications of multiple exciton generation to third-generation photovoltaic solar cells. *Chem. Rev*. 110, 6873–6890. doi:10.1021/cr900289f.

Oguri, T., Schneider, B., and Reitzer, L. (2012). Cysteine catabolism and cysteine desulfhydrase (CdsH/STM0458) in *Salmonella enterica* serovar typhimurium. *Biochem. J*. 194, 4366-4376. doi:10.1128/JB.00729-12

Oliva-Arancibia, B., Órdenes-Aenishanslins, N., Bruna, N., Ibarra, P. S., Zacconi, F. C., Pérez-Donoso, J. M., et al. (2017). Co-synthesis of medium-chain-length

polyhydroxyalkanoates and CdS quantum dots nanoparticles in *Pseudomonas putida* KT2440. J. Biotechnol. 264, 29–37. doi:10.1016/j.jbiotec.2017.10.013.

Orellana-Saez, M., Pacheco, N., Costa, J. I., Mendez, K. N., Miossec, M. J., Meneses, C., et al. (2019). In-depth genomic and phenotypic characterization of the Antarctic psychrotolerant strain *Pseudomonas* sp. MPC6 reveals unique metabolic features, plasticity, and biotechnological potential. *Front. Microbiol*. 10, 1154.

doi: https://doi.org/10.3389/fmicb.2019.01154

Pal, C., Asiani, K., Arya, S., Rensing, C., Stekel, D. J., Larsson, D. J., et al. (2017). Metal resistance and its association with antibiotic resistance. *Adv. Microb. Physiol*. 70, 261–313. doi:https://doi.org/10.1016/bs.ampbs.2017.02.001

Pal, C., Bengtsson-Palme, J., Rensing, C., Kristiansson, E., Larsson, D. J. (2014). BacMet: antibacterial biocide and metal resistance genes database. *Nucleic. Acids. Research*. 42, D737-D743. doi: https://doi.org/10.1093/nar/gkt1252

Pandiyan, A., and Ray, M. K. (2013). Draft genome sequence of the Antarctic psychrophilic bacterium *Pseudomonas syringae* strain Lz4W. *Genome Announc*. 1, e00377-13. doi: 10.1128/genomeA.00377-13

Parks, D. H., Imelfort, M., Skennerton C. T., Hugenholtz P., Tyson G. W. (2015). CheckM: assessing the quality of microbial genomes recovered from isolates, single cells, and metagenomes. *Genome. Res*. 25, 1043–1055. doi:10.1101/gr.186072.114

Papaleo, M., Fondi, M., Maida, I., Perrin, E., Lo Giudice, A., Michaud, L., et al. (2012). Sponge-associated microbial Antarctic communities exhibiting antimicrobial activity against *Burkholderia* cepacia complex bacteria. *Biotech. Adv*. 30, 272–293. doi: https://doi.org/10.1016/j.biotechadv.2011.06.011

Peix, A., Ramírez-Bahena, M.-H., and Velázquez, E. (2018). The current status on the taxonomy of *Pseudomonas* revisited: an update. *Infect. Genet. Evol*. 57, 106–116. doi: 10.1016/j.meegid.2017.10.026

Permina, E. A., Kazakov, A. E., Kalinina, O. V., and Gelfand, M. S. (2006). Comparative genomics of regulation of heavy metal resistance in *Eubacteria*. *BMC Microbiol*. 6, 49. doi:https://doi.org/10.1186/1471-2180-6-49

Perron, K., Caille, O., Rossier, C., Delden, C. V., Dumas, J., and Kohler, T. (2004). CzcR-CzcS, a two-component system involved in heavy metal and carbapenem resistance in *Pseudomonas aeruginosa*. *J. Biol. Chem*. 279, 8761–8768. doi: 10.1074/jbc.M312080200

Perumal, D., Lim, C. S., Chow, V. T., Sakharkar, K. R., and Sakharkar, M. K. (2008). A combined computational-experimental analyses of selected metabolic enzymes in *Pseudomonas* species. *Int. J. Biol. Sci*. 4, 309-317. doi:10.7150/ijbs.4.309.

Plaza, D. O., Gallardo, C., Straub, Y. D., Bravo, D., and Pérez-Donoso, J. M. (2016). Biological synthesis of fluorescent nanoparticles by cadmium and tellurite resistant Antarctic bacteria: Exploring novel natural nanofactories. *Microb. Cell Fact*. 15, 1–11. doi:10.1186/s12934-016-0477-8.

Prabhakaran, R., Rajkumar, S. N., Ramprasath, T., and Selvam, G. S. (2018). Identification of promoter P *cadR*, in silico characterization of cadmium resistant gene *cadR* and molecular cloning of promoter P *cadR* from *Pseudomonas aeruginosa* BC15. *Toxicol. Ind. Health* 34, 819-833. doi:https://doi.org/10.1177/0748233718795934

Prasad, R., Pandey, R., and Barman, I. (2016). Engineering tailored nanoparticles with microbes: quo vadis?. *Wiley Interdiscip. Rev. Nanomed. Nanobiotechnol*. 8, 316-330. doi:https://doi.org/10.1002/wnan.1363

Pritchard, L., Glover, R. H., Humphris, S., Elphinstone, J. G., Toth, I. K. (2016). Genomics and taxonomy in diagnostics for food secu-rity: soft-rotting enterobacterial plant pathogens. *Anal. Methods* 8, 12-24. doi: 10.1039/C5AY02550H

Qin, Z., Yue, Q., Liang, Y., Zhang, J., Zhou, L., Hidalgo, O. B., et al. (2018). Extracellular biosynthesis of biocompatible cadmium sulfide quantum dots using *Trametes versicolor*. *J. Biotechnol*. 284, 52–56. doi:10.1016/j.jbiotec.2018.08.004.

Qin, W., Zhao, J., Yu, X., Liu, X., Chu, X., Tian, J. et al. (2019) Improving Cadmium Resistance in *Escherichia coli* Through Continuous Genome Evolution. *Front. Microbiol*. 10, 278. doi:10.3389/fmicb.2019.00278

Rengers, C., Nikolai, G., and Eychmüller, A. (2019). "Quantum dots and quantum rods," in Biological Responses to Nanoscale Particles. *NanoScienc*, eds., Gehr, P., and Zellner, R. (Cham: Springer). doi:https://doi.org/10.1007/978-3-030-12461-8_2

Richards, S., Baker, M. A., Wilson, M. D., Lohstroh, A., and Seller, P. (2016). Femtosecond laser ablation of cadmium tungstate for scintillator arrays. Opt. Lasers Eng. 83, 116–125. doi:10.1016/j.optlaseng.2016.03.004.

Romoli, R., Papaleo, M., de Pascale, D., Tutino, M., Michaud, L., LoGiudice, A., et al. (2011). Characterization of the volatile profile of Antarctic bacteria by using solid-phase microextraction– gas chromatography-mass spectrometry. *J. Mass Spectr*. 46, 1051–1059. doi: https://doi.org/10.1002/jms.1987

Rossbach, S., Wilson, T. L., Kukuk, M. L., Carty, H. A. (2000). Elevated zinc induces siderophore biosynthesis genes and a zntA-like gene in *Pseudomonas fluorescens*. *FEMS Microbiol. Lett. 191,* 61-70. doi:https://doi.org/10.1111/j.1574-6968.2000.tb09320.x

Sambrook, J. and Russell, D. W. (2001). Molecular Cloning, A Laboratory Manual 3rd edition. Cold Spring Harbor Laboratory Press.

Sanchez, F., and Sobolev, K. (2010). Nanotechnology in concrete - A review. *Constr. Build. Mater*. 24, 2060–2071. doi:10.1016/j.conbuildmat.2010.03.014.

Sankhla, A., Sharma, R., Yadav, R. S., Kashyap, D., Kothari, S. L., and Kachhwaha, S. (2016). Biosynthesis and characterization of cadmium sulfide nanoparticles - An emphasis of zeta potential behavior due to capping. *Mater. Chem. Phys*. 170, 44–51. doi:10.1016/j.matchemphys.2015.12.017.

Scherer, J., and Nies, D. H. (2009). CzcP is a novel efflux system contributing to transition metal resistance in *Cupriavidus* metal-lidurans CH34. *Mol. Microbiol*. 73, 601-621. doi: https://doi.org/10.1111/j.1365-2958.2009.06792.x

Schulz, S., and Dickschat, J. S. (2007). Bacterial volatiles: The smell of small organisms. *Nat. Prod. Rep*. 24, 814–842. doi:10.1039/b507392h.

See-Too, W. S., Lim, Y.-L., Ee, R., Convey, P., Pearce, D. A., et al. (2016). Complete genome of *Pseudomonas* sp. strain L10.10, a psychrotolerant biofertilizer that could promote plant growth. *J. Biotechnol*. 222, 84-5. doi:10.1016/j.jbiotec.2016.02.017

Seemann T. (2014). Prokka: rapid prokaryotic genome annotation. *Bioinformatics* 30, 2068–2069. doi: https://doi.org/10.1093/bioinformatics/btu153

Seiflein, T. A., and Lawrence, J. G. (2006).Two transsulfurylation pathways in *Klebsiella pneumoniae*. *J. Bacteriol*. 188, 5762-5774. doi: 10.1128/JB.00347-06

Seiflein, T. A. and Lawrence, J. G. (2001). Methionine-to-Cysteine Recycling in *Klebsiella aerogenes*. *J. Bacteriol*. 183, 336-346. doi:10.1128/JB.183.1.336-346.2001

Sekar, P. V., and Parvathi, V. D. (2019). Green nanotechnology in cadmium sulphide nanoparticles and understanding its toxicity and antimicrobial properties. doi:10.35841/biomedicalresearch.30-19-324

Shatalin, K., Shatalina, E., Mironov, A., and Nudler, E. (2011). H_2S: A Universal Defense Against Antibiotics in Bacteria. *Science* 334, 986–990. doi:10.1126/science.1209855.

Shim, J., Shin, Y., Lee, I., and Kim, S. Y. (2016). "L-methionine production", in Amino Acid Fermentation, eds., Yokota A., and Ikeda M. Springer, Tokyo, Volume 159, pp. 153-177. doi:https://doi.org/10.1007/10_2016_30

Shivashankarappa, A., and Sanjay, K. R. (2020). *Escherichia coli*-based synthesis of cadmium sulfide nanoparticles, characterization, antimicrobial and cytotoxicity studies. *Braz. J. Microbiol*. 51, 939–948. doi: https://doi.org/10.1007/s42770-020-00238-9

Siegbahn, K., Nordling, C., Fahlman, A., Nordberg, R., and Hamrin, K. (1967). ESCA-atomic, molecular and solid state structure studied by means of electron spectroscopy Nova Acta Regiae Soc. Sci. Upsaliensis Ser. IV 20:84.

Singha, L. P., Kotoky, R., and Pandey, P. (2017). Draft genome sequence of *Pseudomonas fragi* strain DBC, which has the ability to degrade high-molecular-weight polyaromatic hydrocarbons. *Genome Announc*. 5, e01347-17. doi:10.1128/genomeA.01347-17

Solomon, A. (2018). The Emergence of Nanotechnology and its Applications. *Res. J. Nanosci. Eng.* 2, 8–12.

Song, Y., Huang, M., Luo, D., Zhong, D., and Hou, H. (2014). Effect of CdS QDs linked functional groups on interaction between CdS QDs and EcoRI. *Colloids Surfaces A Physicochem. Eng. Asp.* 444, 299–306. doi:10.1016/j.colsurfa.2013.12.074.

Stafford, S. J., Humphreys, D. P., Lund, P. A. (1999). Mutations in *dsbA* and *dsbB,* but not *dsbC*, lead to an enhanced sensitivity of *Escherichia coli* to Hg^{2+} and Cd^{2+}. *FEMS Microbiol. Lett*. 174, 179-184. doi:https://doi.org/10.1111/j.1574-6968.1999.tb13566.x

Stoffels, L., Krehenbrink, M., Berks, B. C., and Unden, G. (2012). Thiosulfate reduction in *Salmonella enterica* is driven by the proton motive force. *J. Bacteriol* 194, 475-485. doi:10.1128/JB.06014-11

Stover, C. K., Pham, X. Q., Erwin, A. L., Mizoguchi, S. D., Warrener, P., Hickey, M. J., et al. (2000). Complete genome sequence of *Pseudomonas aeruginosa* PAO1, an opportunistic pathogen. Nature 2000, 406, 959-964. doi: https://doi.org/10.1038/35023079

Syed, A., and Ahmad, A. (2013). Extracellular biosynthesis of CdTe quantum dots by the fungus *Fusarium oxysporum* and their anti-bacterial activity. *Spectrochim. Acta Part A Mol. Biomol. Spectrosc*. 106, 41–47. doi:10.1016/j.saa.2013.01.002.

Tandon, S., and Vats, S. (2016). Microbial Biosynthesis of Cadmium Sulfide (Cds) Nanoparticles and Their Characterization. *Eur. J. Pharm. Med. Res*. 3, 545–550.

Tatusov, R. L., Galperin, M. Y., Natale, D. A., and Koonin, E. V. (2000). The COG database: a tool for genome-scale analysis of protein functions and evolution. *Nucleic Acids Res*. 28, 33-36. doi:https://doi.org/10.1093/nar/28.1.33

Ulloa, G., Collao, B., Araneda, M., Escobar, B., Álvarez, S., Bravo, D., et al. (2016). "Use of acidophilic bacteria of the genus *Acidithiobacillus* to biosynthesize CdS fluorescent nanoparticles (quantum dots) with high tolerance to acidic pH." *Enzyme Microb. Technol*. 95, 217–224. doi:10.1016/j.enzmictec.2016.09.005.

Ulloa, G., Quezada, C. P., Araneda, M., Escobar, B., Fuentes, E., álvarez, S. A., et al. (2018). Phosphate favors the biosynthesis of CdS quantum dots in *Acidithiobacillus thiooxidans* ATCC 19703 by improving metal uptake and tolerance. *Front. Microbiol*. 9, 1–10. doi:10.3389/fmicb.2018.00234.

Valencia, E. Y., Braz, V. S., Guzzo, C., and Marques, M. V. (2013). Two RND proteins involved in heavy metal efflux in *Caulobacter crescentus* belong to separate clusters within proteobacteria. *BMC Microbiol*. 13, 79. doi: https://doi.org/10.1186/1471-2180-13-79

Veselova, M. A., Plyuta, V. A., and Khmel, I. A. (2019). Volatile Compounds of Bacterial Origin: Structure, Biosynthesis, and Biological Activity. *Microbiology* 88, 261-274. doi:https://doi.org/10.1134/S0026261719030160

Venegas, F. A., Saona, L. A., Monrás, J. P., Órdenes-Aenishanslins, N., Giordana, M. F., Ulloa, G., et al. (2017). Biological phosphorylated molecules participate in the biomimetic and biological synthesis of cadmium sulphide quantum dots by promoting H_2S release from cellular thiols. *RSC Adv.* 7, 40270–40278. doi:10.1039/c7ra03578k.

Vermeij, P., and Kertesz, M. A. (1999). Pathways of assimilative sulfur metabolism in *Pseudomonas putida*. *J. Bacteriol*. 181, 5833–5837.
doi:http://dx.doi.org/10.3122/jabfm.2015.01.140017.

Vidhyaparkavi, A., Osborne, J., and Babu, S. (2017). Analysis of *zntA* gene in environmental *Escherichia coli* and additional implications on its role in zinc translocation. *3 Biotech* 7, 9. doi:10.1007/s13205-017-0613-0

von Neubeck, M., Huptas, C., Glück, C., Krewinkel, M., Stoeckel, M., Stressler, T., et al. (2016). *Pseudomonas helleri* sp. nov. and *Pseudomonas weihenstephanensis* sp. nov., isolated from raw cow's milk. *Int. J. Syst. Evol*. 66, 1163-1173.

Wada, M., and Takagi, H. (2006). Metabolic pathways and biotechnological production of L-cysteine. *Appl. Microbiol. Biotechnol*. 73, 48-54. doi:https://doi.org/10.1007/s00253-006-0587-z

Wagner, A. M., Knipe, J. M., Orive, G., and Peppas, N. A. (2019). Quantum dots in biomedical applications. *Acta Biomater*. 3321961.

Waly, S. A., Shehata, M. M., and Mahmoud, H. H. (2017). Synthesis and characterization of CdS nanoparticles prepared by precipitation in the presence of span 20 as surfactant. *Russ. J. Appl. Chem*. 90, 292–297. doi:10.1134/S1070427217020203.

Wagner, A. M., Knipe, J. M., Orive, G., and Peppas, N. A. (2019). Quantum dots in biomedical applications. *Acta Biomater*. 94, 44-63. doi:https://doi.org/10.1016/j.actbio.2019.05.022

Wang, A., and Crowley, D. E. (2005). Global gene expression responses to cadmium toxicity in *Escherichia coli*. *J. Bacteriol*. 187, 3259-3266. doi:10.1128/JB.187.9.3259-3266.2005

Wang, D., Chen, W., Huang, S., He, Y., Liu, X., Hu, Q., et al. (2017). Structural basis of Zn (II) induced metal detoxification and antibiotic resistance by histidine kinase CzcS in *Pseudomonas aeruginosa*. *PLoS Pathog*. 13, e1006533. doi:https://doi.org/10.1371/journal.ppat.1006533

Wang, D., Li, X., Zheng, L. L., Qin, L. M., Li, S., Ye, P., et al. (2018). Size-controlled synthesis of CdS nanoparticles confined on covalent triazine-based frameworks for durable photocatalytic hydrogen evolution under visible light. *Nanoscale* 10, 19509–19516. doi:10.1039/c8nr06691d.

Wasley, J., Robinson, S. A., Lovelock, C. E., and Popp, M. (2006). Climate change manipulations show Antarctic flora is more strongly affected by elevated nutrients than water. *Change Biol*. 12, 1800-1812. doi: https://doi.org/10.1111/j.1365-2486.2006.01209.x

Wickham, H. (2016). ggplot2: Elegant Graphics for Data Analysis. 2nd ed.; Springer-Verlag: New York.

Wu, R., Wang, C., Shen, J., and Zhao, F. (2015). A role for biosynthetic CdS quantum dots in extracellular electron transfer of *Saccharomyces cerevisiae*. *Process Biochem*. 50, 2061–2065. doi:10.1016/j.procbio.2015.10.005.

Wüthrich, D., Wenzel, C., Bavan, T., Bruggmann, R., Berthoud, H., and Irmler, S. (2018). Transcriptional regulation of cysteine and methionine metabolism in *Lactobacillus paracasei* FAM18149. *Front. Microbiol.* 9, 1261. doi:https://doi.org/10.3389/fmicb.2018.01261

Xia, Y., Lü, C., Hou, N., Xin, Y., Liu, J., Liu, H., et al. (2017). Sulfide production and oxidation by heterotrophic bacteria under aerobic conditions. *ISME J*. 11, 2754-2766. doi:https://doi.org/10.1038/ismej.2017.125

Yan, Z., Li, M., Wang, J., and Pan, J. (2019). Genome Analysis Revealing the Potential Mechanisms for the Heavy Metal Resistance of *Pseudomonas* sp. P11, Isolated from Industrial Wastewater Sediment. *Curr. Microbiol*. 76, 1361-1368.
doi: https://doi.org/10.1007/s00284-019-01728-2

Yang, W., Guo, W., Chang, J., and Zhang, B. (2017). Protein/peptide-templated biomimetic synthesis of inorganic nanoparticles for biomedical applications. *Mater. Chem. B* 5, 401-417. doi: https://doi.org/10.1039/C6TB02308H

Yang, Z., Lu, L., Berard, V. F., He, Q., Kiely, C. J., Berger, B. W., et al. (2015). Biomanufacturing of CdS quantum dots. *Green Chem*. 17, 3775–3782. doi:10.1039/c5gc00194c.

Yang, Z., Lu, L., Kiely, C. J., Berger, B. W., and McIntosh, S. (2016). Biomineralized CdS quantum dot nanocrystals: Optimizing synthesis conditions and improving functional properties by surface modification. *Ind. Eng. Chem. Res*. 55, 11235–11244. doi:10.1021/acs.iecr.6b03487.

Yanzhen, M., Yang, L., Xiangting, X., and Wei, H. (2016). Complete genome sequence of a bacterium *Pseudomonas fragi* P121, a strain with degradation of toxic compounds. *J. Biotechnol*. 224, 68-69. doi: https://doi.org/10.1016/j.jbiotec.2016.03.019

Yu, Y., Bai, G., Liu, C., Li, Y., Jin, Y., and Yang, W. (2007). Cloning, expression and characterization of L-cysteine desulfhydrase gene from *Pseudomonas* sp. TS1138. *Front. Biol. China* 2, 391–396. DOI:https://doi.org/10.1007/s11515-007-0059-6

Zhou, M., and Ghosh, I. (2007). Quantum dots and peptides: a bright future together. *N. Z. Med. J*. 88, 325–339. doi:10.1002/bip.

Zdych, E., Peist, R., Reidl, J., and Boos, W. (1995). MalY of *Escherichia coli* is an enzyme with the activity of a beta CS lyase (cystathionase). *J. Bacteriol*. 177, 5035-5039. doi:10.1128/jb.177.17.5035-5039.1995

Annex 1

Supporting information of Biosynthesis of CdS Quantum Dots Mediated by Volatile Sulfur Compounds Released by Antarctic Pseudomonas fragi

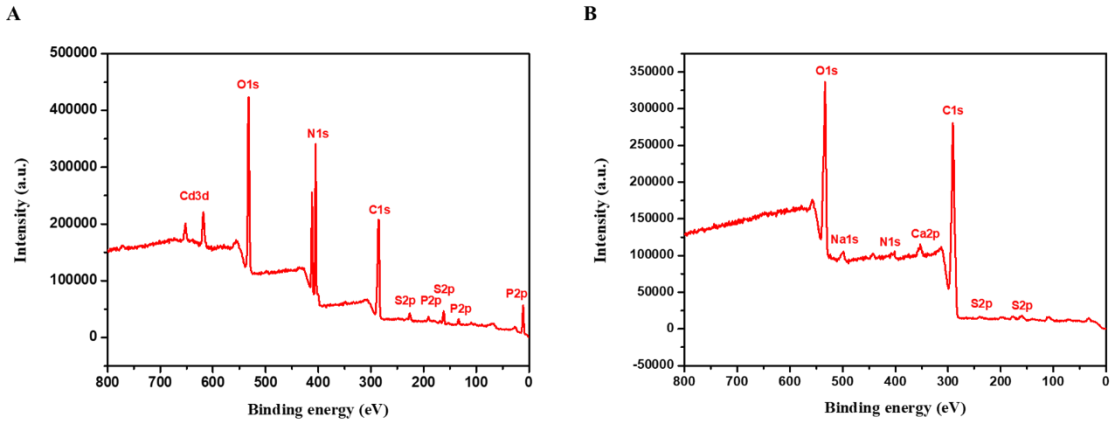

Supplementary Figure S1.1. XPS survey spectra of CdS nanoparticles obtained with (A) Cys, (B) Met.

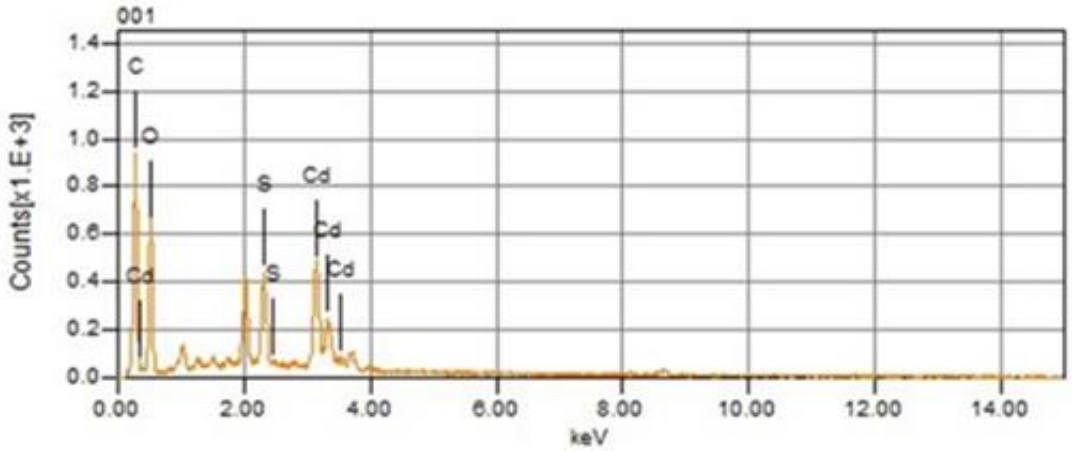

Supplementary Figure S1.2. EDX graph of CdS QDs biosynthesized by *P. fragi* GC01 with Cys for 3h (orange).

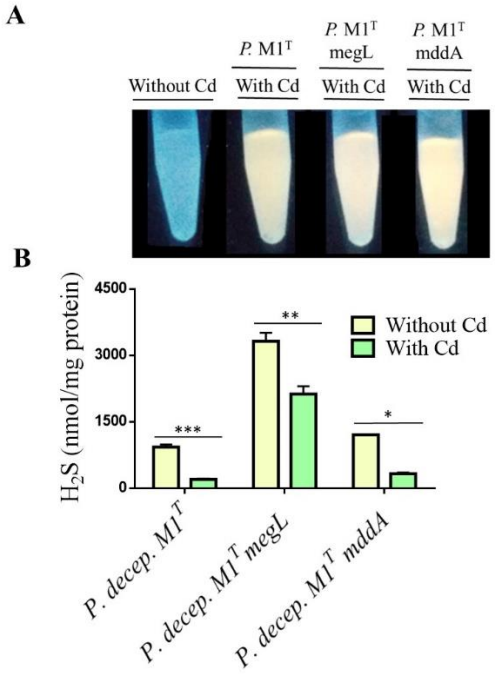

Supplementary Figure S1.3. VSCs produced by *Pseudomonas deceptionensis* M^{1T} strains under biosynthesis conditions with Cys. (A) Fluorescence of bacterial supernatants under biosynthesis conditions during 1 h after UV light exposure. (B) Quantification of H2S by GC after 1 h incubation. Bacterial strains were grown under biosynthesis conditions in M9 medium with 2mM cysteine, in presence or absence of CdCl2 20 µg mL at 28°C. Error bars represent standard deviation (n=3). Student's t-test ($P<0.05$): Comparison between treatments without and with cadmium (Cd). *Statistically significant differences.

Annex 2

Supporting information of Genomics Insights on Pseudomonas sp. CG01: an Antarctic Cadmium Resistant Strain Capable to Biosynthesize CdS Nanoparticles using Methionine as S-source

Supplementary Table S2.1. Accession numbers and data for the selected 28 *Pseudomonas* strains genomes.

Species	**Strain**	**BioSample**	**BioProject**	**Sample**	**Geographic location**
Pseudomonas sp	Lz4W	SAMN02469436	PRJNA170013	Soil	Schirmacher Oasis, Antarctica
Pseudomonas sp	L10.10	SAMN04076495	PRJNA295629	Soil	Antarctica
Pseudomonas sp	ADAK18	SAMN14692983	PRJNA627971	boreal fostest	Alaska, USA
Pseudomonas psychrophila	KM02	PRJNA509367	SAMN14133006	Food spoilage microflora	Poland
Pseudomonas psychrophila	BS3667	SAMN04490201	PRJEB16505	missing	missing
Pseudomonas taetrolens	NCTC10697	SAMEA3711430	PRJEB6403	not available	not available
Pseudomonas taetrolens	NCTC8067	SAMEA26390668	PRJEB6403	not available	not available
Pseudomonas fragi	P121	SAMN04371283	PRJNA307076	Sediment	Artic
Pseudomonas fragi	NMC25	SAMN06628701	PRJNA380155	meat	China
Pseudomonas fragi	DBC	SAMN07187748	PRJNA388845	PAH contaminated soil	India
Pseudomonas chlororaphis	R47	SAMN06241861	PRJNA355625	rhizosphere soil	Switzerland
Pseudomonas chlororaphis subsp. aureofaciens	ChPhzTR39	SAMN08359181	PRJNA433211	tomato rhizosphere	France: Provence-Alpes-Cote d'Azur, Chateaurenard
Pseudomonas chlororaphis subsp. aurantiaca	PCM 2210	SAMN08359189	PRJNA433211	sugar-beetroot rhizosphere	Poland
Pseudomonas protegens	H78	SAMN04240923	PRJNA301182	soil	China
Pseudomonas protegens	UCT	SAMN05964115	PRJNA299395	contaminated site	Czech Republic

Pseudomonas fluorescens	L321	SAMN04992557	PRJNA320923	temperate forest	Ireland
Pseudomonas fluorescens	L111	SAMN04992704	PRJNA320923	temperate forest	Ireland
Pseudomonas frederiksbergensis	ERDD5:01	SAMN05947123	PRJNA350793	glacier stream	India
Pseudomonas frederiksbergensis	AS1	SAMN06102480	PRJNA343270	arsenic-contaminated soil	South Korea
Pseudomonas mucidolens	LMG2223	SAMN05216202	PRJEB16499	missing	missing
Pseudomonas mucidolens	NCTC8068	SAMEA4040591	PRJEB6403	missing	missing
Pseudomonas yamanorum	LMG 27247	SAMN05216237	PRJEB16453	missing	missing
Pseudomonas yamanorum	LBUM636	SAMN03981702	PRJNA292571	field soil	Canada
Pseudomonas sp.	GC01	SAMN14766589	PRJNA629082	soil	Antarctica: Deception Island, South Shetland Archipelago
Pseudomonas aeruginosa	NCTC10332	SAMEA2479570	PRJEB6403	not available	Czech Republic
Pseudomonas aeruginosa	PAO1	SAMN02603714	PRJNA331	not available	missing
Pseudomonas deceptionensis	LMG 25555	SAMN04489800	PRJEB16503	missing	missing
Pseudomonas deceptionensis	DSM 26521	SAMN03328792	PRJNA274345	marine sediment	Antartica

Supplementary Table S2.2. Cadmium-resistance Genes Database described in the literature to *Pseudomonas*.

Gene	Family	Substrates	Organism	Reference
cadA	P-type ATPases	Cd^{2+}, Zn^{2+}	*P. putida* 06909	Lee et al., 2001
			P. sp. MPC6	Orellana-Saez et al., 2019
cadA2R			*P. putida* CD2	Hu and Zhao, 2007
czcA	Cation diffusion facilitator	Cd^{2+}, Zn^{2+}, Co^{2+}	*P. aeruginosa*	Joonu, and Averal, 2016
			P. sp. MPC6	Orellana-Saez et al., 2019
			P. sp. P11	Yan et al., 2019
czcB	Membrane fusion protein	Cd^{2+}, Zn^{2+}, Co^{2+}	*P. aeruginosa*	Joonu, and Averal, 2016
			P. KT2440	Orellana-Saez et al., 2019
czcC	Cation diffusion facilitator	Cd^{2+}, Zn^{2+}, Co^{2+}	*P. aeruginosa*	Joonu, and Averal, 2016
			P. putida KT2440	Orellana-Saez et al., 2019
czcR *czcS*	Regulator	Cd^{2+}, Zn^{2+}, Co^{2+}	*P.* sp. MPC6	Orellana-Saez et al., 2019
			P. aeruginosa	Wang et al., 2017
			P. aeruginosa PAO1	Perron et al., 2004
			P. putida X4	Liu et al., 2015
CzrA *CzrB* *CzrC*	RND Efflux	Cd^{2+}, Zn^{2+}	*P. aeruginosa* CMG103	Hassan et al., 1999
ZntA	P-type ATPases	Pb^{2+}, Cd^{2+}, Zn^{2+}	*Pseudomonas fluorescens* strain ATCC 13525	Rossbach et al., 2000

RND: Resistance-nodulation-division.

Supplementary Table S2.3. Genes Classification for each strain in the pangenome compartments.

Strain	Total Proteins	Accessory	Disposable	Core
P. aeruginosa NCTC10332	5704	2736 (48.0%)	944 (16.5%)	2024 (35.5%)
P. aeruginosa PAO1	5694	2720 (47.8%)	950 (16.7%)	2024 (35.5%)
P. chlororaphis R47	6042	1038 (17.2%)	2980 (49.3%)	2024 (33.5%)
P. chlororaphis subsp. Aurantiaca PCM2210	5631	726 (12.9%)	2881 (51.2%)	2024 (35.9%)
P. chlororaphis subsp. aureofaciens ChPhzTR39	5911	979 (16.6%)	2908 (49.2%)	2024 (34.2%)
P. deceptionensis DSM26521	4560	386 (8.5%)	2150 (47.1%)	2024 (44.4%)
P. deceptionensis LMG25555	4561	387 (8.5%)	2150 (47.1%)	2024 (44.4%)
P. fluorescens L111	5820	1042 (17.9%)	2754 (47.3%)	2024 (34.8%)
P. fluorescens L321	5844	1042 (17.8%)	2778 (47.5%)	2024 (34.6%)
P. fragi DBC	3908	180 (4.6%)	1704 (43.6%)	2024 (51.8%)
P. fragi NMC25	4182	247 (5.9%)	1911 (45.7%)	2024 (48.4%)
P. fragi P121	4316	359 (8.3%)	1933 (44.8%)	2024 (46.9%)
P. frederiksbergensis AS1	4495	285 (6.3%)	2186 (48.6%)	2024 (45.0%)
P. frederiksbergensis ERDD5:01	4197	336 (8.0%)	1837 (43.8%)	2024 (48.2%)
P. mucidolens LMG2223	5242	981 (18.7%)	2237 (42.7%)	2024 (38.6%)
P. mucidolens NCTC8068	5241	980 (18.7%)	2237 (42.7%)	2024 (38.6%)
P. protegens H78	5494	790 (14.4%)	2680 (48.8%)	2024 (36.8%)
P. protegens UCT	4379	804 (18.4%)	1551 (35.4%)	2024 (46.2%)
P. psychrophila BS3667	4710	529 (11.2%)	2157 (45.8%)	2024 (43.0%)
P. psychrophila KM02	4717	532 (11.3%)	2161 (45.8%)	2024 (42.9%)

P. sp. ADAK18	5031	334 (6.6%)	2673 (53.1%)	2024 (40.2%)
P. sp. GC01	4875	271 (5.6%)	2580 (52.9%)	2024 (41.5%)
P. sp. L10.10	4132	167 (4.0%)	1941 (47.0%)	2024 (49.0%)
P. sp. Lz4W	4298	277 (6.4%)	1997 (46.5%)	2024 (47.1%)
P. taetrolens NCTC10697	4305	536 (12.5%)	1745 (40.5%)	2024 (47.0%)
P. taetrolens NCTC8067	4368	562 (12.9%)	1782 (40.8%)	2024 (46.3%)
P. yamanorum LBUM636	5907	879 (14.9%)	3004 (50.9%)	2024 (34.3%)
P. yamanorum LMG27247	5929	893 (15.1%)	3012 (50.8%)	2024 (34.1%)